TRANSIENT STABILITY ANALYSIS OF MULTIMACHINE POWER SYSTEMS BY CATASTROPHE THEORY

by

ALI MOHAMED MIHIRIG
B.Sc., University of Al Fateh, 1978
M.A.Sc., University of British Columbia, 1984

A THESIS SUBMITTED IN PARTIAL FULFILMENT OF

THE REQUIREMENTS FOR THE DEGREE OF

DOCTOR OF PHILOSOPHY

in

THE FACULTY OF GRADUATE STUDIES

DEPARTMENT OF ELECTRICAL ENGINEERING

We accept this thesis as conforming

to the required standard

THE UNIVERSITY OF BRITISH COLUMBIA

December 1987

In presenting this thesis in partial fulfilment of the requirements for an advanced degree at the University of British Columbia, I agree that the Library shall make it freely available for reference and study. I further agree that permission for extensive copying of this thesis for scholarly purposes may be granted by the head of my department or by his or her representatives. It is understood that copying or publication of this thesis for financial gain shall not be allowed without my written permission.

Department of Electrical Engineering

The University of British Columbia
1956 Main Mall
Vancouver, Canada
V6T 1Y3

Date March 15, 1988

ABSTRACT

Transient stability analysis is an important part of power system planning and operation. For large power systems, such analysis is very demanding in computation time. On-line transient stability assessment will be necessary for secure and reliable operation of power systems in the near future because systems are operated close to their maximum limits.

In the last two decades, a vast amount of research work has been done in the area of fast transient stability assessment by direct methods. The major difficulties associated with direct methods are the limitations in the power system model, determination of transient stability regions and adaptation to changes in operating conditions. In this thesis catastrophe theory is used to determine the transient stability regions. Taylor series expansion is used to find the energy balance equation in terms of clearing time and system transient parameters. The energy function is then put in the form of a catastrophe manifold from which the bifurcation set is extracted. The bifurcation set represents the transient stability region in terms of the power system transient parameters bounded by the transient stability limits. The transient stability regions determined are valid for any changes in loading conditions and fault location. The transient stability problem is dealt with in the two dimensions of transient stability limits and critical clearing times. Transient stability limits are given by the bifurcation set and the critical clearing times are calculated from the catastrophe manifold equation. The method achieves a breakthrough in the modelling problem because the effects of exciter response, flux decay and

systems damping can all be included in the transient stability analysis. Numerical examples of one-machine infinite-bus and multi-machine power systems show very good agreement with the time solution in the practical range of first swing stability analysis. The method presented fulfills all requirements for on-line assessment of transient stability of power systems.

TABLE OF CONTENTS

Page

LIST OF TABLES

LIST OF FIGURES

Page

Page

ACKNOWLEDGEMENT

I would like to thank Dr. M.D. Wvong for his continual encouragement and invaluable guidance throughout the course of this research.

I would like to express my sincere appreciation and indebteness to Dr. H.W. Dommel for his encouragement and financial assistance.

I am also indebted to the B.C. Hydro and Power Authority for the financial support and to the Electrical Engineering Department for the computing support and the teaching assistantships provided.

I wish to thank my wife, Najwa, for her encouragement and patience throughout my graduate program.

Thanks are extended to Gail Schmidt for her pleasant attitude and skilled typing of the manuscript.

CHAPTER 1

INTRODUCTION

The stability of a power system implies that all its generators remain in synchronism through normal and abnormal operating conditions. Transient stability arises when a large disturbance such as a loss of generation, load or transmission lines takes place in the power system. The question of whether the power system will settle to a new stable operating state or not is known as the transient stability problem.

The ever increasing demand for electrical energy requires ever larger interconnected power systems and a maximum generation. This raises great concern about the security of power systems when subjected to large disturbances. Transient stability, therefore, becomes an increasingly important consideration in system planning and operation. Extensive stability studies are needed in order to ensure system security before a planning or operating decision is made. Each contingency for each disturbance considered requires a large number of stability studies to determine the critical clearing time or system stability limits.

A typical transient stability study consists of obtaining the time solution to the power system differential and algebraic equations starting with the system conditions prior to the transient. The power system equations should include all significant parameters that influence stability such as generator controls, stability controls and protective devices. The desired objectives of a transient stability analysis are:

i. The stability of the power system. Is it stable or not, to what degree is it stable, and how far is it from the stability limits?

ii. Time responses of generator variables, bus voltages, currents, and active and reactive power.

iii. System quantities that affect the performance of protective devices.

The above objectives are key issues in power system design, planning and operation to ensure system stability for different prescribed disturbances.

The time solution method of stability analysis, although it is very reliable, accurate, and suitable for different modelling orders, has the following disadvantages;

1. The method involves numerical integration of a large number of differential equations for each disturbance considered. A large number of repetitive simulations is required for each case to determine either the stability limits or the critical clearing time. This procedure is very time consuming in the system planning stage where a large number of cases need to be considered.

2. In system operations, there are situations where fast solution is needed to make operational decisions. These situations could be different from those previously considered during planning. Since the time solution method is slow, the system operator has either to overreact to ensure system security or to make decisions that may put stability of the system at risk.

3. The power system operating conditions change during the course of the day and year, while stability studies are done off-line for certain

severe cases. This leads to improper decisions in some cases and, therefore, may increase operational expenditures.

From the above, it is clear that the power industry greatly needs an alternative method to solve the transient stability problem. The alternative method cannot entirely replace the time solution, but it should reduce the number of simulations for each case and hence save a great deal of computation time. A new method is also needed for system operations where the system operator has only minutes or hours to make an important operational decision. The best solution, of course, is to have an on-line method that deals with system operations on a real-time basis.

The desired method for fast analysis of transient stability should satisfy the following important requirements.

1. Provide fast and reliable answers to the transient stability problem when a specified disturbance is given. The answer must particularly indicate whether the system is stable or not.
2. Include sufficient modelling options so that the answer provided is in the range of the actual system response.
3. Provide the necessary information about the degree of stability and system security so that the operator can make proper decisions to ensure system security.
4. If this fast method is to be used for real-time system operations, it should be adaptable to changes in operating conditions, different disturbances, and stability controls.

Although extensive research has been conducted in this area, little of the previous requirements have been achieved so far. A great deal of

research is still needed to either improve the existing methods or propose new methods in order to fulfill all these requirements.

This research is motivated by the challenging problem of developing a satisfactory fast direct method for the assessment of transient stability. The main objectives of this thesis are:

1. To develop a fast, reliable direct method for the assessment of transient stability of power systems.
2. To improve the power system model used by including all necessary options to get as accurate a system response as possible.
3. To predict the comprehensive transient stability region with security boundaries for possible on-line assessment of transient stability.

A review of the literature on the transient stability problem and presently available solutions are given in Chapter 2. In Chapter 3 a new direct method for stability assessment is introduced with preliminary applications on a simple one-machine infinite-bus power system. In Chapter 4, the technique is applied to multi-machine power systems using dynamic equivalents and Taylor series expansions. Transient stability regions are also given by using the catastrophe theory. Chapter 5 presents the capability of the new method to include excitation, flux decay and system damping in the power system model. Chapter 6 summarizes the conclusions and achievements of this project.

CHAPTER 2

REVIEW OF STABILITY PROBLEM AND ITS SOLUTION

2.1 Introduction

The stability problem of power systems has been given new importance since the famous blackout in Northeast U.S.A. in 1965. Considerable research effort has gone into the stability investigation both for off-line and on-line purposes. It started a chain reaction affecting planning, operation and control procedures of electric power systems. Since then several studies have been conducted and new concepts and directions have been suggested to prevent instability and ensure security and reliability of power systems.

In this chapter, a brief review of the stability problem is presented, followed by a literature review of the different methods used and suggested to analyze it.

2.2 The Stability Problem

A stable power system implies that all its interconnected generators are operating in synchronism with the network and with each other. Problems arise when the generators oscillate because of disturbances that occur from transmission faults on switching operations.

There are two types of stability problem in power systems. Firstly, the steady state stability problem which refers to the stability of power systems when a small disturbance occurs in the power systems such as a gradual change in loads, manual or automatic changes in excitation,

irregularities in prime-mover input. Obviously these small disturbances cannot cause loss of synchronism unless the system is operating at, or very near, its steady state stability limit. This limit is the greatest power that can be transmitted on a specified circuit, under certain operating conditions in the steady state, without loss of synchronism. The analysis of steady state stability requires the solution of power flow equations and swing equations over a period of a few miniutes. Governor and exciters should also be included in the steady state stability analysis.

Secondly, there is the transient stability problem which arises from a large disturbance in the power system such as a sudden loss of generators or loads, switching operations, or faults with subsequent circuit isolation. Such large disturbances create a power unbalance between supply and demand in the system. This unbalance takes place at the generator shafts and causes the rotors to oscillate until a new steady state operating point is reached; or until the rotors continue to oscillate and deviate from each other and finally some generators will lose synchronism.

Loss of synchronism must be prevented or controlled because it has a disturbing effect on voltages, frequency and power, and it may cause serious damage to generators, which are the most expensive elements in power systems [1]. The generators which tend to lose synchronism should be tripped, i.e. disconnected from the system before any serious damage occurs, and subsequently brought back to synchronism. While this can be done readily with gas and water turbine generators, steam turbine generators require many hours to rebuild steam and the operator has to shed load to compensate for the loss of generators. Loss of synchronism may also cause some protective

relays to operate falsely and trip the circuit breakers of unfaulted lines. In such cases the problem becomes very complicated and may result in more generators losing synchronism.

2.3 Basic Power System Stability Model

The equation of motion of n generator rotors in a power system of n-machines is given by

$$M_i \ddot{\delta}_i + D_i \dot{\delta}_i = P_i - P_{ei} = P_{ai} \quad , i = 1,2, \ldots n \tag{2.1}$$

where

$$P_{ei} = \sum_{j=1}^{n} (G_{ij} E_i E_j \cos \delta_{ij} + B_{ij} E_i E_j \sin \delta_{ij}) \tag{2.2}$$

δ_i: internal rotor angle of machine 2.

M_i: ωI_i = inertia constant.

I_i: moment of inertia.

ω : angular speed.

D_i: damping coefficient.

P_i: mechanical power input.

P_{ei}: electrical power output.

P_{ai}: accelerating power.

G_{ij}, B_{ij}: real and imaginary parts of reduced nodal admittance matrix.

δ_{ij}: $\delta_i - \delta_j$.

E_i, E_j: internal voltages of machine i,j.

Under steady state conditions, $P_{ai}=0$, and δ_i is constant. When a disturbance occurs, P_{ai} becomes different from zero and equation (2.1) describes the behaviour of δ_i with time. For machine i to be stable, δ_i

must settle to a constant value again and P_{ai} must return to zero. For a power system of n machines, n swing equations have to be solved in order to decide whether the power system is stable or not when a specific disturbance occurs. The solution of the swing equations obtained depends upon the model of the power system elements such as generators (machine, exciter and governor), transmission lines and loads. Furthermore, the choice of the power system model will depend upon the stability study to be carried out and the period of analysis [2].

2.3.1 Synchronous Generator

The most simplified model of the sychronous generator is the so-called classical model. In this model the generator is described by a constant voltage behind transient impedance. This model is acceptable for the first swing transient stability analysis which has a period of one second or less [2]. The internal voltage is constant in magnitude only. This representation neglects the effect of saliency and assumes constant flux linkages and a small change in speed. The voltage equation is given by

$$|E| \underline{/\delta} = V_t + r_a I_t + j x'_d I_t \tag{2.3}$$

where $|E|$: magnitude of voltage behind transient impedance.

δ: angle of $|E|$ (variable).

V_t: terminal voltage.

r_a: armature resistance.

X'_d: transient reactance.

I_t: terminal current.

When saliency and changes in field flux linkages are taken into account, it is no longer possible to represent the generator completely by an equivalent circuit. The resulting equations have time-dependent coefficients unless they are transformed by the use of Park's transformation into the so-called direct- and quadrature-axis variables [2]. The model then involves both differential and phasor-algebraic equations [3]. The differential equation is:

$$\frac{dE_q'}{dt} = \frac{1}{T_{do}'}\left(E_{fd} - E_I\right) \tag{2.4}$$

where E_q' is the voltage proportional to field flux linkage, T_{do}' is the direct-axis transient open-circuit time constant, E_{fd} is the quadrature-axis field voltage and E_I is the voltage proportional to field current. The phasor equations of the above quantities are:

$$E_q' = E_q - j(x_q - x_d')I_d \tag{2.5}$$

$$E_I = V_t + r_a I_t + jx_d I_d + jr_q I_q \tag{2.6}$$

$$E_q = V_t + r_a I_t + jx_q I_t \tag{2.7}$$

where E_q is the voltage behind quadrature-axis reactance x_q, I_d, I_q are the components of I_t along the direct- and quadrature-axes, respectively. Here the machine angle δ is the angle of E_q.

The above model is desirable in the transient stability analysis for the cases when a longer period of analysis is needed when a high-speed voltage-regulator is considered [2].

2.3.2 Exciter and Governor Control Systems

The exciter is a device that supplies flux to the synchronous generator and directly controls the output voltage of the generator. The exciter control system provides the proper field voltage to maintain a desired system voltage during transient and steady state operations. There are many types of exciter control systems in use in power systems [2]. The basic components of an exciter control system are the regulator, amplifier and exciter. The regulator measures the actual regulated voltage and determines the voltage deviation. The deviation signal is then amplified to provide the signal required to control the exciter field current that changes the exciter output voltage and hence results in a new excitation level for the generator. Reference [3] gives the detailed differential equations of the exciter control system.

The exciter control system must be included in the transient stability studies if the period of analysis is longer than one second. Modern fast high-ceiling exciters operate even within a period of one second and if such an exciter is considered then the exciter control system must be included in the generator model.

The rotor speed of the synchronous generator is controlled by the governor control system by varying the mechanical power input. The governor control system can be taken into account in the stability studies by solving its differential equations simultaneously with the rest of the system equations. It is necessary to include the governor effect if the period of analysis is longer than one second [3].

2.3.3 Transmission System and Loads

Transmission lines are usually represented by nodal type equations. Current equations are written for each node in the following manner:

$$I_i = \sum_{j=1}^{n} Y_{ij} E_j \tag{2.8}$$

where E_j are nodal voltages, Y_{ij} are the coefficients of the ith row of the network admittance matrix and I_i is the input current into node i due to a generator or load. The power input into the network at node i is given by

$$P_{ei} = R_e\left(E_i \; I_i^*\right) \tag{2.9}$$

Loads are usually represented as constant complex power, constant impedance or constant current at constant power factor. The equation for constant complex power is

$$S_i = P_i + jQ_i = E_i \; I_i^* = \text{constant} \tag{2.10}$$

for constant impedance is

$$Z_i = \frac{E_i}{I_i} = \text{constant} \tag{2.11}$$

and for constant current at constant power factor is

$$|I_i| = \frac{|S_i|}{|E_i|} \tag{2.12}$$

Transmission lines and loads affect directly the stability limits [4]. The types of load models mentioned above are not adequate models if the load is of a dynamic type. It is very important to use more advanced load models

for dynamic loads especially when high voltage variations are expected [5,6].

2.4 Solution of the Transient Stability Problem

Transient stability refers to the amount of power that can be stably transmitted when the power system is subjected to a large disturbance such as, faults, loss of lines, loss of generators or loads and sudden changes in the tie-line flow. The main objective of a transient stability study is to assess the possible loss of synchronism due to such large disturbances. Transient stability studies enable power engineers to set up protective devices and to design proper stability controls that ensure no loss of synchronism.

The growth of large interconnected power systems demands careful transient stability studies because some large disturbances could have catastrophic results. On the other hand, rapid growth makes it extremely difficult to carry out such careful and detailed stability studies. An easily reached conclusion is that an exact answer is difficult to obtain [7].

There are three main approaches to solving the transient stability problem. These approaches will be discussed in the following sections.

2.4.1. Numerical Integration Methods

These methods solve the power system differential equations (swing equations) during and after the transient period. From the response of

the swing curves of the generators in the power system an experienced power engineer can assess the stability of the power system.

The numerical integration methods can be divided into two basic types:

1. One-step methods: these methods require only information concerning the previous time point to calculate the values at the next time point. Consider a set of non-linear differential equations

$$\frac{dy}{dt} = f(y,t) \tag{2.13}$$

where y represents a set of n variables and f a vector of n functions. The one-step method calculates at point 1 starting from point 0 using a straight line defined by the derivative at point 0

$$y_1 = y_0 + \frac{dy}{dt}\Big|_0 h \tag{2.14}$$

where h is the time interval, $t_1 - t_0$. The new point can be used to calculate the next one, and the iteration continues until the solution is obtained. These methods have high accuracy when the time interval is small, but the accuracy decreases rapidly as the time interval increases. Euler's method and the step by step method given in [1] are typical one-step methods.

2. Multi-step methods: these methods require for each new point, information about two or more preceding points. The predictor-corrector method [8] calculate a point y_{n+1} as follows

$$y_{n+1} = \sum_{k=0}^{p} a_k \, y_{n-k} + h \sum_{k=-1}^{p} b_k \, f\left(y_{n-k}, \, t_{n-k}\right) \tag{2.15}$$

where appropriate values for the a and b constants are chosen for the predictor and corrector formulas. f(y,t) indicates the derivative with respect to time. Equation (2.15) is the same as equation (2.14) for the one-step method with $a_n = b_n = 1$, and all other constants equal to zero.

The number series approach [3] is another type of multi-step method where the generator angles versus time are obtained using the following iterative equation

$$\delta_{n+2} = \delta_n + \frac{(\Delta t)^2}{M} + \frac{(\Delta t)^2}{M} P_{a\ n+1} \tag{2.16}$$

Equation (2.16) is derived from the swing equation by evaluating $\delta(t)$ integration by the trapezoidal rule.

Other methods have been applied to this problem such as Runge-Kutta method [10], an improved Gauss-Seidel approach [11], and the phase-plane techniques [12]. The main advantage of multistep methods is that long time intervals can be used with high accuracy and stability.

In general, the numerical integration methods are widely accepted and used because of the fact that these methods provide detailed results and are capable of including detailed models of power system elements.

The main disadvantage of the numerical integration methods for transient stability studies are the formidable computation time required, the need for human interpretation of the swing curves for assessing the transient stability and the fact that the method cannot be used for on-line assessments of stability.

In spite of the high speed computation of modern computers and several refinements and developments of the technique [13-15] the digital analysis of even a moderate sized power system is still too time consuming. Analog and hybrid simulation [16] have been suggested. In these schemes, all the differential and algebric equations are solved in analog form and the rest of the work (initialization, switching and logic operations) is taken care of by the digital computer. But this approach is still too slow for on-line applications.

2.4.2 Lyapunov's Direct Method

To improve on the slow computational speed of numerical integration methods, Lyapunov's stability theory has been applied to the transient stability problem.

Let the system be represented by a set of differential equations

$$\frac{dX_i}{dt} = f_i\ (X_1,\ X_2,\ \ldots\ X_n,\ t), \quad i = 1,\ldots n. \tag{2.17}$$

The origin of the state vector X is considered to be stable, i.e. $f_i(0,0\ \ldots\ 0,t) = 0, \quad i = 1,\ldots n.$

When the set of initial conditions at the start of the disturbance are all known, Lyapunov's direct method will determine, without finding the actual trajectory of the state variables, if the systm will asymptotically reach a stable point. Therefore, much integration time can be saved as stability can be determined directly from initial conditions.

The method assumes a scalar, continuous Lyapunov function V(X,t) exists in the neighborhood of the origin such that,

1. $V(0,t) = 0$

2. $V(X,t) > 0 \qquad X \in R,\ X \neq 0$

3. $\dfrac{dV(C,t)}{dt} < 0 \qquad X \in R$

where R is a region around the stable point X=0 and is called the region of stability. If the above conditions are valid for V(X,t), it can be shown that for a disturbance $X \in R$ $(X \neq 0)$ then $X \in R$ as $t \to \infty$. The main difficulty here is that the determination of the boundary of the stability region is very time consuming.

The application of this method to the transient stability problem of power systems can be summarized in the following steps [17-19].

1. Initial conditions are determined by a load flow study.
2. The admittance matrix of the power system is reduced to the number of generating buses for during-disturbance and post-disturbance conditions.
3. The steady state equilibrium point of the post-disturbance system is found by solving the equation

   $$P_i - P_{ei} = 0 \quad , \quad i = 1, \ldots n$$

   where P_i and P_{ei} are the mechanical input power and the electrical output power, respectively. The same equation has also to be solved to find the closest unstable equilibrium point. Such a point helps to define the region of stability around the stable state point.
4. The Lypanov's function V(X,t) is found and calculated. Thus the stability regions for V=constant can be found.

5. Integration of the differential equations for the during-disturbance period. At each new point, the function V is calculated with post-disturbance conditions to determine whether the system is stable when the disturbance is cleared. The first instance of instability defines the critical clearing time for the disturbance.

Numerous methods have been suggested to derive a Lyapunov function with the desired properties [20,21]. It should be noted here that different V functions may yield different answers in the sense that they comprise different subregions of the stability region around the stable point [15].

The transient energy function method [22] is the most promising approach among the direct methods. Remarkable progess has been made in recent years [23,24]. However, the method is still not suitable for on-line application because of some practical and computational difficulties [25].

The advantages which Lyapunov's direct method has over numerical integration methods are the following:

1. This method is computationally faster. Here the critical clearing time can be obtained in a single integration while the simulation technique requires repetitive integration for different assumed clearing times.
2. For a given clearing time, this method will indicate whether the system is stable or not. This solution is direct and it does not require the integration of the system differential equations beyond the clearing time.
3. It is shown that the value of the Lyapunov function and the critical clearing time are related [26]. Hence, this method can yield stability margins or stability indices without making actual calculations. Looked

at from another angle, this method can indicate whether a clearing time is adequate or not.

Despite the above attractive features, Lyapunov's direct method has not received general acceptance from the utilities. The main reasons for this are the following practical difficulties associated with this method:

1. Approximate mathematical model of the system; many simplifying assumptions have been made in arriving at a mathematical model of the power system to make it suitable for its analysis by Lyapunov's direct method. The critics of this method question the validity of the simplifications which are necessary for construction of a proper Lyapunov function. Moreoever, the Lyapunov functions are not unique and several such functions can be constructed by using different dynamic models of the power system.
2. The method is conservative and, although some stable point are readily identified, others are inconclusive. Also, the method cannot predict instability, therefore, it may produce too many false alarms.
3. Determination of the region of stability; from a practical application point of view, this has been the most consuming part of this method. In power systems, this requires determination of the unstable equilibrium points closest to the post fault stable equilibrium points, and involves the solution of n-nonlinear algebraic equations.

2.4.3 Pattern Recognition Method

The object of this method is to determine a function S(X) [27] such that:

$$S(X) = \begin{cases} > 0 \text{ for stable } X \\ < 0 \text{ for unstable } X \end{cases}$$

S(X) is called the decision function and X is the state variable , where $(X = X_1, X_2 \ldots X_n)$.

The classification procedure in the pattern recognition method is shown in Fig. (2.1) and summarized in the following steps:

Figure (2.1)

1. Training Set:

In order to obtain S(X), a training set of various operating conditions must be available. Each operating condition or state is specified by variables such as injection powers, loads, generation powers, load flows, voltage magnitudes and rotor angles. Each variable describing a particular X condition constitutes a component of the pattern vector $X = (X_1, X_2 \ldots X_n)$. Ideally, every conceivable pattern should be included in the training set so that it covers the whole spectrum of the system operating conditions. Each pattern of the training set must be classified whether it is stable or unstable.

2. Feature extraction:

The number of variables obtainable from the training set can be very large. In pattern recognition, it is not desirable nor is it necessary to use all the available variables to obtain the classifier function. Therefore, we have to choose the most important variables that contain the necessary information about stability. This can be done by practical experience with the power system or by using statistical measures. The following function F [28] provides an easy and straightforward measure of the information in each variable.

$$F = \frac{|m_s - m_u|}{\sigma_s + \sigma_u}$$

where

m_s = mean of the variable in the stable class.

m_u = mean of the variable in the unstable class.

σ_s = variance of the variable in the stable class.

σ_u = variance of the variable in the unstable class.

Feature extraction begins with the computations of the F values for all the components of the pattern vectors in the training set. The variable with the largest F is selected as the first feature. Then the redundant information is removed by calculating the correlation factor between the first feature and the rest of the variables, excluding variables with high correlation factor with the first feature. The procedure of calculating F with the rest of the features is repeated and selection continues [27].

3. Training Procedure:

Having selected the significant features, the next step is to obtain the decision function S(X). This function can be first order such as

$$S(X) = W_o + W_1 X_1 + \dots + W_m X_m$$

The weighting coefficients (W_o, W_1 ... W_m) are determined such that

$S(X) > 0$ if X is stable

and $S(X) < 0$ if X is unstable

There are many training procedures available such as the least squares method [29,30], linear programming [30,31] and an optimal search algorithm [32].

Another possible classifier function is of second order or quadratic form [27] given below

$$S(X) = W_o + \sum_{i=1}^{m} W_i Z_i + \sum_{i=1}^{m} \sum_{j=1}^{m} W_{ij} Z_i Z_j$$

After the weights are determined, their performance are checked by using them to classify the patterns in the training set.

This method has been improved [33-34], and it is found that non-parametric approaches are more reliable than the parametric approaches mentioned above.

The non-parametric approaches rely on experience to select the proper variables to be used in stability classification [35].

The main advantages of pattern recognition are:

1. It is suitable for on-line assessment of transient stability if a reliable decision function is determined.

2. The method is independent of the model of the power system that is used.

The main disadvantages of pattern recognition are:

1. Off-line computations to obtain the decision function are excessive.
2. The decision function S(X) may very well be sensitive to system configuration so that a different S(X) is needed for any change in the system configuration.
3. Correct classification of 100% cannot be achieved with large power systems because it involves unlimited off-line computations.

2.5 Discussion of Existing Methods

The growth of large interconnected power systems dictates the necessity for on-line transient stability assessment to ensure the security of the power system and maintain reliable service. The main problem of large power systems is that it is impossible to simulate exactly for on-line purposes. Most direct methods provide global solution to the stability problem with high approximation, except the method using the energy-type Lyapunov function [24] which yields solution for the individual machine. But with this method the problem is how to define the stability region for an individual machine and that only a simplified power system model is used.

One may expect better results from the pattern recognition method because of the fact that it is independent of the model used to simulate the power system. This method can be used for an on-line assessment of stability even for individual machines, but it cannot be generalized because

each decision function is good only for the system trained for.

The motivation for this work is to search for a method which is suitable for an on-line assessment of transient stability that can be used for every individual generator in the power system. If such a method can be found then the problem of transient stability can be dealt with on-line. The most suitable method (from among the existing methods) for such an application is pattern recognition because of the fact that it is independent of the systems equations which couple the generators together.

2.4.1 Application of Pattern Recognition to a Simple Power System

A recent technique of pattern recognition [35] is applied to a single machine-infinite bus system shown in Fig. 2.2. Two indices are used as state variables, the kinetic energy (K.E) and transmission margin (TM), where

$$K.E = \frac{1}{2} MW^2$$

and

$$TM = P_{max} - P_c$$

M = inertia constant of the machine

W = speed

p_{max} = maximum power for post-fault condition

P_c = line power at the instant a fault is cleared

K.E and TM have opposite characteristics with loading conditions as shown in Fig. 2.3.

The decision function S(X) in terms of K.E. and TM can be written in the form

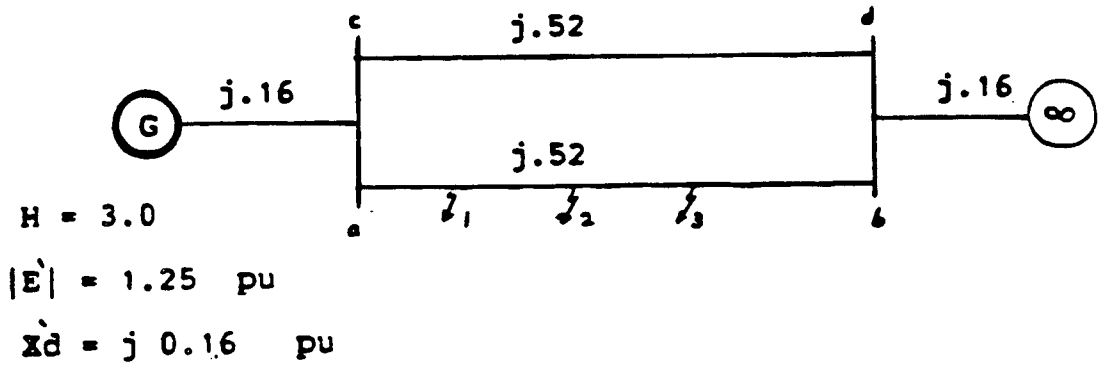

Fig. 2.2 One machine infinite-bus power system

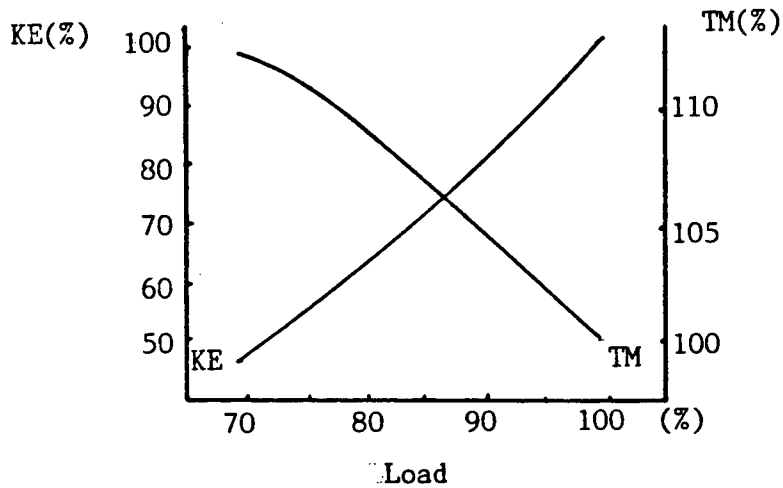

Fig. 2.3 Characteristics of KE and TM with load variation

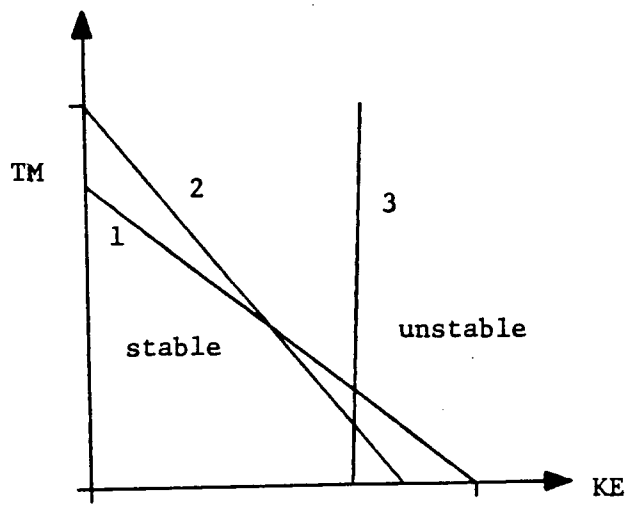

Fig. 2.4 The decision function for three different fault locations

$S(X) = W_x^t + \phi_o$

$S(X) > 0$: stable

$S(X) < 0$: unstable

where $X = (K.E, TM)$, W is coefficient vector

ϕ_o = constant

The technique is applied to the system shown in Fig. 2.2 for three different fault locations indicated. Three different decision functions were determined for the three fault locations as shown in Fig. 2.4.

For fault location (1), $S_1(X) = -TM + 20.71\ K.E + 2.44$.

For fault location (2), $S_2(X) = -TM + 31.51\ K.E + 3.09$

For fault location (3), $S_3(X) = -TM - 681.8\ K.E + 56.1$.

In conclusion, to represent all possible fault locations we have to build up a surface that consists of all possible fault locations. This surface should contain a large number of lines in order to cover the whole region of stability. Therefore, the decision function S(X) should represent the equilibrium surface of the stability region. This conclusion brought up the idea of using catastrophe theory to define the stability region.

CHAPTER 3

APPLICATION OF CATASTROPHE THEORY TO POWER SYSTEM STABILITY

A preliminary application of the catastrophe theory, a mathematical method, to the stability assessment of power systems is introduced in this chapter. The theory is reviewed in Section 3.2 followed by applications to both steady state and transient stability of a simple one-machine infinite-bus power system. This method provides a very good tool to visualize steady state and transient stability regions.

3.1 Introduction

The sustained increasing demand for electrical power requires larger interconnected power systems and operation at or near to full capacity. Therefore, transient stability of power systems becomes a major factor in planning and day-to-day operations and there is a need for fast on-line solution of transient stability to predict any possible loss of synchronism and to take the necessary measures to restore stability.

Lyapunov's direct method and pattern recognition have been introduced for fast assessment of transient stability and eventually to implement these methods for on-line applications.

Catastrophe theory has been applied to the study of stability of various dynamic systems [36] and in recent years to the steady state stability problem of power systems by Sallam and Dineley [37]. An attractive feature of catastrophe theory is that the stability regions are

defined in terms of the system parameters bounded by the lines of stability limits.

The application of catastrophe theory is extended to the transient stability problem. A well defined transient stability region in terms of system parameters is obtained; these regions are suitable for fast on-line applications.

3.2 Catastrophe Theory

It is a natural phenomenon that sudden changes can occur as a result of smooth or gradual changes. Examples might include the breakdown of an insulator when voltage is built up gradually, the collapse of a bridge by gradual load increases and the loss of synchronism of generators in a power system when subject to smooth changes in operating conditions. The term "catastrophe" is used for such sudden changes that are caused by smooth alterations.

Catastrophe theory was originally presented by the French mathematician Rene Thom and published in his book "Structural Stability and Morphogenesis" [38]. Thom used differential topology to explain sudden changes in morphogenesis. The idea then attracted the attention of many scientists and has been applied to a variety of sciences [36].

Catastrophe theory is a theory that explores the region of sudden changes in dynamic systems and deals with the properties of discontinuities directly. It has been defined as the study from a qualitative point of view of the ways the solutions to differential equations may change [39].

Consider a system whose behaviour is usually smooth but which sometimes (or in some places) exhibits discontinuities. Suppose the system has n state variables and controlled by m independent variables, and suppose a smooth potential function to describe the system dynamics exists. Given such a system, what catastrophe theory tells us is the following: The number of qualitative different configurations of discontinuities that can occur depends not on the number of state variables, which may be very large, but on the number of control variables, which is generally small. Particularly, if the number of control variables is not greater than four, then there are only seven distinct types of catastrophes known as the seven elementary catastrophes, and in none of these are more than two state variables involved [40].

3.2.1. Catastrophe Theory and Bifurcation Analysis

Consider a continuous potential function V(X,C) which represents the system behaviour, where X are the state variables and C are the control variables. The potential function V(V,C) can be mapped in terms of its control variables C to define the continuous region. Let the potential function be represented as

$$V(X,C) \quad : \quad M \times C \rightarrow R \tag{3.1}$$

where M, C are manifolds in the state space R^n and the control space R^r respectively.

Now we define the catastrophe manifold M as the equilibrium surface that represents all critical points of V(X,C). It is the subset $R^n \times R^r$ defined by

$$\nabla_X V_C(X) = 0 \tag{3.2}$$

where $V_C(X) = V(X,C)$ and ∇_X is partial derivative with respect to X. Equation (3.2) is the set of all critical points of the function V(X,C).

Next we find the singularity set, S, which is the subset of M that consists of all degenerate critical points of V. These are the points at which

$$\nabla_X V_C(X) = 0$$

and $$\nabla_X^2 V_C(X) = 0 \qquad (3.3)$$

The singularity set, S, is then projected down onto the control space R^r by eliminating the state variables X using (3.3) and (3.2), to obtain the bifurcation set, B. The bifurcation set provides a projection of the stability region of the function V(X,C), i.e. it contains all non-degenerate critical points of the function V bounded by the degenerate critical point at which the system exhibits sudden changes when it is subject to small changes.

The seven elementary catastrophes of $r \leq 4$ are listed in Table (3.1). The geometric analysis of the catastrophes that are used in this thesis are presented in detail in Appendix (A1). A simplified analysis of the seven elementary catastrophes is given in Reference [40].

3.3 Applications to the Steady State Stability Problem

The application of catastrophe theory to the steady state stability of power systems was first introduced in Reference [37]. However, that application was limited only to salient-pole type synchronous generators. When the same procedure was applied to cylindrical-rotor generators,

Catastrophe	Control Space Dimension	State Space Dimension	Function	Catastrophe Manifold
Fold	1	1	$1/3\ x^3-ax$	x^2-a
Cusp	2	1	$x^4-ax-1/2\ bx^2$	x^3-a-bx
Swallowtail	3	1	$1/5\ x^5-ax-1/2\ bx^2-1/3\ cx^3$	$x^4-a-bx-cx^2$
Butterfly	4	1	$1/6\ x^6-ax-1/2\ bx^2-1/3\ cx^3-dx^4$	$x^5-a-bx-cx^2-dx^3$
Hyberbolit	3	2	$x^3+y^3+ax+by+cxy$	$3x^2+a+cy$ $3y^2+b+cx$
Eliptic	3	2	$x^3-xy^2+ax+by+cx^2+cy^2$	$3x^2-y^2+a+2cx$ $-2xy+b+2cy$
Parabolic	4	2	$x^2y+y^4+ax+by+cx^2+dy^2$	$2xy+a+2cx$ $x^2+4y^3+b+2dy$

Table 3.1 The Seven-Elementary Catastrophes

unjustified answers were obtained [37]. In this section, a new procedure for applying catastrophe theory to the steady state stability of cylindrical rotor generators is presented using Taylor series expansion around the initial steady state operating point. This section is a complement to the work done by Sallam and Dineley and it introduces a general procedure which is applicable to all types of generators. Furthermore, the damping and governor effects can also be included using this method.

3.3.1 Cylindrical-rotor Infinite-bus Power System

Consider the one-machine infinite-bus power system of Fig. 3.1. The steady state output power P_e is given by

$$P_e = P_m \sin \delta \tag{3.4}$$

where $P_m = \frac{EV}{X_d}$

E is the machine internal voltage, V is the infinite-bus voltage, X_d is the mchine reactance and δ is the rotor angle (angle of internal voltage E). The power angle curve is given in Fig. 3.2.

Suppose the input power to the machine is increased smoothly from P_o to P_i. The machine will oscillate between δ_0 and δ_2 as shown in Fig. 3.2. If the new operating angle is higher than the maximum power limit, the machine will lose synchronism.

The energy of oscillations between δ_o and δ_2 is given by

$$\int_{\delta_o}^{\delta_2} P_a \, d\delta \tag{3.5}$$

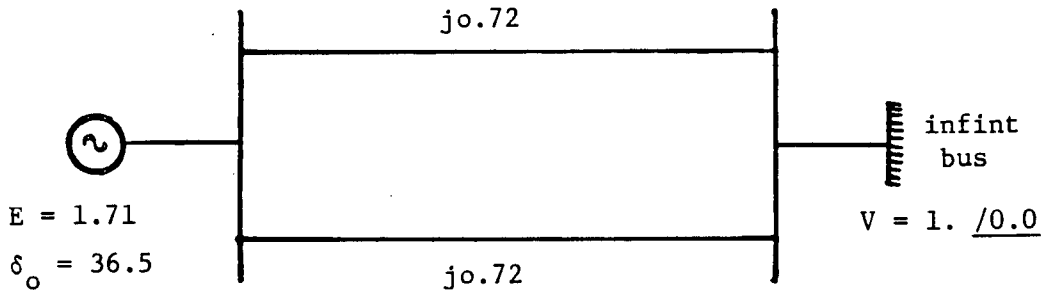

Fig. 3.1

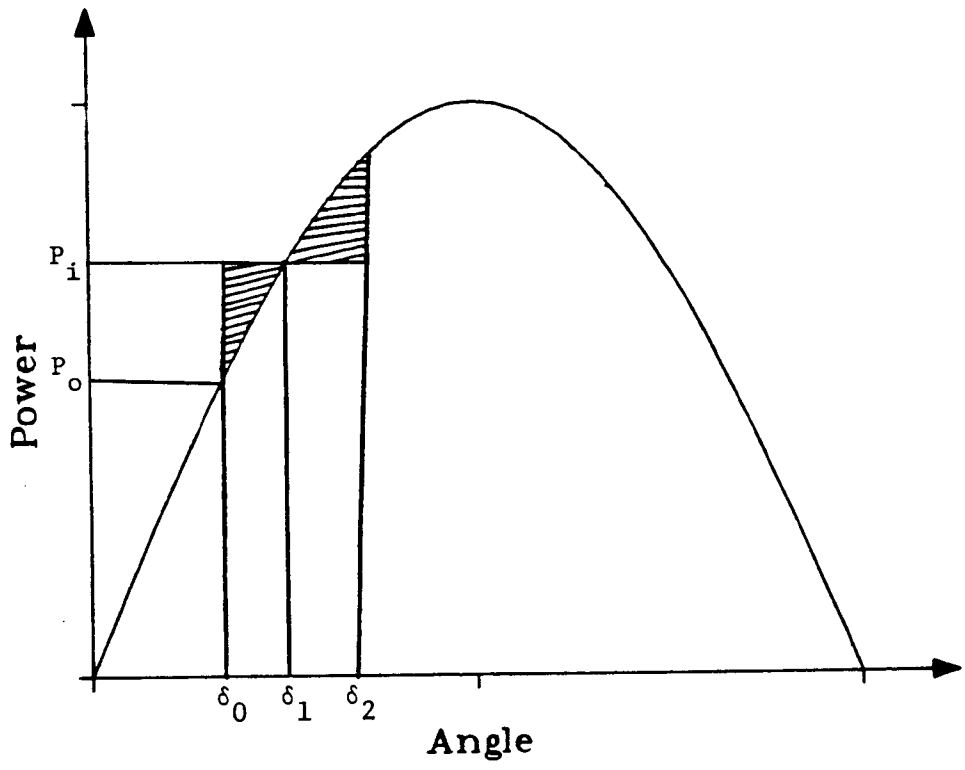

Fig. 3.2 The power-angle curve

$$P_a = P_i - P_m \sin \delta \tag{3.6}$$

P_a is the accelerating power.

We now expand equation (3.6) by Taylor series around δ_o at t=0, P_a becomes

$$P_a(t) = P_a^{(0)} + P_a^{(1)}t + \frac{P_a^{(2)}t^2}{2!} + \ldots \tag{3.7}$$

where

$$P_a^{(m)} = \left.\frac{d^m P_a}{d\,t^m}\right|_{\delta_o} \tag{3.8}$$

Therefore

$$P_a^{(0)} = P_i - P_m \sin \delta_o$$

$$P_a^{(1)} = \left.\frac{d\,P_a}{d\,t}\right|_{\delta_o} = - P_m \cos \delta_o \dot{\delta} = 0$$

$$P_a^{(2)} = \left.\frac{d\,P_a^{(1)}}{d\,t}\right|_{\delta_o} = P_m \sin \delta_o \dot{\delta}^2 - P_m \cos \delta_o \ddot{\delta} \tag{3.9}$$

$$= -P_m \cos \delta_0 \ddot{\delta}$$

$$P_a^{(3)} = \left.\frac{d\,P_a^{(2)}}{d\,t}\right|_{\delta_o} = P_m \cos\delta_o \dot{\delta}^3 + P_m \sin\delta_o (2\dot{\delta})\ddot{\delta}$$

$$+ P_m \sin\delta_o\, \dot{\delta}\,\ddot{\delta} - P_m \cos\delta_o\, \ddot{\delta} = 0$$

$$P_a^{(4)} = \left.\frac{d\,P_a^{(3)}}{dt}\right|_{\delta_0} = - P_m \cos\delta_0 \cdot \dot{\delta}\cdot\cdot + 3P_m \sin\delta_0\, \ddot{\delta}^2$$

where $\dot{\delta} = 0$ at $t = 0$

Since the change in the power input of the machine is smooth and small, the Taylor series expansion determines the exact region of oscillation, from δ_o to δ_2. The accelerating power is then given by

$$P_a(t) = P_a^{(0)} + \frac{P_a^{(2)} t^2}{2!} + \frac{P_a^{(2)} t^4}{4!} + \frac{P_a^{(6)} t^6}{6!} \tag{3.10}$$

Let $\delta = \delta_0 + \frac{1}{2}\gamma t^2$, $(\delta - \delta_0) = \frac{1}{2}\gamma t^2$, $\delta' = \frac{1}{2}\gamma t^2$

where $\gamma = \dfrac{P_a^{(0)}}{M}$

Put $\delta - \delta_0 = \delta' = \frac{1}{2}\gamma t^2$ and substitute in equation (3.10) to obtain

$$P_a(\delta') = P_a^{(0)} + \frac{P_a^{(0)}\delta'}{\gamma} + \frac{P_a^{(4)}}{6\gamma^2}\delta'^2 + \frac{P_a^{(6)}}{18\,\gamma^3}\delta'^3 \tag{3.11}$$

δ' represents the change in rotor angle corresponding to changes in power i.e. at $t = 0$, $\delta' = 0$

Evaluating equation (3.5) to obtain the energy function form δ_0 to

δ_2, we obtain the energy function,

$$V = P_a^{(0)}\ \delta' + \frac{P_a^{(1)}\delta'^2}{2} + \frac{P_a^{(2)}\delta'^3}{3!} + \frac{P_a^{(3)}\delta'^4}{4!} \tag{3.12}$$

Equation (3.12) represents a catastrophe cusp equation, see Table (3.1). The first derivative of the energy function (3.12) that represents the catastrophe manifold (equilibrium surface) of all operating points of the power system is given by

$$\nabla_{\delta'} V = P_a^{(0)} + P_a^{(1)}\ \delta' + P_a^{(2)}\ \frac{\delta'^2}{2!} + \frac{P_a^{(3)}\ \delta'^3}{3!} \tag{3.13}$$

To put equation (3.12) in the cusp catastrophe manifold, the second order term must be eliminated.

Let $\delta' = X - \alpha$

$$\text{and} \quad \alpha = \frac{-P_a^{(2)}}{P_a^{(3)}} \tag{3.14}$$

Substitute equation (3.14) in (3.13) to obtain

$$\nabla_X V = (P_a^{(0)} + K_\alpha) + (P_a^{(1)} - \frac{P_a^{(2)^2}}{2P_a^{(3)}})\ X + \frac{P_a^{(3)}}{6}\ X^3 = 0$$

$$= X^3 + \frac{6}{P_a^{(3)}}\ (P_a^{(1)} - \frac{P_a^{(2)^2}}{2P_a^{(3)}})\ X + \frac{6}{P_a^{(3)}}\ (P_a^{(0)} + K_\alpha) = 0$$

$$= X^3 + a\,X + b = 0 \tag{3.15}$$

where

$$a = \frac{6}{P_a^{(3)}}\left(P_a^{(1)} - \frac{P_a^{(2)^2}}{2P_a^{(3)}}\right)$$

$$b = \frac{6}{P_a^{(3)}}\left(P_a^{(0)} + K_\alpha\right)$$

$$K_\alpha = P_a^{(1)} + \frac{P_a^{(2)}}{2!}\,\alpha^2 + \frac{P_a^{(3)}\,\alpha^3}{3!}$$

Equation (3.15) is exactly the cusp catastrophe manifold (see Appendix B). The steady state stability region is calculated from equation (3.15) by projecting it down onto the control space (a,b), where:

$$\nabla_X^2\, V = 3\,X^2 + a = 0 \tag{3.16}$$

From equation (3.16) and equation (3.15) the state variable X can now be eliminated to get the bifurcation set B,

$$4\,a^3 + 27\,b^2 = 0 \tag{3.17}$$

Equation (3.17) represents the steady state stability limits of the power system in terms of the control parameters a and b as shown in Fig. 3.3.

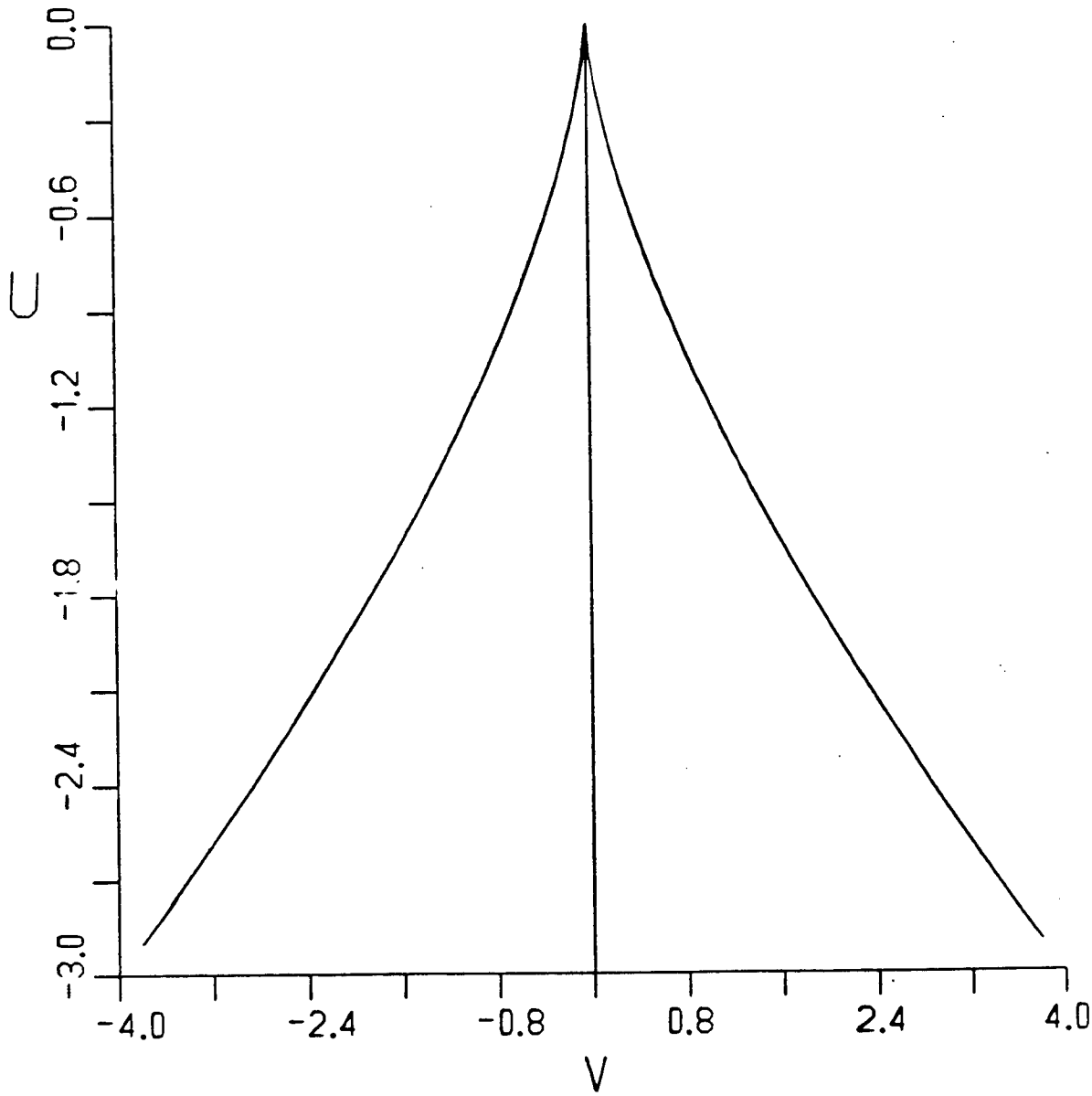

Fig. 3.3 The bifurcation set of the cusp catastrophe which represents the steady state stability region.

3.3.2 Numerical Results

Consider the one-machine infinite-bus system of Fig. 3.1, given the following data

$H = 3$ s , $V_\infty = 1. \underline{/0.0}$ pu

$E = 1.71$ pu , $\delta_o = 36.5$ pu

$X_d = 1.05$ pu , $X_t = 0.36$ pu

Following the procedure in the previous section, the solution of equation (3.15) will give the new operating angle for any change in the input power. The steady state stability region is shown in Fig. 3.3. For any loading condition, the location of the control parameters (a,b) on the bifurcation set of Fig. 3.3 will determine the steady state stability of the system.

The results obtained in Fig. 3.3 agree with the power equation (3.4). It should be clear that the change in the loading condition must be small and within the determining region of the Taylor series order used. However, a higher order Taylor series can be used with a suitable higher catastrophe.

This method can be extended further to include the speed governor effect.

3.4 Application to the Transient Stability Problem

The application of the catastrophe theory to the steady state stability problem is fairly straightforward, as shown in the previous section. In the case of transient stability, the situation is different because there are two switchings (discontinuities) during the transient

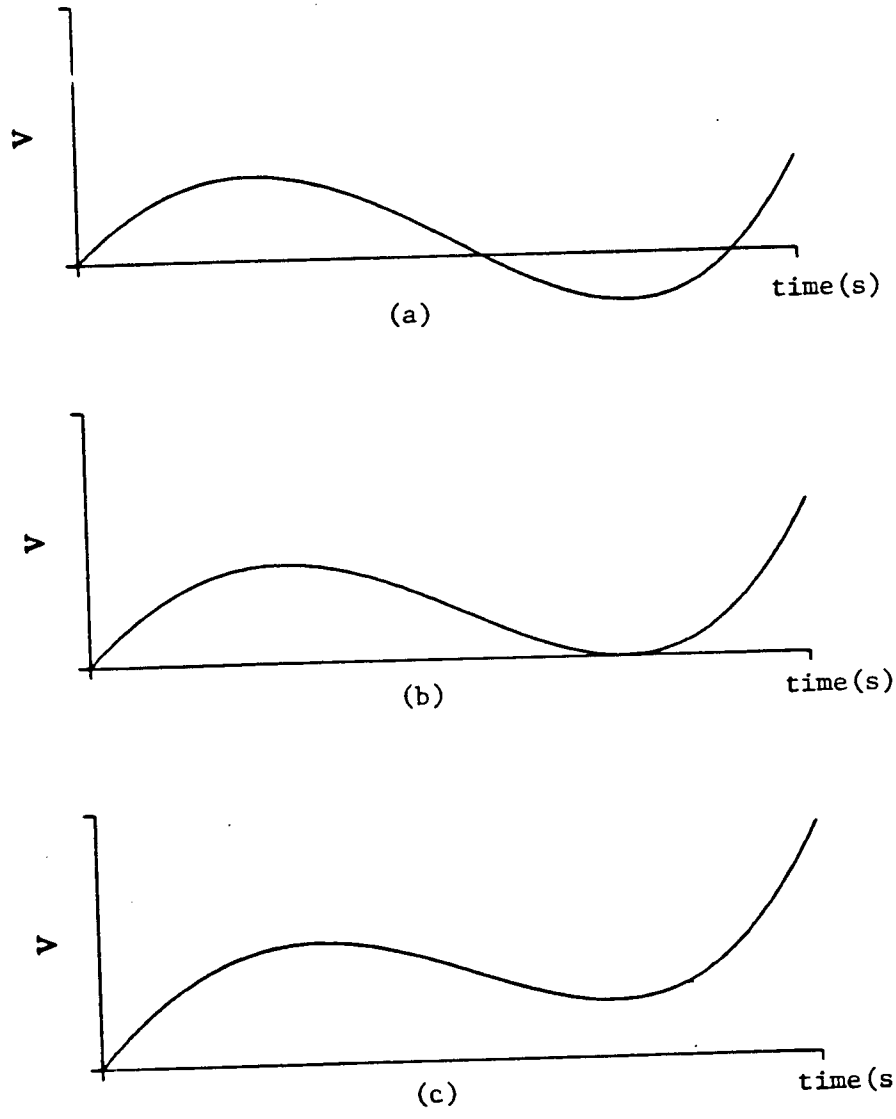

Fig. 3.4 The energy function stability criteria
a. stable
b. critically stable
c. unstable

period, one at fault occurrence and the other at fault clearance. Before we attempt to apply the catastrophe theory we need to find a continuous function that represents the system behaviour during the transient period. We need also to define the degenerate and non-degenerate critical points in terms of transient stability.

Consider again the one-machine infinite-bus system of Fig. 3.1. If a fault occurs on one of the lines near the machine bus, the rotor will accelerate and gain kinetic energy. If the fault is cleared at the critical clearing time, the kinetic energy generated by the fault will be absorbed by the system and the gained energy at the end of the transient period will be exactly zero; the system is considered to be critically stable. A typical energy curve for a fault cleared at different clearing times is shown in Fig. 3.4. In terms of catastrophe theory, curve (b) of Fig. 3.4 can be considered as the energy equilibrium surface or catastrophe manifold at which the kinetic energy equals the potential energy of the system. All non-degenerate critical points lie on the energy equilibrium surface which corresponds to critical clearing times. The degenerate critical points which are defined by the bifurcation set, are the points which correspond to the transient stability limits of the power system at which any small disturbance of the power system will drive the system unstable regardless of the clearing time.

In summary, since the energy function during the transient period is continuous and represents the power system behaviour, the energy balance equation will represent the equilibrium surface that decides the critical

clearing time and the transient stability limits define the degenerate critical points.

3.4.1 Single-Machine Infinite-bus Power System [42]

Consider the power system of Fig. 3.5 which consists of one machine, an infinite bus and two transmission lines ab and dc. Representing the synchronous machine by a constant voltage source behind a reactance (the classical model [2]), the swing equation representing the system behaviour is given by

$$M \frac{d^2\delta}{dt^2} = P_i - P_e = P_a \tag{3.18}$$

where $P_e = P_{max} \sin \delta'$ is the electrical power output.

M = inertia constant of the machine.

P_i = mechanical input power (constant during transient).

P_a = accelerating power.

δ = rotor angle.

Consider a three-phase fault on line ab cleared at the critical clearing time t_c. The accelerating power P_a will exhibit two discontinuities, one when the fault occurs and the other when the fault is cleared. Multiply equation (3.18) by $\dot{\delta}$ and integrate with respect to time using the post-fault network conditions to obtain

$$\frac{1}{2} M \dot{\delta}_c^2 = P_m \cos \delta_c + P_i \delta_c - P_m \cos \delta_m - P_i \delta_m \tag{3.19}$$

where

δ_c = critical clearing angle.

$\dot{\delta}_c = w_c$ = speed at critical clearing.

P_m = maximum power of post-fault network.

δ_m = unstable equilibrium angle (maximum angle).

The L.H.S. of equation (3.19) represents the kinetic energy (K.E) generated during the fault-on period and the R.H.S. represents the potential energy (P.E) of the post-fault network. If the fault is cleared at the critical clearing time, then

$$K.E = P.E$$

or

$$K.E - P.E = 0 \tag{3.20}$$

and for stability

$$K.E < P.E \tag{3.21}$$

Thus equation (3.19) represents the equilibrium surface for the transient stability or in terms of catastrophe theory it represents the catastrophe manifold, N, which is the gradient of the energy integral function $V(\delta_c)$.

$$N = \nabla_{\delta_c} V(\delta_c) = \frac{1}{2} M \dot{\delta}_c^{\,2} - P_m \cos \delta_c - P_i \delta_c + P_m \cos \delta_m + P_i \delta_m = 0 \tag{3.22}$$

We define also the singularity set, S, as the set of transient stability limits of the power system as

$$\nabla_{\delta_c}^{2} V(\delta_c) = 0 \tag{3.23}$$

Using Taylor series expansion to approximate δ_c and $\dot{\delta}_c$ as a function of time (which has been reported to be a very good approximation for the first swing transient stability analysis [43]) we get

$$\dot{\delta}_c = W_c = \gamma t_c \text{ and } \delta_c = \delta_o + \frac{1}{2}\ \gamma t_c^{\ 2} \tag{3.24}$$

where γ = acceleration at the instant of fault occurrence

$$\gamma = \frac{1}{M}\left[P_i - P_e(t_{o+})\right] \tag{3.25}$$

Let $$X = \frac{1}{2}\gamma\ t_c^{\ 2} \tag{3.26}$$

and $K = p_m\ \delta_m + p_m \cos\ \delta_m$

Substituting for $\dot{\delta}_c$ and δ_c by equations (3.24) and (3.26), replacing the cosine term ($\cos\ \delta_c$) by its expansion, then equation (3.22) becomes

$$N = \nabla_{\delta_c} V(\delta_c) = M\gamma X - P_{ma}\left[1 - \frac{(\delta_o + X)^2}{2!} + \frac{(\delta_o + X)^4}{4!}\ldots\right] - P_i(\delta_o + X) + K = 0 \tag{3.27}$$

Truncating the cosine expansion to the fourth order we get

$$N = M\gamma X - P_{ma} + \frac{(\delta_o + X)^2}{2!}\ P_{ma} - \frac{(\delta_o + X)^4}{4!}\ P_{ma} - P_i(\delta_o + X) + K = 0 \tag{3.28}$$

Since equation (3.28) is a function of clearing time which is usually small, thus the fourth-order truncation would be enough to represent the equilibrium surface N.

$$N = -\frac{P_{ma}}{24} X^4 - \frac{P_{ma}}{6} \delta_o X^3 + \left(\frac{2-\delta_o^{\,2}}{4}\right) P_{ma} X^2 + \left(M\gamma + \delta_o P_{ma} - \frac{P_{ma}}{6} \delta_o^{\,3} - P_i\right)X$$

$$+ \left(\frac{P_{ma}}{2} \delta_o^{\,2} - \frac{P_{ma}}{24} \delta_o^{\,4} - P_{ma} - P_i \delta_o + K\right) = 0$$

Let $A = \frac{P_{ma}}{24}$, $B = \frac{P_{ma}}{6} \delta_o$

$C = \left(\frac{2-\delta_o^{\,2}}{4}\right) P_{ma}$, $D = (M\gamma + \delta_o P_{ma} - \frac{P_{ma}}{6} \delta_o^{\,3} - P_i)$

and $E = \frac{P_{ma}}{2} \delta_o^{\,2} - \frac{P_{ma}}{24} \delta_o^{\,4} - P_{ma} - P_i \delta_o + K)$

$$N = -AX^4 - BX^3 + CX^2 + DX + E = 0 \qquad (3.29)$$

Equation (3.29) is structurally stable and in the form of the swallowtail catastrophe (Appendix A) except we need to eliminate the cubic term.

Let $X = y - \alpha$

$$N = -A(y-\alpha)^4 - B(y-\alpha)^3 + C(y-\alpha)^2 + D(y-\alpha) + E = 0$$

$$= -Ay^4 + (4A\alpha - B)y^3 + (C-6A\alpha^2 + 3B\alpha)y^2$$

$$+ (D - 2c\alpha - 3B\alpha^2 + 4A\alpha^3)y - A\alpha^4 + B\alpha^3 + C\alpha^2 - D\alpha + E = 0$$

then $\alpha = \frac{1}{4}\frac{B}{A}$

Substitute for α and get

$$N = -Ay^4 + \left(C + \frac{3}{8}\frac{B^2}{A}\right)y^2 + \left(D - \frac{1}{2}\frac{CB}{B} - \frac{1}{8}\frac{B^3}{A^2}\right)y$$

$$+ \left(E - \frac{D}{4}\frac{B}{A} + \frac{C}{16}\frac{B^2}{A^2} + \frac{3}{256}\frac{B^4}{A^3}\right) = 0$$

divide by -A

$$N = y^4 - \left(\frac{C}{A} + \frac{3}{8}\frac{B^2}{A^2}\right)y^2 - \left(\frac{D}{A} - \frac{1}{2}\frac{CB}{A^2} - \frac{1}{8}\frac{B^3}{A^3}\right)y$$

$$- \frac{E}{A} + \frac{D}{4}\frac{B^2}{A^2} - \frac{C}{16}\frac{B^2}{A^3} - \frac{3}{256}\frac{B^4}{A^4} = 0$$

Let

$$u = -\left(\frac{C}{A} + \frac{3}{8}\frac{B^2}{A^2}\right)$$

$$\upsilon = -\left(\frac{D}{A} - \frac{1}{2}C\frac{B}{A^2} - \frac{1}{8}\frac{B^3}{A^3}\right) \tag{3.30}$$

and $\quad w = -\frac{E}{A} + \frac{D}{4}\frac{B}{A^2} - \frac{C}{16}\frac{B^2}{A^3} - \frac{3}{256}\frac{B^4}{A^4}$

then N becomes

$$N = y^4 + uy^4 + \upsilon y + w = 0 \tag{3.31}$$

Equation (3.31) is the manifold of the swallowtail catastrophe

$$V(y) = \frac{1}{5} y^5 + \frac{1}{3} uy^3 + \frac{1}{2} \upsilon y^2 + wy \tag{3.32}$$

We need to find the singularity set, S, which is the subset of N that consists of all the degenerate critical points of V. These are the points at which

$$\nabla_y V(y) = M = 0$$

and $$\nabla_y^2 V(y) = 0 \tag{3.33}$$

$$\nabla_y^2 V(y) = 4y^3 + 2uy + \upsilon = 0 \tag{3.34}$$

It is interesting to note that the control variable (U) in this case is constant and negative.

We have $$u = -\left(\frac{C}{A} + \frac{3}{8}\frac{B^2}{A^2}\right)$$

where $$A = \frac{P_{ma}}{24}, \qquad B = \frac{P_{ma}}{6}\delta_o$$

and $$C = P_{ma}\left(\frac{2 - \delta_o^2}{4}\right)$$

thus,

$$u = -\left(12 - 6\delta_o^2 + 6\delta_o^2\right) = -12$$

This result reduces the bifurcation manifold from three dimensions to only two dimensions in υ and W. We can plot the bifurcation set of the

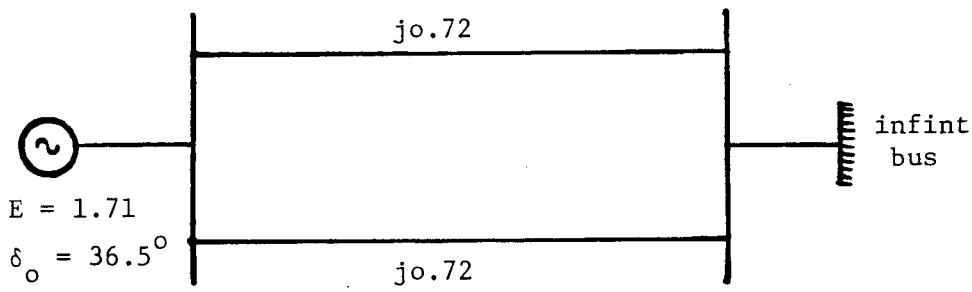

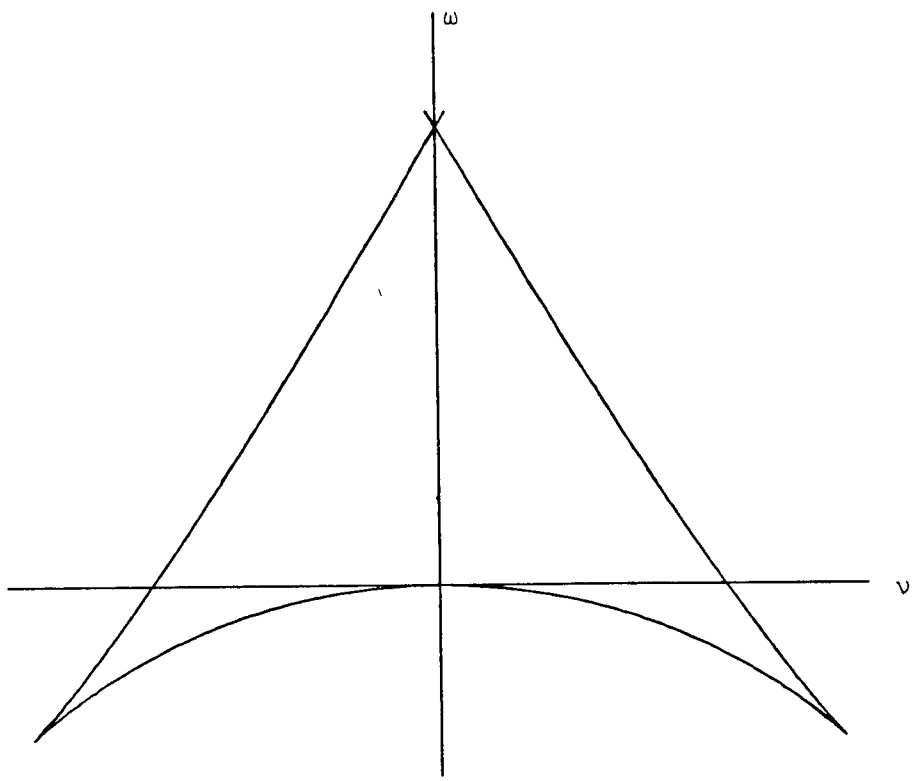

Fig. 3.6 The transient stability limits given by the swallowtail catastrophe for the power system of Fig. 3.5

power system using equations (3.31) and (3.34) (see Appendix A for details). The boundaries of the bifurcation set of Fig. 3.6 represent the degenerate transient stability limits of the power system.

It should be noted that for a generator the control variables υ and W are positive and for a motor they are negative.

The region of transient stability of the power system has to be inside the positive side of Fig. 3.6 and the following conditions have to be met:

Since $X = \frac{1}{2} \gamma t_c^{\,2} > 0$

where t_c is the critical clearing time

and $X = y - \alpha$

then $y - \alpha > 0$ (3.35)

or $y > \alpha$ (3.36)

we have $\alpha = \frac{1}{4} \frac{B}{A} = \delta_0$

hence, $y > \delta_o$ (3.37)

For the stability region bounded by equation (3.31), (3.34) and the constraints $y > \delta_o$ equation (3.31) has four critical points, two maxima and two minima. The critical clearing time is represented by the first positive critical point of $y > \delta_o$.

3.4.2 Results

The transient stability region of the system shown in Fig. 3.5 is defined by equations (3.31), (3.34) and (3.37). Changing the fault

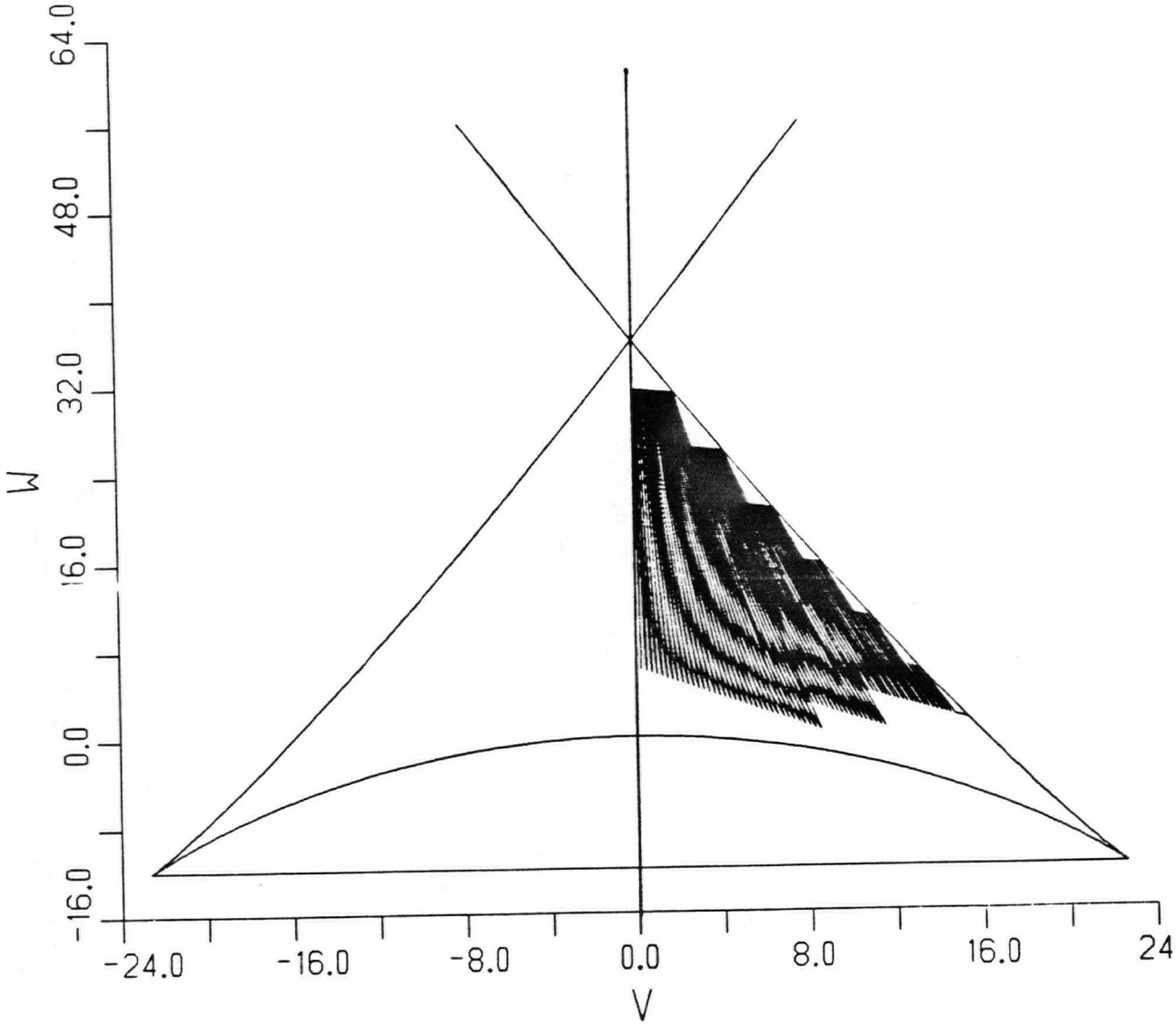

Fig. 3.7 Transient stability region for all possible fault locations and loading conditions.

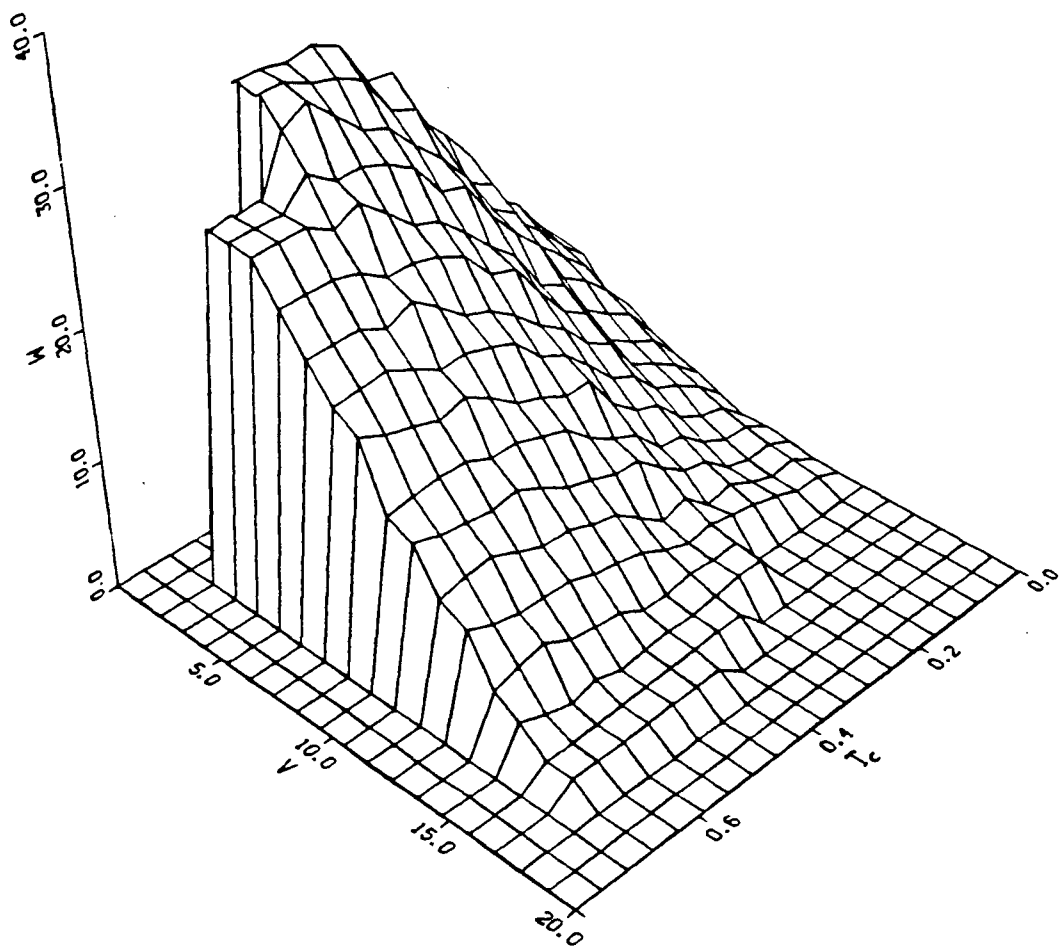

Fig. 3.8 The transient stability region in terms of stability limits and critical clearing times.

location, and for each fault the loading condition (P_i) is changed from .1 to 1.2 pu. The shaded areas of Figure 3.7 represent the region of transient stability for all possible fault locations and loading conditions. A more comprehensive view of the stability region can be visualized by plotting the region in three dimensions where y is the singularity ($y > \alpha > 0$) representing the critical clearing time

$$T_c = \sqrt{\frac{2(y - \alpha)}{\gamma}} \tag{3.38}$$

Figure 3.8 shows the transient stability region in three dimensions υ, W and t_c. The third dimension t_c is calculated from the catastrophe manifold and plotted over the shaded arc of Figure 3.7. This qualitative view of the stability region cannot be achieved by other direct methods of transient stability, because these other methods use state variables to define the region of stability which depends on operating conditions, fault locations and time. But by using the catastrophe theory, the stability region is defined by two control variables, υ and W, only and includes all possible fault locations and loading conditions. The control variables υ and W can be written as a function of operating conditions and fault locations by using equations (3.30) and substituting for A, B, C, D and E to get

$$\upsilon = \frac{24}{P_{ma}}\left(M\gamma + P_i\right) + 8\left(\delta_o^{\,3} - \delta_o\right) \tag{3.39}$$

$$w = 24\left(\delta_o^{\,2} + \frac{2\,P_i}{P_{ma}}\,\delta_o + \frac{M\gamma}{P_{ma}}\,\delta_o - \frac{K}{P_{ma}} + 1\right)$$

In fact the region of stability defined by υ, W and T_c is fixed and

the machine is stable when it is operating inside the region. These results are identical to that of the time solution.

3.4.3 Equivalent Two Machine Power System [44]

Consider the power system of Fig. 3.9 which consists of three power plants A, B and C. A three-phase fault is applied on line 5-6 near bus 6. It is found that machines B and C are swinging coherently against machine A. In this case B and C can be combined together to form a large machine B+C, and the system can be reduced to a two-machine power system. The swing equation of machine A against the equivalent machine (B+C) can be written in the form

$$M \frac{d^2\delta}{dt^2} = P_i - \left(P_c + P_m \sin(\delta - \alpha)\right) \tag{3.40}$$

The same procedure of the previous section can be applied to calculate the equilibrium surface from the energy balance equation [44]. Similar transient stability regions of Figs. 3.7 and 3.8 are also obtained in this case.

The critical clearing time calculated from the catastrophe manifold equation for this case is .348 seconds and that calculated by time solution is .35 seconds. The method shows very close agreement with the numerical integration method. When either the fault location or the loading conditions are changed, the machines may respond to the disturbance in different coherency. This dictates different equivalence calculations for different fault locations and loading conditions. Therefore, a faster method

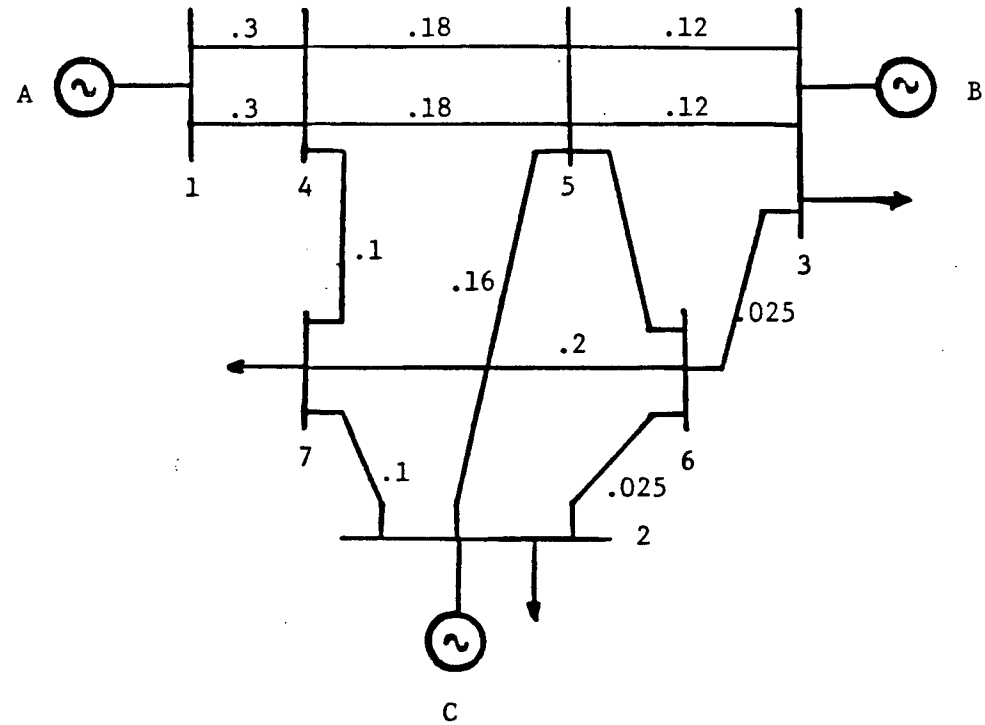

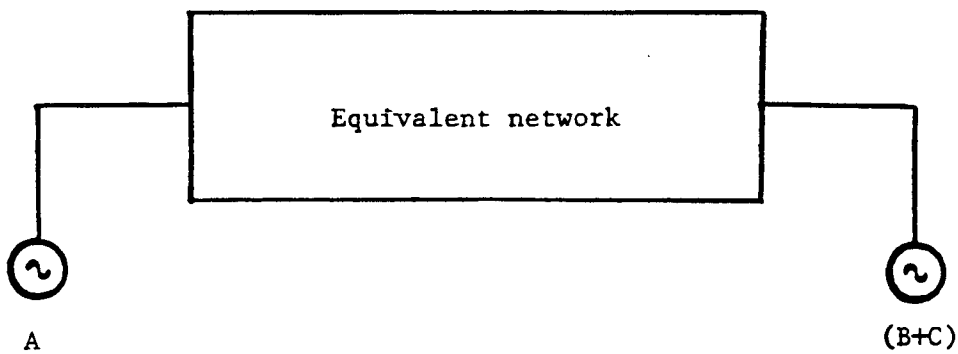

Fig. 3.9 The equivalent two machine power system

is needed to assess the response of the system to different contingencies. This problem will be addressed in the next chapter.

3.5 Summary

The preliminary applications of catastrophe theory to the transient stability problems of simple power systems have shown three attractive advantages:

1. The transient stability region is well defined in terms of the control variables (system parameters) regardless of the state variables. The stability regions are bounded by the stability limits which provide very good insight to the security boundaries. Adequate stability controls can be also designed and applied according to the transient stability limits.

2. Extremely few computations are needed to define the stability region, each transient case can be easily calculated in terms of the system parameters without repetitive iterations.

3. The method is a serious candidate to be used for on-line assessment of transient stability, security analysis and for the application of transient stability controls such as dynamic breaking, fast valving, etc.

CHAPTER 4

TRANSIENT STABILITY REGIONS OF MULTIMACHINE POWER SYSTEMS

4.1 Introduction

The transient stability problem of multi-machine power systems is much more complicated than the simple power systems analyzed in Chapter 3. The analysis in this case involves every machine in the power system without equivalencing any machine. The swing equation of each machine depends upon the movements of the other machines coupled to it.

There have been some major difficulties associated with the application of direct methods to the transient stability problem of multi-machine power systems. Although noticeable progress has been reported in dealing with these difficulties [45-48], the challenge of fast on-line transient stability assessment is still not overcome. These challenging problems are [49]:

i. Power system model: applications of direct methods are limited to the classical model of power systems. In this model, generators are represented by constant voltage magnitude behind transient reactance, loads are represented by constant impedances, transfer conductances are usually neglected or approximated, although they are significant network elements [50].

ii. Although fast exciters respond within the first swing period (.1 second), none of the existing direct methods consider excitation effects.

iii. In practice, power engineers are usually not interested in the critical clearing time (which is the main goal of direct methods) but rather in the amount of power that can be delivered without risking system security for specified clearing times.

iv. Network reduction and calculations of stable and unstable equilibrium points for large power systems are time consuming. For unstable equilibrium points, existing algorithms cannot always be relied upon to converge to the right solution.

Two methods will be introduced in this chapter to provide an energy function suitable for the application of catastrophe theory, namely the critical machines dynamic equivalent method and a method using Taylor series expansion of the accelerating power during the transient period. Both methods need the identification of the critical machines for each disturbance considerd.

The transient stability regions are then defined in terms of the system parameters which enable power engineers to define the security regions and apply preventative control methods.

The difficulties mentioned above will be dealt with in the proposed methods. Transfer conductance will be fully included; damping and excitation response will be also included and discussed in Chapter 5.

4.2 Dynamic Equivalent of the Critical Machines

The equation of motion of machine i in a multi-machine power system, using classical model representation is given by

$$\dot{\delta}_i = \omega_i \qquad i = 1, \ldots n$$

$$M_i \ddot{\delta}_i = P_{mi} - P_{ei} \tag{4.1}$$

where $$P_{ei} = \sum_{j=1}^{n} E_i E_j (g_{ij} \cos \delta_{ij} + b_{ij} \sin \delta_{ij}) \tag{4.2}$$

= electrical power output of machines

P_{mi} = mechanical power input

M_i = intertia constant

δ_i = rotor angle

ω_i = speed deviation

E_i = internal voltage

g_{ij} = transfer conductance

b_{ij} = transfer susceptance

$\delta_{ij} = \delta_i - \delta_j$

When a fault occurs in a large power system only a few machines actively response to the fault and tend to lose synchronism. These machines are known as the critical machines [45,47]. Therefore, it is enough to study the behaviour of the critical machines with respect to the rest of the power system in order to evaluate the transient stability of the system for a specific fault.

Consider that machine k is the critical machine(s) for a specific disturbance. This machine is considered to be oscillating against the rest of the power system which is not significantly affected by the disturbance and will be considered moving as one machine

Let $$M_0 = \sum_{i \neq k}^{n} M_i \tag{4.3}$$

$$\delta_0 = \frac{1}{M_0} \sum_{i \neq k}^{n} M_i \delta_i \tag{4.4}$$

M_0 and δ_0 are, respectively, the inertia constant and the angle of the center of angle of the power system excluding the critical machine.

Let $\Theta_k = \delta_k - \delta_0$

$$= \delta_k - \frac{1}{M_0} \sum_{i \neq k}^{n} (M_i \delta_i)$$

also

$$\dot{\Theta}_k = \dot{\delta}_k - \frac{1}{M_0} \sum_{i \neq k}^{n} M_i \dot{\delta}_i$$

$$\ddot{\Theta}_k = \ddot{\delta}_k - \frac{1}{M_0} \sum_{i \neq k}^{n} (M_i \ddot{\delta}_i) \tag{4.5}$$

We substitute equation (4.1) into (4.5) to obtain the swing equation of machine k with respect to the center of angle (COA).

$$\ddot{\Theta}_k = \frac{P_{mk} - P_{ek}}{M_k} - \frac{1}{M_0} \sum_{i \neq k}^{n} (P_{mi} - P_{ei}) \tag{4.6}$$

$$M_k \ddot{\Theta}_k = P_{mk} - P_{ek} - \frac{M_k}{M_0} \sum_{i \neq k}^{n} (P_{mi} - P_{ei}) \tag{4.7}$$

Substituting for P_{ek} and P_{ei} from equation (4.2) and separating Θ_k from the rest of the system we get the swing equation of the critical machine k against the rest of the power system. This is explained in the following steps:

First we let $D_{ij} = E_i E_j g_{ij}$

and $C_{ij} = E_i E_j b_{ij}$

Equation (4.7) becomes

$$M_k \ddot{\Theta}_k = P_{mk} - D_{kk} - \sum_{i \neq k}^{n} (D_{ij} \cos \Theta_{kj} + C_{kj} \sin \Theta_{kj})$$

$$- \frac{M_k}{M_0} \sum_{i \neq k}^{n} \left(P_{mi} - \sum_{j=1}^{n} (D_{ij} \cos \Theta_{ij} + C_{ij} \sin \Theta_{ij})\right)$$

Separate the term B_{ik} from the last term and obtain

$$M_k \ddot{\Theta}_k = P_{mk} - D_{kk} - \frac{M_k}{M_0} \sum_{i \neq k}^{n} \left(P_{mi} - \sum_{j \neq k}^{n} (D_{ij} \cos \Theta_{ij} + C_{ij} \sin \Theta_{ij})\right)$$

$$+ \frac{M_k}{M_0} \sum_{i \neq k}^{n} (D_{ik} \cos \Theta_{ik} + C_{ik} \sin \Theta_{ik})$$

$$- \sum_{j \neq k}^{n} (D_{kj} \cos \Theta_{kj} + C_{kj} \sin \Theta_{kj})$$

Let $P_k = P_{mk} - D_{kk} - \frac{M_k}{M_0} \sum_{i \neq k}^{n} \left(P_{mi} - \sum_{j \neq k}^{n} (D_{ij} \cos \Theta_{ij} + C_{ij} \sin \Theta_{ij})\right)$ (4.8)

then

$$M_k \ddot{\Theta}_k = P_k - [b \sin \Theta_k - a \cos \Theta_k] \tag{4.9}$$

where

$$a = \frac{M_k}{M_0} \sum_{i \neq k}^{n} (D_{ik} \cos \Theta_i + C_{ik} \sin \Theta_i) - \sum_{j \neq k}^{n} (C_{ij} \sin \Theta_j - D_{kj} \cos \Theta_j)$$

$$b = \sum_{j \neq k}^{n} (D_{kj} \sin \Theta_j + C_{ij} \cos \Theta_j) - \frac{M_k}{M_0} \sum_{i \neq k}^{n} (D_{ik} \sin \Theta_i - C_{ik} \cos \Theta_i)$$

Equation (4.9) can be written in a more convenient form

$$M_k \ddot{\delta}_k = P_k - T_k \sin (\Theta_k - \alpha_k) \tag{4.10}$$

where

$$\alpha_k = \tan^{-1} \frac{a}{b}$$

and $\quad T_k = (a^2 + b^2)^{1/2}$

Equation (4.10) is a simple form representing the motion of the critical machine for a certain disturbance. Since we assumed that the rest of the system is not responding to the disturbance, it is reasonable to use the pre-disturbance angles Θ_o to calculate the parameters P_k, T_k and α_k.

The stable and unstable equilibrium points of equation (4.10) can be easily computed by solving equation (4.11) for Θ_k^s

$$P_k - T_k \sin (\Theta_k^s - \alpha_k) = 0 \tag{4.11}$$

and the unstable equilibrium point (UEP) is

$$\Theta_k^u = \Pi - \Theta_k^s \tag{4.12}$$

We note here that we have two sets of the parameters P_k, T_n and α_k; one set for the fault-on network and another for the post-fault network.

4.2.1 The Transient Stability Region

During the transient period, an exchange of energy takes place between the rotor of the critical machine and the post-fault network. The kinetic energy generated by the accelerating power during the fault-on period must be fully absorbed by the post-fault network in order to maintain stability.

Multiplying equation (4.10) by $\dot{\Theta}_k$ and integrating between Θ_k^C and Θ_k^0 with respect to time for the fault-on network parameters we obtain the kinetic energy generated by the fault

$$K.E = \frac{1}{2} M_k \dot{\Theta}_k^{C\,2} = P_k^f (\Theta_k^C - \Theta_k^0) - T_k^f [\cos(\Theta_k^0 - \alpha_k^f) - \cos (\Theta_k^C - \alpha_k^f)] \tag{4.13}$$

where P_k^f, T_k^f and α_k^f are the system parameters for fault-on network and Θ_k^C is the clearing angle.

The potential energy of the post-fault network is derived in the same manner by integrating equation (4.10) between Θ_k^C and Θ_k^u using the post-fault network parameters, we obtain

$$-\frac{1}{2} M_k \dot{\Theta}_k^{C\,2} = P_k^f (\Theta_k^u - \Theta_k^C) - T_k^p[\cos(\Theta_k^C - \alpha_k^p) - \cos(\Theta_k^u - \alpha_k^p)] \tag{4.14}$$

Note that the speed deviation at the unstable equilibrium point Θ_k^u is zero ($\dot{\Theta}_k^u = 0$).

Equation (4.14) represents the energy function of the critical machine during the transient period. The L.H.S. represents the fault kinetic energy and the R.H.S. represents the potential energy for the post-fault network. The energy balance equation for critical clearing becomes:

$$\frac{1}{2} M \dot{\Theta}_k^{C^2} - P_k^p \Theta_k^C - T_k^P \cos(\Theta_k^C - \alpha_k^P) + k^u = 0 \quad .. \tag{4.15}$$

where $k^u = P_k^p \Theta_k^u + T_k^p \cos(\Theta_k^u - \alpha_k^p)$

again we represent Θ_k^C by Taylor series expansion

$$\Theta_k^C = \Theta_k^0 + \frac{1}{2} \gamma_k t_C^2$$

and

$$\dot{\Theta}_k^C = \gamma_k t_C$$

where $\gamma_k = \frac{1}{M_k} [P_k - P_{ek}^t(t_{0+}]$

Let $x = \frac{1}{2} \gamma_k t_C^2$

By replacing $\cos(\Theta_k^C - \alpha_k^p)$ in equation (4.15) with the cosine series expansion up to the fourth order, we obtain

$$M \gamma_k x - P_k^p(\Theta_k^0 + x) - T_k^p[1 - \frac{(x + \Theta_2^0 - \alpha_k^p)^2}{2!} + \frac{(x + \Theta_x^0 - \alpha_k^p)^4}{4!} + k^u = 0$$

Let $\beta = \Theta_k^0 - \alpha_k^p$

then we get the catastrophe manifold equation

$$- \frac{T_k^p x^4}{24} + \frac{T_k^p}{6} \beta x^3 + \frac{T_k^p}{2} (1 - \frac{B^2}{2})x^2 + (M\gamma_k - P_k^p)^2 + T_k^p \beta - \frac{T_k}{6} \beta^3)x$$

$$+ (k^u - T_k^p - P_k^p \Theta_k^0 + \frac{T_k^p}{2} \beta^2 - \frac{T_k}{24} \beta^4) = 0 \qquad (4.16)$$

Multiply equation (4.16) by $- \frac{24}{T_f^p}$ to give:

$$X^4 - 4\beta X^3 - 12(1 - \frac{B^2}{2})X^2 - \frac{24}{T_k^p} (M\gamma_k - P_k^p + T_k^p \beta - \frac{T_k}{6} \beta^3)X$$

$$- \frac{24}{T_k^p} (k^u - T_k^p - P_k^p \Theta_k^0 + \frac{T_k^p}{2} \beta^2 - \frac{T_k^p}{24} \beta^4) = 0 \qquad (4.17)$$

We need to eliminate the third order term in order to have equation (4.17) in the swallowtail catastrophe manifold form

Let $A_3 = - 4\beta$

$$A_2 = - 12(1 - \frac{\beta^2}{2})$$

$$A_1 = - \frac{24}{T_k^p} (M\gamma_k - P_k^p + T_k^p \beta - \frac{T_k^p}{6} \beta^3)$$

$$A_0 = -\frac{24}{T_k^p}\left(k^u - T_k^p - P_k^p\,\Theta_k^p + \frac{T_k^p}{2}B^2 - \frac{T_k^p}{24}B^4\right)$$

and $$x = y - \mu \tag{4.18}$$

$$\mu = \frac{A^3}{4} \tag{4.19}$$

We obtain the swallowtail catastrophe manifold

$$y^4 + uy^2 + \upsilon y + w = 0 \tag{4.20}$$

where $u = (A_2 - \frac{3}{8}A_3{}^2)$

$$\upsilon = (A_1 - \frac{A_2A_3}{2} + \frac{A_3{}^3}{8})$$

$$w = (A_0 - \frac{A_1A_3}{4} + \frac{A_2A_3{}^2}{16} - \frac{3}{256}A_3{}^4)$$

The bifurcation set B can then be defined by

$$4y^3 + 2uy + \upsilon = 0 \ldots \tag{4.21}$$

The transient stability region is formed in the shape of the swallowtail bifurcation set (see Appendix A) bounded by the transient stability limits. The region is defined in terms of the system parameters which can be easily calculated.

In summary, the procedure of calculating the transient stability regions for multi-machine power systems using the critical-machines dynamic-equivalent method is outlined in the following steps:

1. Define the critical machine(s) for the fault considered.
2. Calculate the parameters P_k, T_k and α_k to form the dynamic equivalent of the critical machine(s).
3. Calculate the catastrophe manifold parameters u, υ and w from which the critical clearing time and the degree of stability are determined.

It is important to note that the transient stability region using this method is the same shape regardless of fault location and loading condition. This makes the method a good candidate for on-line assessment of the transient stability and the degree of security of power systems.

4.3 Taylor Expansion of the Accelerating Power

The chaotic nature of the swing equations of multi-machine power systems is a major difficulty in solving the transient problem and in trying to include more detailed system models in direct methods.

Recalling the swing equation of machine i in an n-machine power system from section (4.2):

$$M_i \ddot{\delta}_i = P_{mi} - \sum_{j=1}^{n} (D_{ij} \cos \delta_{ij} + C_{ij} \sin \delta_{ij})$$

$$= P_{ai} \qquad (i = 1, \ldots n) \qquad (4.22)$$

where P_{ai} is the accelerating power of machine i.

In the conventional time solution, equations (4.22) are solved by numerical integration for the transient period ($t_0 \rightarrow t_u$), from the instant

of fault occurrence to the unstable equilibrium point. It is already known that each post-fault network has a fixed energy-absorbing capacity, called the critical energy [51]. The critical energy can be calculated off-line for any post-fault condition. This energy is the numerical integration of the post-fault accelerating power from the stable equilibrium point to the unstable equilibrium point.

We suggest using Taylor series expansion to find the energy function as a function of time by expanding the accelerating power equation around the instant of fault occurrence at t=0. This provides the advantage of eliminating the calculations of the stabel and unstable equilibrium points on-line and simplifies the procedure of defining the critical machines.

The energy function of machine i in a multi-mchine power system during the transient period is given by:

$$V_i = \int_0^{t_c} P_{ai}^f(t)\, dt + \int_{t_s}^{t_c} P_{ai}^p(t)\, dt + \int_{t_s}^{t_u} P_{ai}^p(t) dt \qquad (4.23)$$

where P_{ai}^f is fault-on accelerating power.

$P_{ai}^p(t)$ is post-fault accelerating power.

t_c is the clearing time.

t_s, t_u is the times at SEP and UEP.

The first two terms of the R.H.S. of equation (4.23) are the kinetic energy generated during fault-on, and the third term is the critical energy of the post-fault network. The portion of the kinetic energy needed to move

the rotor from δ_0 to δ_s of the post-fault network does not contribute to the instability [51]. Therefore, it should be subtracted from the energy function in order to write the energy balance equation; this portion is

$$\int_0^{t_s} P_{ai}^{p}(t)\, dt \tag{4.24}$$

Subtracting (4.24) from (4.23), and assuming that machine i is the critical machine and the fault is cleared at critical clearing, we obtain the energy balance equation,

$$V_i = \int_0^{t_c} \left(P_a^f(t) - P_a^p(t)\right)dt + \int_{t_s}^{t_u} P_a^p(t)\, dt = 0 \tag{4.25}$$

Equation (4.25) is evaluated by replacing $P_a^f(t)$ and $P_a^p(t)$ with their Taylor series expressions, in the form:

$$P_a(t) = P_a^{(0)} + \frac{1}{1!} P_a^{(1)} t + \frac{1}{2!} P_a^{(2)} t^2 + \tag{4.26}$$

where $$P_a^{(m)} = \left.\frac{d^m P_a}{dt^m}\right|_{t=0} \tag{4.27}$$

and the accelerating power of machine i

$$P_{ai} = P_{mi} - \sum_{i=1}^{n} (D_{ij} \cos \delta_{ij} + C_{ij} \sin \delta_{ij})$$

We note that at $t=0$

$$\omega_i = 0$$

and $\delta_i = \delta_i^0$ (initial operating condition)

Therefore $P_{ai}^{(0)} = P_{mi} - P_{ei}$ $(t = 0)$

$$= P_{mi} - \sum_{j=1}^{n} (D_{ij} \cos \delta_{ij}^0 + C_{ij} \sin \delta_{ij}^0) \tag{4.28}$$

$$P_{ai}^{(1)} = \frac{d}{dt} (P_{ai})\Big|_{t=0} = \sum_{j=1}^{n} (D_{ij} \sin \delta_{ij}^0 - C_{ij} \cos \delta_{ij}^0)\dot{\delta}_{ij}$$

Since $\dot{\delta}_{ij}\Big|_{t=0} = 0$

Therefore $P_{ai}^{(1)} = 0$ (4.29)

$$P_{ai}^{(2)} = \frac{d}{dt} (P_{ai}^{(1)})\Big|_{t=0} = \sum_{j=1}^{n} (D_{ij} \cos \delta_{ij}^0 + C_{ij} \sin \delta_{ij}^0)\dot{\delta}_{ij}^2$$

$$+ \sum_{j=1}^{n} (D_{ij} \sin \delta_{ij}^0 - C_{ij} \cos \delta_{ij}^0)\ddot{\delta}_{ij}$$

Since $\dot{\delta}_{ij} = 0$

$$P_{ai}^{(2)} = \sum_{j=1}^{n} (D_{ij} \sin \delta_{ij}^0 - C_{ij} \cos \delta_{ij}^0 \ddot{\delta}_{ij}^0 \tag{4.30}$$

where $\ddot{\delta}_{ij}^0 = P_{ai}^{(0)}/M_i$ (initial acceleration)

The derivations of the rest of the Taylor series coefficients are given in Appendix C. It is found that all odd order coefficients are zeros;

this reduces the number of Taylor series coefficients to one half. Therefore,

$$P_{ai} = P_a^{(0)} + \frac{1}{2!} P_a^{(2)} t^2 + \frac{1}{4!} P_a^{(4)} t^4 + \ldots \tag{4.31}$$

The accelerating power coefficients have to be calculated for the system during the fault and for the post fault condition.

Usually in large power systems the critical clearing time is very small (typically < .5 second). For this period we will use up to the sixth order of the accelerating power expansion for both fault-on and post-fault conditions. Thus equation (4.25) becomes;

$$V_i = \int_0^{t_c} \left((P_a^{(0)^f} - P_a^{(0)^p}) + \left(\frac{P_a^{(2)^f} - P_a^{(2)^p}}{2!}\right)t^2 + \left(\frac{P_a^{(4)^f} - P_a^{(4)^p}}{4!}\right) t^4 + \left(\frac{P_a^{(6)^f} - P_a^{(6)^p}}{6!}\right) t^6\right)dt + \int_{t_s}^{t_u} P_a^p(t)\, dt = 0 \tag{4.32}$$

The last term is the critical energy of each specific post-fault condition. The critical energy is evaluated off-line for each post-fault condition by the trapezoidal rule as follows

$$V_{cr} = \int_{t_s}^{t_u} P_a^p(t)\, dt$$

$$V_{cr}(1+1) = V_{cr}(k) + \frac{1}{2} (P_a(t)(k+1) - P_a(t)(k)) - (t(k+1) - t(k))$$

4.3.1 Transient Stability Regions Using Taylor Expansion

The Taylor series expansion of the accelerating power provides flexible choice over the seven elementary catastrophes of Table (3.1). The choice of a specific catastrophe type depends on the highest order of the Taylor series that will give the best required results. It is needless to add that the lower order catastrophes are easier to visualize.

We start with the resultant Taylor series expansion of equation (4.32).

$$P_a(t) = P_a(0) + \frac{P_a^{(2)}}{2!} t^2 + \frac{P_a^{(4)}}{4!} t^4 + \ldots$$

The rotor angle can also be represented by the form

$$\delta_i = \delta_{0i} + \frac{1}{2} \gamma_i t^2$$

which provides good agreement with the time solution for $t \leq .5$ second [52].

We let $x = \delta_i - \delta_{0i} = \frac{1}{2} \gamma_i t^2$

substitute for t^2 in the accelerating power series

$$P_a(x) = P_a^{(0)} + \frac{P_a^{(2)}}{\gamma_i} X + \frac{P_a^{(4)}}{6\gamma_i^2} X^2 + \ldots \tag{4.33}$$

The energy balance equation can be evaluated with respect to the angle advances x

$$V_i = \int_0^{x_c} P_a(x)dx + V_{cr} = 0$$

$$= P_a^{(0)}x + \frac{P_a^{(3)}}{2\gamma_i} x^2 + \frac{P_a^{(4)} x^3}{18\gamma_i^2} + \ldots + V_{cr} = 0 \tag{4.34}$$

The choice of the determinant order decides the catastrophe manifold type as follows

X^2 = fold

X^3 = cusp

X^4 = swallowtail

X^5 = butterfly

Here we consider the cusp catastrophe manifold given in Appendix B.

The cusp catastrophe manifold from equation (4.24) is given by

$$V = \frac{P_a^{(4)}}{18\gamma^2} X^3 + \frac{P_a^{(2)}}{2\gamma_i} X^2 + P_a^{(0)}X + V_{cr} = 0$$

$$= X^3 + \frac{9\gamma_i P_a^{(2)}}{P_a^{(4)}} X^2 + \frac{18\ \gamma_i^2 P_a^{(0)}}{P_a^{(4)}} X + \frac{18\ \gamma_i^2}{P_a^{(4)}} V_{cr} = 0 \tag{4.35}$$

$$= X^3 + A_2X^2 + A_1X + A_0 = 0 \tag{4.36}$$

In order to put equation (4.36) in the standard cusp manifold we need to eliminate the second order term (X^2).

We let $X = y - \beta$

$$\beta = \frac{A_2}{3}$$

We get

$$y^3 + (A_1 - \frac{A_2^2}{3})\, y + (A_0 + \frac{2A_2^2}{27} - \frac{A_1 A_2}{3}) = 0 \tag{4.37}$$

or

$$y^3 + u\, y + \upsilon = 0 \tag{4.38}$$

where

$$u = (A_1 - \frac{A_2^2}{3})$$

$$\upsilon = (A_0 + \frac{2A_2^3}{27} - \frac{A_1 A_2}{3})$$

Equation (4.38) is in the standard form of the cusp catastrophe.

The bifurcation set is defined by equation (4.38) and the set of degenerate critical points.

$$3y^2 + u = 0 \tag{4.29}$$

The bifurcation set given in Appendix B consists of all stable points in terms of the system parameters u and υ.

4.4 Identification of the Critical Machines

Both methods presented in Sections (4.2) and (4.3) rely on the accurate identification of the critical machines for a specified disturbance.

Correct identification has been achieved by calculating the unstable equilibrium points for all machines in the power systems; the machine which

has the highest unstable equilibrium point is identified as the critical machine [47]. Although this method provides correct identification, its main drawback is the calculation of the UEP's, which is time consuming, and in some cases, wrong answers may be obtained [48].

Another method is to use the acceleration at the instant of fault occurrence as a first identification and then calculate the critical clearing time for each machine. The machine with the lowest critical clearing time is the critical machine [45].

For small and medium size power systems, the calculation of UEP's is not difficult and usually the correct answer is achieved in a reasonable time, but for large power systems the right answer is not guaranteed.

In this thesis, the critical machines are identified as follows:

i. Calculate the initial acceleration for each machine as follows

$$\gamma_i = \frac{1}{M_i} [P_{mi} - P_{ei} (t_o^+)]$$

where $P_{ei}(t_0^+)$ is the electrical power output during fault at the instant of fault occurrence.

ii. The machines which have high and positive initial accelerations are injecting kinetic energy to the system; therefore, they all contribute to the system instability. These machines are combined to form a critical group.

iii. The critical energies of the critical machines are also added together to form the global energy-absorbing capacity of the critical group.

In most cases critical machines can be identified easily by the first acceleration, especially when the fault is close to one of the generator terminals. The procedure of combining a group of critical machines has to be carried out only when a fault occurs at non-generator buses or far from generator buses.

4.5 Numerical Examples

In this section two examples are presented to demonstrate the validity and advantages of the application of catastrophe theory to transient stability assessment of power systems. Transient stability regions in terms of the system parameters are given for each example. Three and seven machine power systems are used, three-phase short circuits are considered at different locations and a comparison between the presented methods and the step-by-step time solution is given for each example.

Each short-circuit case considered is evaluated by the following steps.

i. Identify the critical machine or machines as explained in Section 4.4.

ii. Dynamic equivalent method; calculate the dynamic equivalent parameters of equation (4.10) for the critical machine(s) (as given in Section 4.2). The bifurcation set parameters and critical clearing time are then calculated.

iii. Taylor series method; calculate the Taylor series coefficients of the accelerating power for the critical machine (as given in Section 4.3). The bifurcation set parameters and the critical clearing time are then calculated and the case is located on the transient stability region.

4.5.1 The Three-Machine System

This system with nine buses, three machines and three loads, is widely referred to in the literature as the Western Systems Coordinating Council (WSCC) test system.

A single-line diagram of the system is shown in Fig. 4.1. Transmission line parameters and loads are given in per unit on a 100-MVA base in Table 4.1. Generator data and initial operating conditions are given in Table 4.2.

	Bus No.	Admittance (pu) G	B
Generators			
1	1-4	0	- 8.446
2	2-7	0	- 5.485
3	3-9	0	- 4.168
Transmission Lines	4-5	1.365	-11.604
	4-6	1.942	-10.511
	5-7	1.188	- 5.975
	6-9	1.282	- 5.588
	7-8	1.617	-13.698
	8-9	1.155	- 9.784
Shunt Admittances			
Load A	5-0	1.261	- 0.263
Load B	6-0	0.878	- 0.035
Loda C	8-0	0.969	- 0.160
	4-0		0.167
	7-0		0.227
	9-0		0.283

Table 4.1 Network parameters of the three-machine system

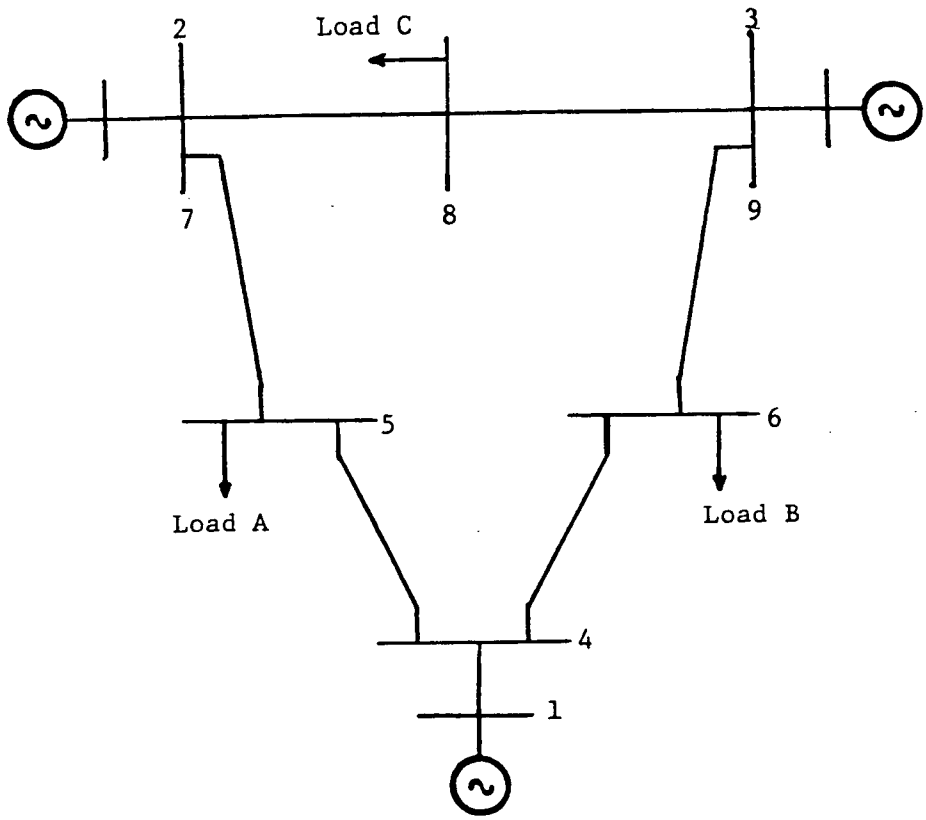

Fig. 4.1 The three-machine power systems

Generator data			Initial Conditions		
Gen. No.	H (MW/MVA)	X'_d (pu)	P_{mo} (pu)	E (pu)	(degree)
1	23.64	.0608	2.269	1.096	6.95
2	6.40	.1198	1.6	1.102	13.49
3	3.01	.1813	1.0	1.024	8.21

Table 4.2 Generator data and initial conditions of the three-machine system

Three-phase short circuits are considered at different locations. The transient stability is evaluated for each fault by the step-by-step time solution, dynamic equivalent and Taylor series methods. A comparison between the three methods is given in Table 4.3 in terms of the critical clearing time. Both methods show very good agreement with the time solution.

Fig. 4.2 shows the accuracy of the Taylor series method using terms up to the second order term for the angle during the fault-on period. Fig. 4.3 shows a comparison between the Taylor series approximation of the accelerating power and the time solution for different fault locations during the transient period.

The transient stability region using the dynamic equivalent method is shown in Fig. 4.4. All stable cases are shown inside the region in terms of the system parameters. Fig. 4.5 show the transient stability region using the Taylor series method. Stable points are marked inside the region.

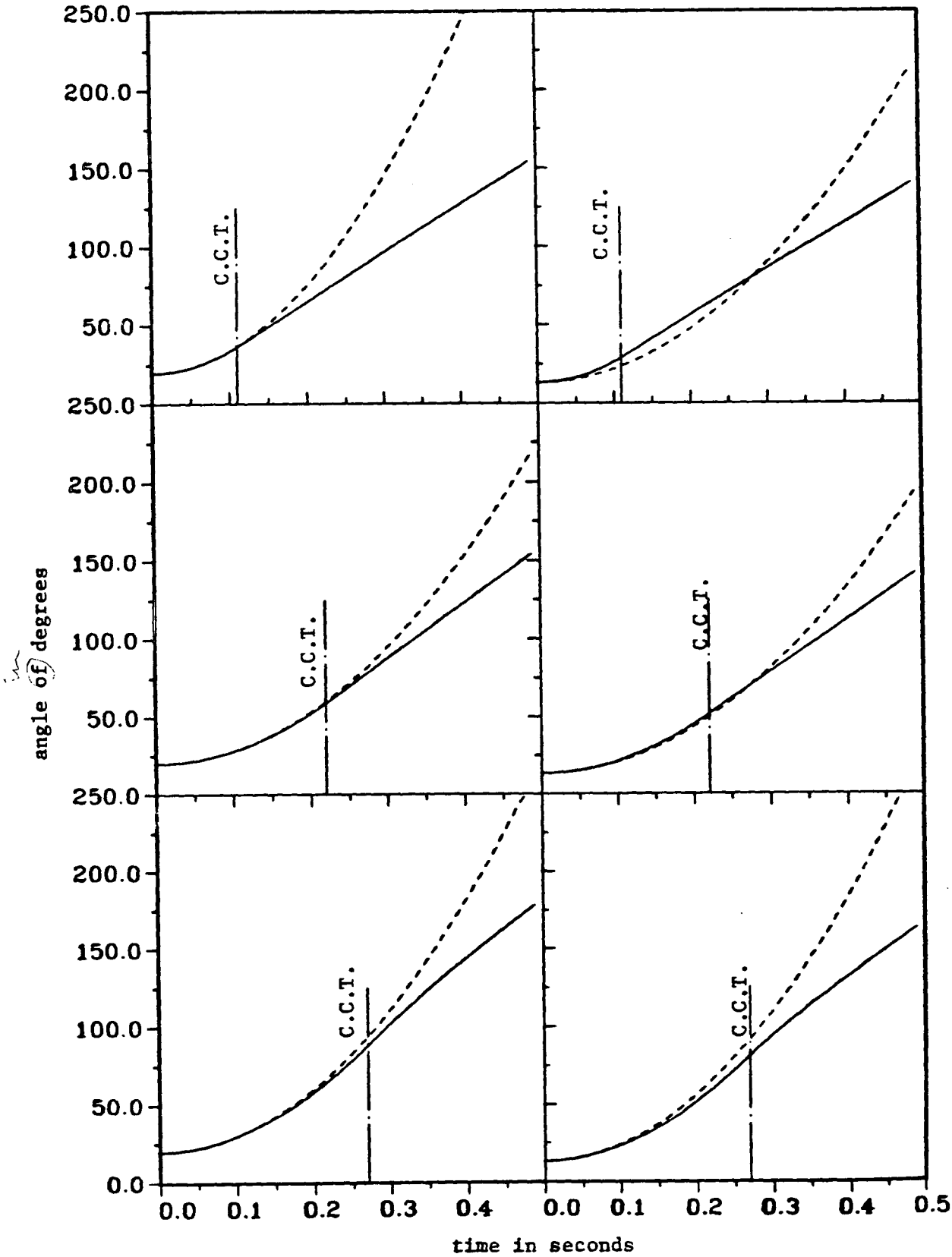

Fig. 4.2 Accuracy of Taylor series during the fault-on period using only the second order term.
—— time solution
--- Taylor series method
C.C.T. critical clearing time

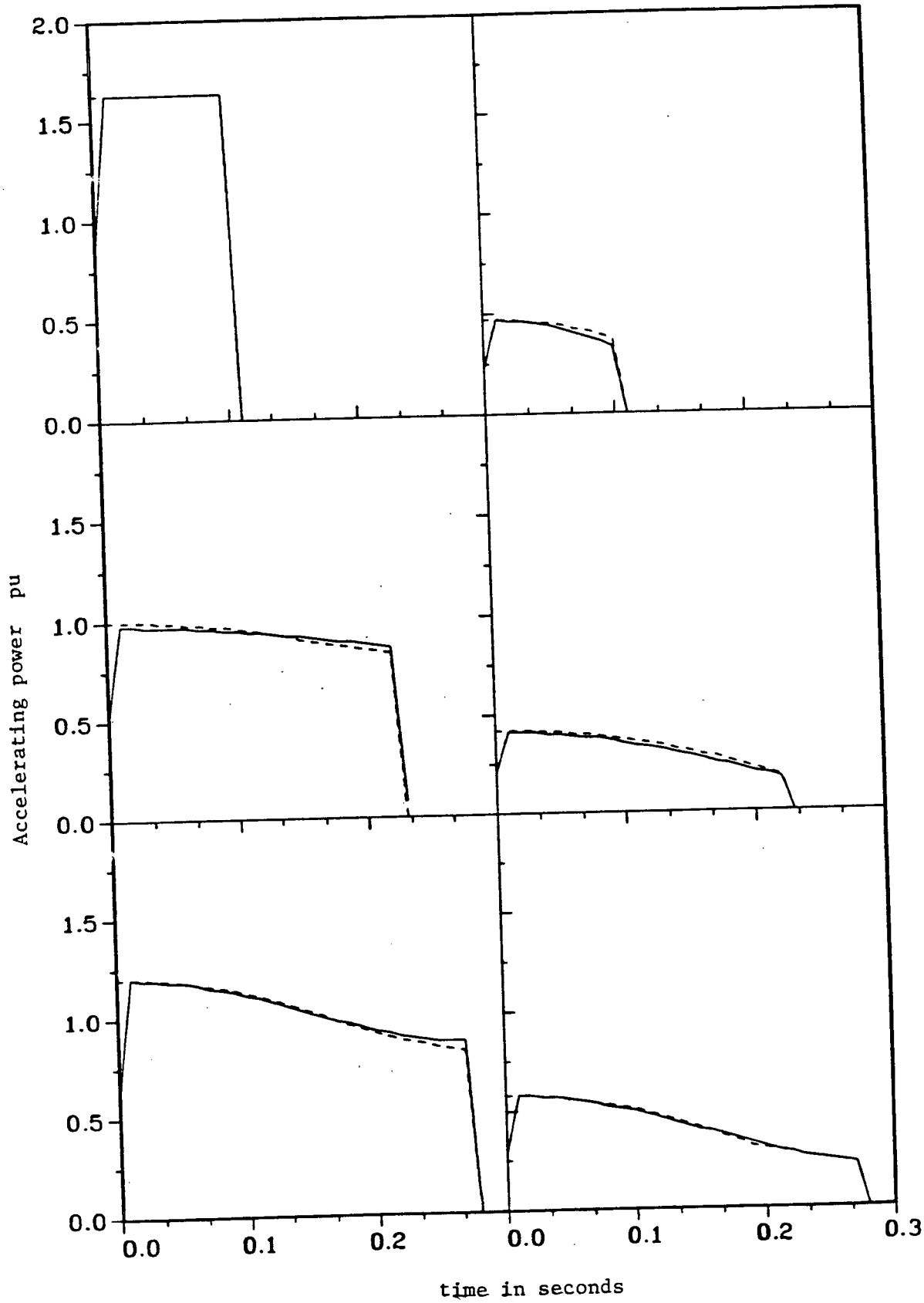

Fig. 4.3 The accelerating power for different fault locations
——— time solution
- - - - Taylor series

Fault at Bus #	Critical Clearing Time (second)		
	Time Solution (step-by-step)	Dynamic equivalent method	Taylor Series method
4	.29-.30	.27	.29
5	.22-.23	.20	.22
6	.51-.52	.46	.49
7	.11-.12	.1	.11
8	.28-.29	.26	.28
9	.40-.41	.38	.41

Table 4.3 Critical clearing time by the time solution and the proposed methods for the 3-machine power system.

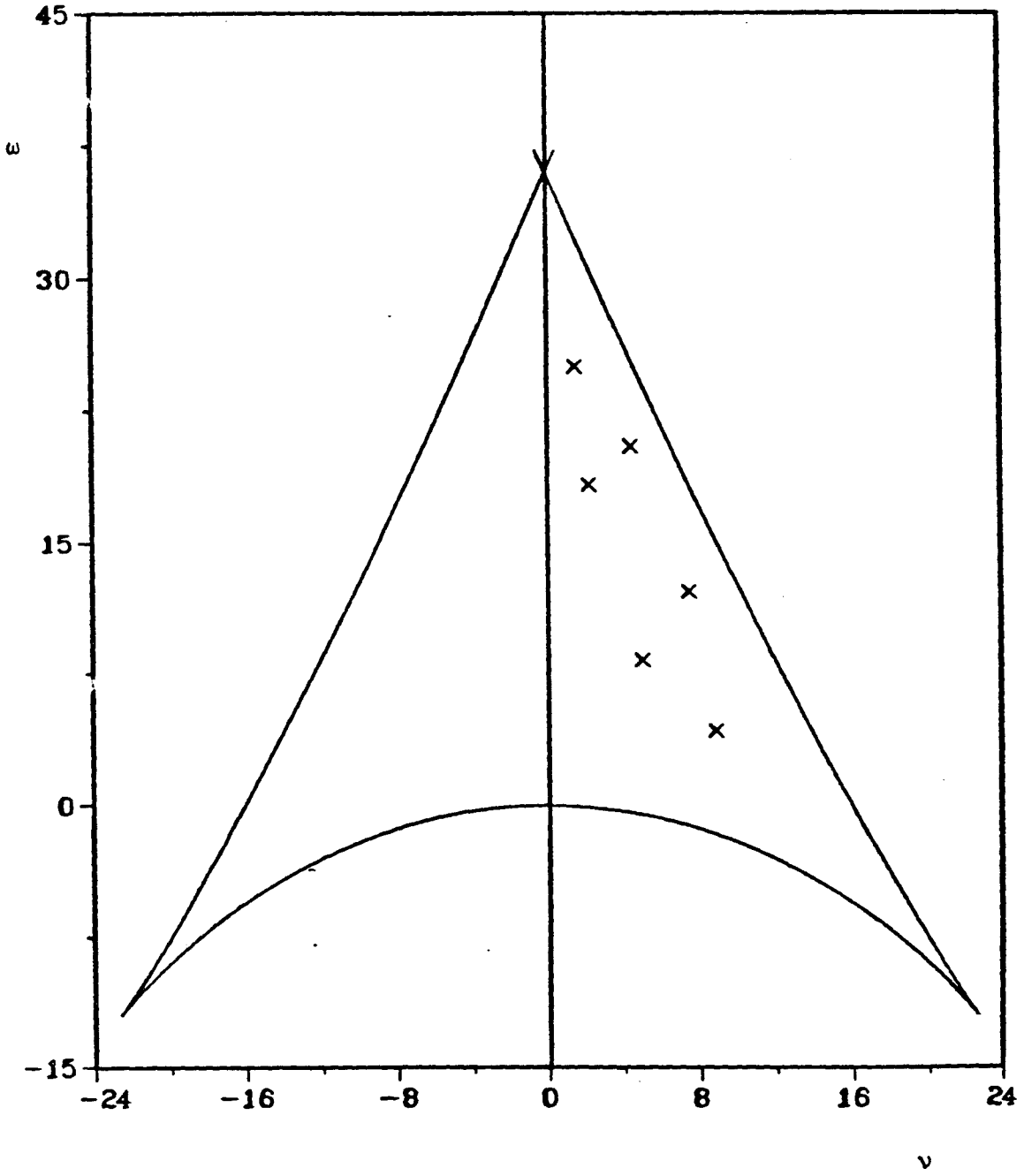

Fig. 4.4 The transient stability region of the 3-machine power system using the dynamic equivalent method. Stable cases are marked (x) inside the region.

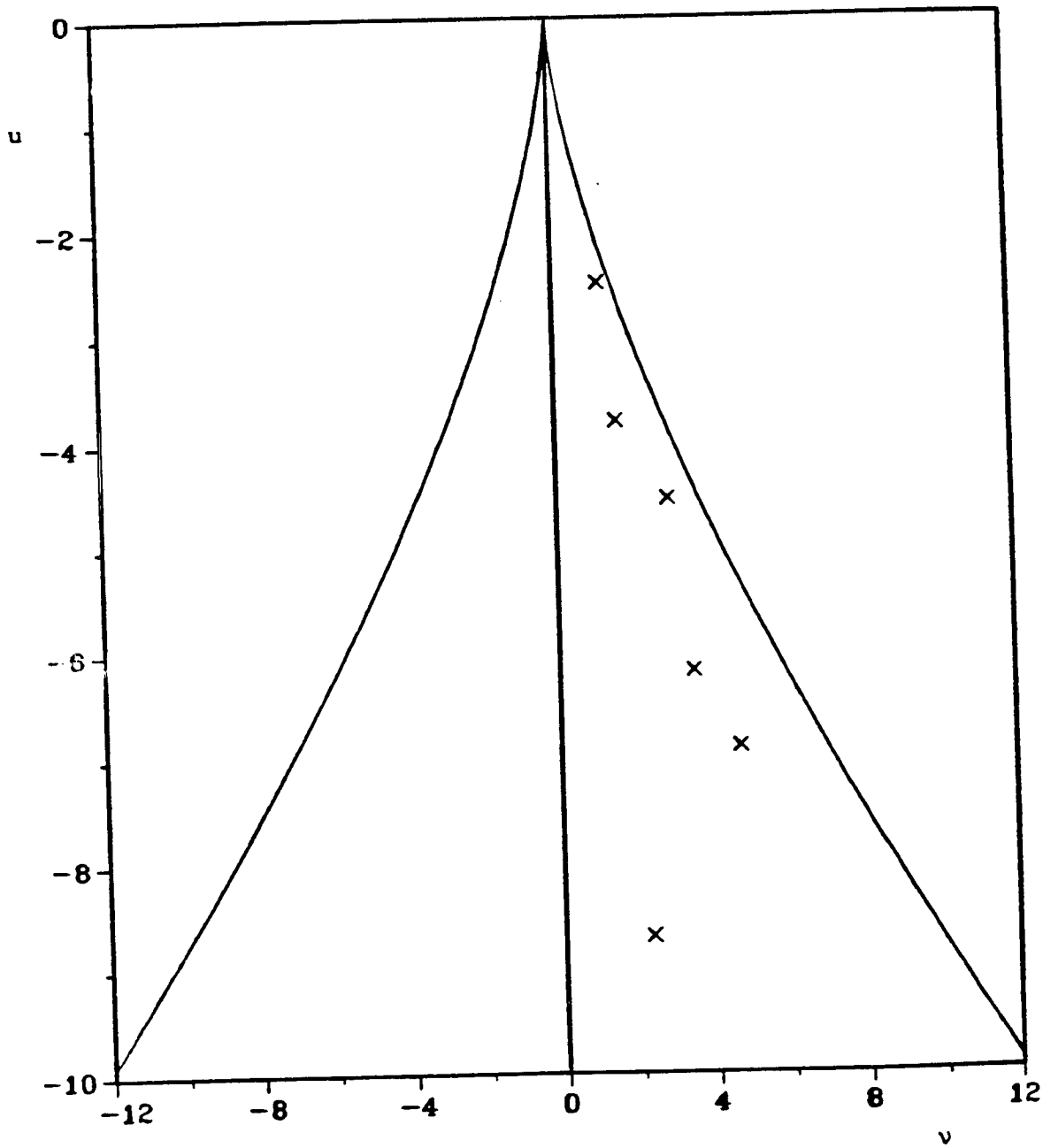

Fig. 4.5 The transient stability region of the 3-machine system using Taylor series method with stable cases marked (x) inside the region.

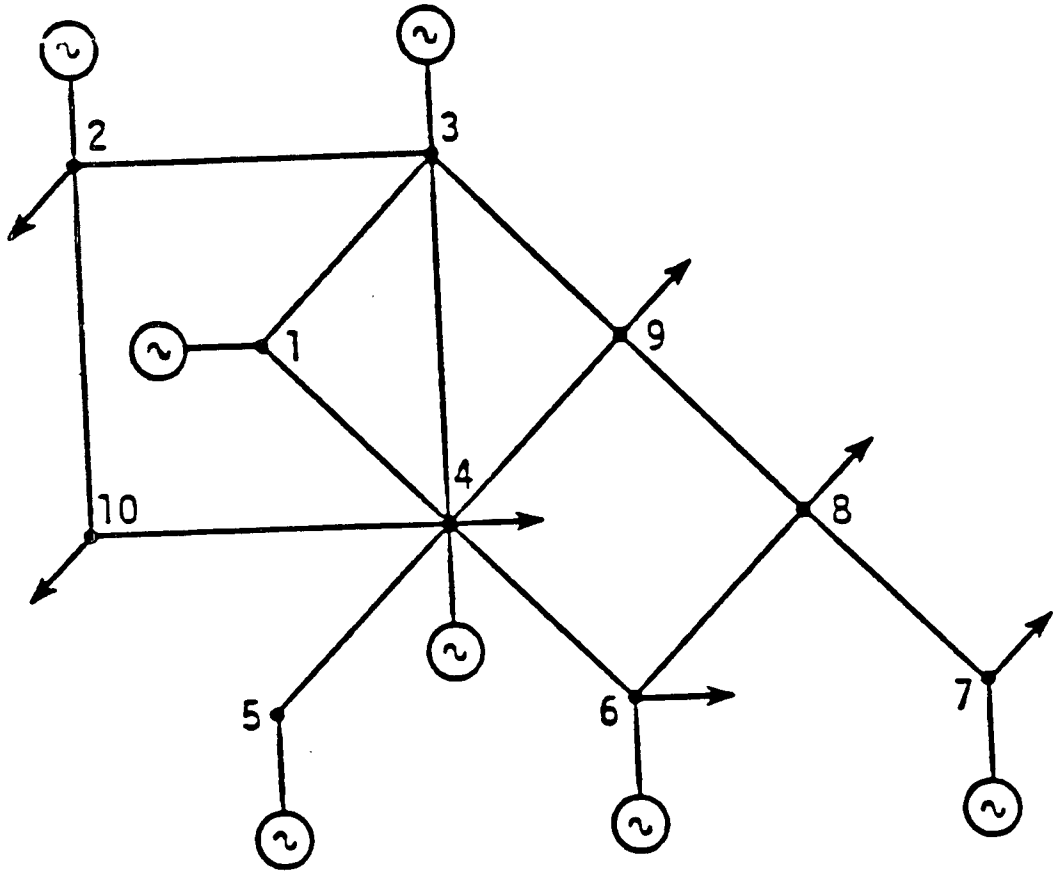

Fig. 4.6 The CIGRE test system.

4.5.2 CIGRE 7-machine Test System

The CIGRE 225 KV test system is shown in Fig. 4.6. It has 10 buses and 13 lines. Buses 1 through 7 are generating buses while loads are located at buses 2, 4, 6, 7, 8, 9 and 10. Generator, load and transmission line data are given in Table 4.4. The base values used are 225 KV and 100 MVA.

Three-phase faults are applied and the transient stability is evaluated for each fault. The critical clearing time is calculated for each case using the three methods. Table 4.5 gives a comparison between the time solution and the two methods presented in this chapter in terms of the critical clearing time.

The transient stablity regions are shown in Figures 4.7 and 4.8. Both methods show very good agreement with the time solution plus well defined transient stability regions in terms of the system parameters valid for all loading conditions and fault locations.

4.6 Discussion of Results

The results of the two examples presented in the previous section have shown the feasibility of catastrophe theory application to multi-machine power systems. The accuracy of the methods is very good when compared with the step-by-step time solution which is used as the benchmark for accuracy. The methods proposed are fast and give the critical clearing time through a single computation instead of using the time solution method repetitively and human interpretation to evaluate a similar case.

GENERATORS						
Bus	P_{base} (MVA)	X (%)([1])	M (MW s^2/rad)	P_m (MW)	E (p.u)	δ^o (°)
1	100	7.4	6.02	217	1.106	7.9
2	100	11.8	4.11	120	1.156	-0.2
3	100	6.2	7.59	256	1.098	6.5
4	100	4.9	9.54	300	1.110	3.9
5	100	7.4	6.02	230	1.118	7.0
6	100	7.1	6.77	160	1.039	3.6
7	100	8.7	5.68	174	1.054	7.9

LOADS					
Bus	P (MW)	Q (MVar)	Bus	P (MW)	Q (MVar)
2	200	120	8	100	50
4	650	405	9	230	140
6	80	30	10	90	45
7	90	40			

LINES			
Bus	R (ohm)	X (ohm)	$\omega C/2$ (μS)
1 - 3	5	24.5	200
1 - 4	5	24.5	100
2 - 3	22.8	62.6	200
2 - 10	8.3	32.3	300
3 - 4	6	39.5	300
3 - 9	5.8	28	200
4 - 5	2	10	200
4 - 6	3.8	10	1200
4 - 9	24.7	97	200
4 - 10	8.3	33	300
6 - 8	9.5	31.8	200
7 - 8	6	39.5	300
8 - 9	24.7	97	200

([1]) These values include the transformer's reactances and are expressed on a 100 MVA base.

Table 4.4 Data for the CIGRE 7-machine system (taken from Ref. [20])

Fault at Bus #	Critical Clearing Time (second)		
	Time Solution (step-by-step)	Dynamic equivalent method	Taylor Series method
1	.35-.36	.34	.36
2	.41-.42	.40	.37
3	.39-.40	.38	.39
4	.50-.51	.52	.48
5	.35-.36	.34	.35
6	.52-.53	.51	.51
7	.33-.34	.33	.33
8	.44-.45	.42	.45

Table 4.5 Critical clearing time by the time solution and the proposed methods for the 7-machine power system.

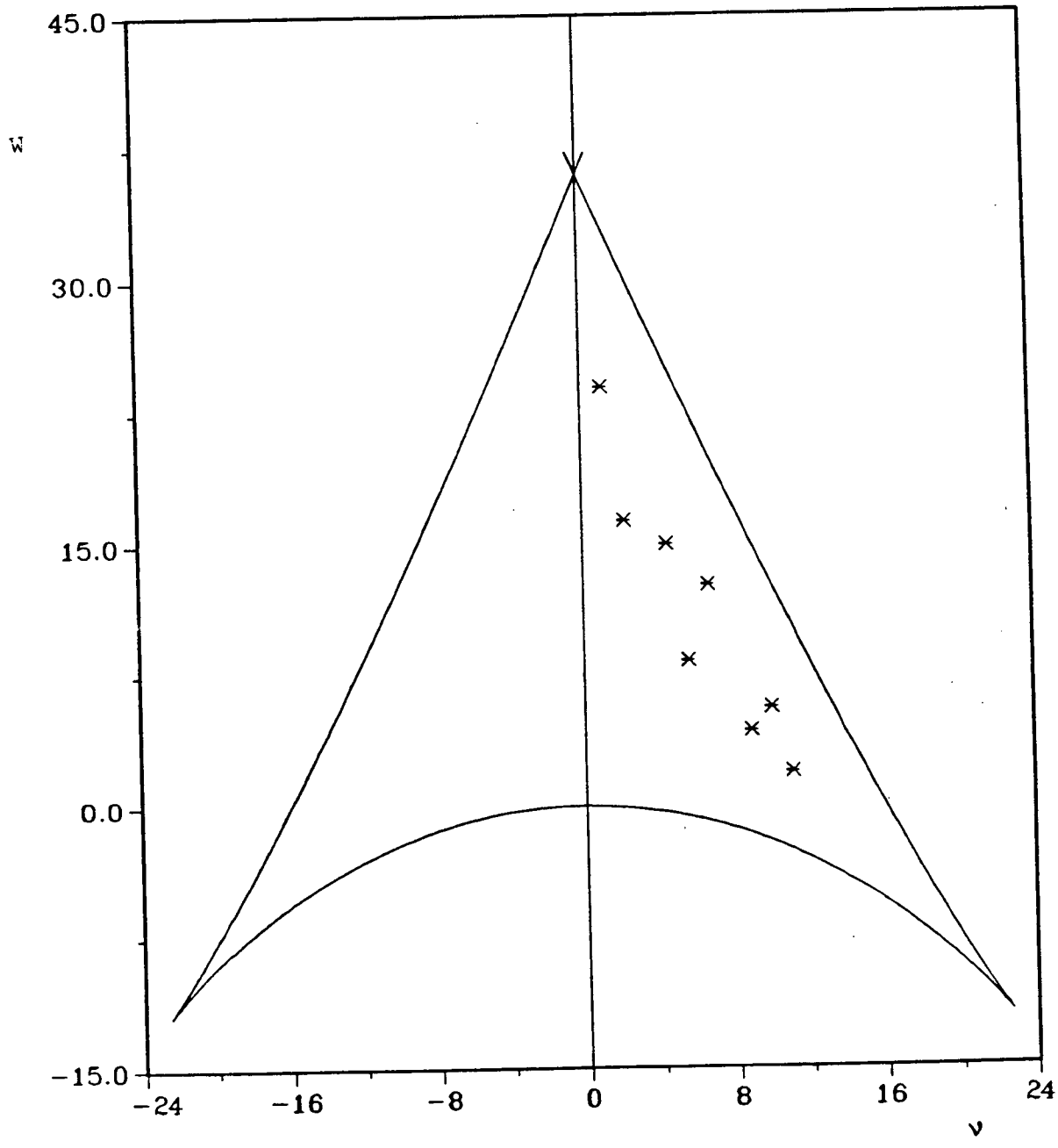

Fig. 4.7 The transient stability region for the CIGRE test system using the dynamic equivalent method.

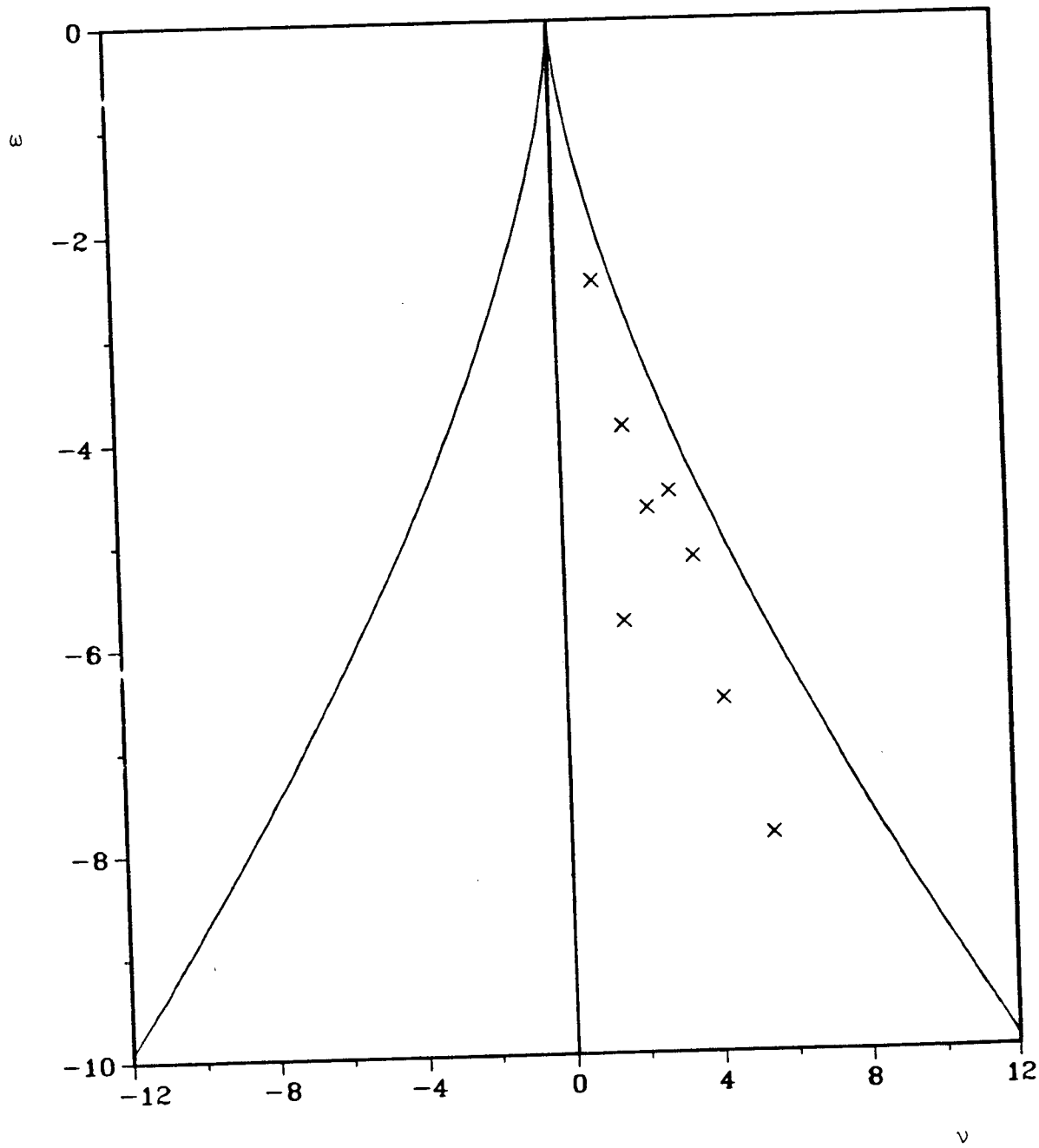

Fig. 4.8 The transient stability region for the CIGRE test system using the Taylor series method.

The importance of the transient stability regions provided by the bifurcation set of the catastrophe manifold is not only in terms of speed and accuracy. It provides another important dimension to the transient stability problem-the stability limits. The method checks for the violations of the transient stability limits of the post-fault network in terms of the system parameters. Of course, if the limits are exceeded the system is unstable. This important feature is not possible with existing direct methods, i.e., the existing direct methods cannot give any solution when the stability limits of the post-fault network are violated.

The accuracy of the Taylor series method becomes a problem when t_c is higher than .5 second [52]. To obtain good accuracy beyond this limit higher order terms have to be included in the computations. This will complicate the stability region and slow down the calculation procedure. In practice, however, this problem is very rare. Faults in large power systems are usually tripped in a few cycles, typically .1 second. Interest is in the delivery of maximum power at low clearing time without risking the power system security. This practical consideration can easily be handled by the proposed methods without loss of accuracy.

The off-line calculations of the critical energy for each case considered can be improved by calculating the closest unstable equilibrium point for the critical machine. This reduces the computation time and simplifies the procedure of finding the critical energy [45].

CHAPTER 5

INCLUSION OF DAMPING, FLUX DECAY AND EXCITATION RESPONSE

The most challenging problem in the application of direct methods to transient stability of power systems is the validity of the simplified model used to represent power systems.

In this Chapter a significant improvement in the modelling problem is presented. The new model proposed includes damping, field flux decay and excitation response.

5.1 Limitation of the Classical Model

Power utilities are hesitant to accept the direct methods of transient stability assessment mainly because they raise doubts about the validity of the classical model. In this model it is assumed that the flux linking the main field winding remains constant during the transient. This may be true only if the exciter does not respond during the first swing period (1 second or less). Modern excitation systems can reach full response within .1 second, so that the classical model assumption is not valid for such exciters. In fact, during the last decade trends in the design of power system components have resulted in more reliance on fast-response and high ceiling voltage exciters [53].

Although fast-response exciters are more desirable and widely used in modern power systems, none of the existing direct methods of transient stability assessment have considered the excitation effect. The reason is

that Lyapunov's function becomes so complicated that the direct methods lose the merit of being fast methods.

In classical model assumptions, damping effects are usually neglected although it affects directly the accelerating power. In some cases the damping power has appreciable value and so affects the first swing stability [54].

5.2 Damping

In power systems there are sources of positive damping which tend to damp out oscillations resulting from disturbances. This damping is due to the characteristics of the mechanical system, generator and loads. The mechanical system damping results from the increase in shaft torque with the decrease in speed. The per unit damping torque coefficient is defined as the negative of the per unit change in torque for each per unit change in speed [54].

The generator electrical damping is associated with the currents that are induced in the rotor windings due to a disturbance or oscillations. The damping torque due to the field winding is usually small because of the relatively long time constant. The damper winding component of the damping torque is quite appreciable and it usually affects accelerating power during disturbances.

Cylindrical rotor generators may develop appreciable torque due to the eddy currents which are induced by asynchronous operation, such as slipping poles or oscillations.

Loads are also a source of damping in power systems. Induction and synchronous motors with their mechanical shaft loads develop damping torque during disturbances.

The damping power ($D\dot{\delta}$) is usually added to the inertial power in the swing equation. The damping coefficient D includes the various damping power components, both mechanical and electrical. The damping coefficients are usually in the range of 1-3 pu. This represents mechanical damping, generator and load damping. Larger values are also reported in the literature [2].

The swing equation of machine i in an n-machine power system is given by

$$M_i \ddot{\delta}_i + D \dot{\delta}_i = P_{mi} - P_{ei} \qquad i = 1, \ldots n \qquad (5.1)$$

where D is the damping coefficient.

The accelerating power becomes

$$P_{ai} = P_{mi} - P_{ei} - D \dot{\delta}_i \qquad (5.2)$$

The same procedure of Section 4.3, is used to expand P_{ai} into a Taylor series to get the energy function during the fault-on period. Recalling equations (4.26) and (4.27)

$$P_{ai}(t) = P_a^{(0)} + \frac{1}{1!} P_a^{(1)} t + \frac{1}{2!} P_a^{(2)} t^2 + \ldots$$

$$P_a^{(m)} = \left. \frac{d^m P_{ai}}{dt^m} \right|_{t=0}$$

we have

$$P_{ai} = P_{mi} - \sum_{j=1}^{n} (D_{ij} \cos \delta_{ij} + C_{ij} \sin \delta_{ij}) - D\dot{\delta}_i \tag{5.3}$$

We note that at $t = 0$, $\dot{\delta}_i = 0$.

Therefore

$$P_{ai}^{(0)} = P_{mi} - \sum_{j=1}^{n} (D_{ij} \cos \delta_{ij}^{0} + C_{ij} \sin \delta_{ij}^{0}) - D(0) \tag{5.4}$$

$$P_{ai}^{(1)} = \left.\frac{d\, P_{ai}}{dt}\right|_{t=0}$$

$$= - \sum_{j=1}^{n} (-D_{ij} \sin \delta_{ij}^{0} + C_{ij} \cos \delta_{ij}^{0}\, \dot{\delta}_{ij} - D)\ddot{\delta}_i^{(0)}$$

$$= - D\, \ddot{\delta}_i^{(0)} \tag{5.5}$$

where $$\ddot{\delta}_i^{(0)} = \frac{P_{ai}^{(0)}}{M_i} \tag{5.6}$$

$$P_{ai}^{(2)} = \left.\frac{d^2 P_{ai}}{dt^2}\right|_{t=0}$$

$$= - \sum_{j=1}^{n} (-D_{ij} \cos \delta_{ij}^{0} - C_{ij} \sin \delta_{ij}^{0})\, (\dot{\delta}_i^{0})^2$$

$$- \sum_{j=1}^{n} (-D_{ij} \sin \delta_{ij}^{0} + C_{ij} \cos \delta_{ij}^{0})\ \ddot{\delta}_{ij}^{0} - D\, \dddot{\delta}_i^{0}$$

$$= \sum_{j=1}^{n} (D_{ij} \sin \delta_{ij}^{0} - C_{ij} \cos \delta_{ij}^{0})\, \ddot{\delta}_{ij}^{0} - D\, \dddot{\delta}_i^{0} \tag{5.7}$$

where $\dddot{\delta}_i^0 = \dfrac{P_{ai}^{(1)}}{M_i}$ (5.8)

Derivation of $P_{ai}^{(3)}$ and $P_{ai}^{(4)}$ are given in Appendix D. We note here that all Taylor series coefficients exist when damping is taken into account.

$$P_{ai} = P_{ai}^{(0)} + P_{ai}^{(1)}t + \frac{P_{ai}^{(2)}}{2!}t^2 + \ldots \tag{5.8}$$

The energy equilibrium surface is then formed using equation (4.23)

$$V_i = \int_0^{t_c} (P_{ai}^f - P_{ai}^p)dt + \int_0^f P_{ai}^p dt + V_{cr} = 0 \tag{5.9}$$

This becomes

$$= A_4t^4 + A_3t^3 + A_2t^2 + A_1t + A_0 + k_s + V_{cr} = 0 \tag{5.10}$$

where $A_n = \dfrac{1}{n!}(P_a^{f(n)} - P_a^{p(n)})$

$$K_s = \int_0^{t_c} P_{ai}^p \, dt = \text{constant}$$

Here V_i is truncated after the 4th order term. We eliminate the 3rd order term to obtain the standard swallowtail catastrophe manifold (Appendix A) as given in Section 3.4.1 to get

$$X^4 + uX^2 + vX + w = 0 \tag{5.11}$$

The transient stability region is defined through of the bifurcation set in terms of the system parameters u, v and w which includes the damping term.

The effect of damping on the accelerating power during the transient period is shown in Fig. 5.1 for a short circuit on the power system of Fig. 3.5. Another example is given in Fig. 5.2 for a short circuit at bus 7 of the three-machine power system given in Fig. 4.1. It is clear that the damping tends to reduce the fault kinetic energy and results in more stable systems.

5.3 Excitation Response and Flux Decay

When a fault occurs near a generator bus, transient currents in the armature circuit induce other currents in the rotor circuit which carries the field current. The flux linking the armature circuit will decay according to the effective time constant of the field circuit. This time constant is in order of several seconds at no load, and one second or higher under load. The flux decay decreases the generator internal voltage and hence reduces the stability limits.

Both steady-state and transient stability can be improved by excitation control systems [55]. Fast speed of response and high ceiling voltage exciters can particularly improve transient stability. With the help of fast transient forcing of excitation and the boost of internal machine flux, the output power of the generator can be increased during the transient period. This reduces the accelerating power and results in improved transient performance. Fast exciters also ensure that subsequent swings are smaller than the first swing. This is important for modern low inertia generators and weakly damped power systems where transient instability after the first swing may occur.

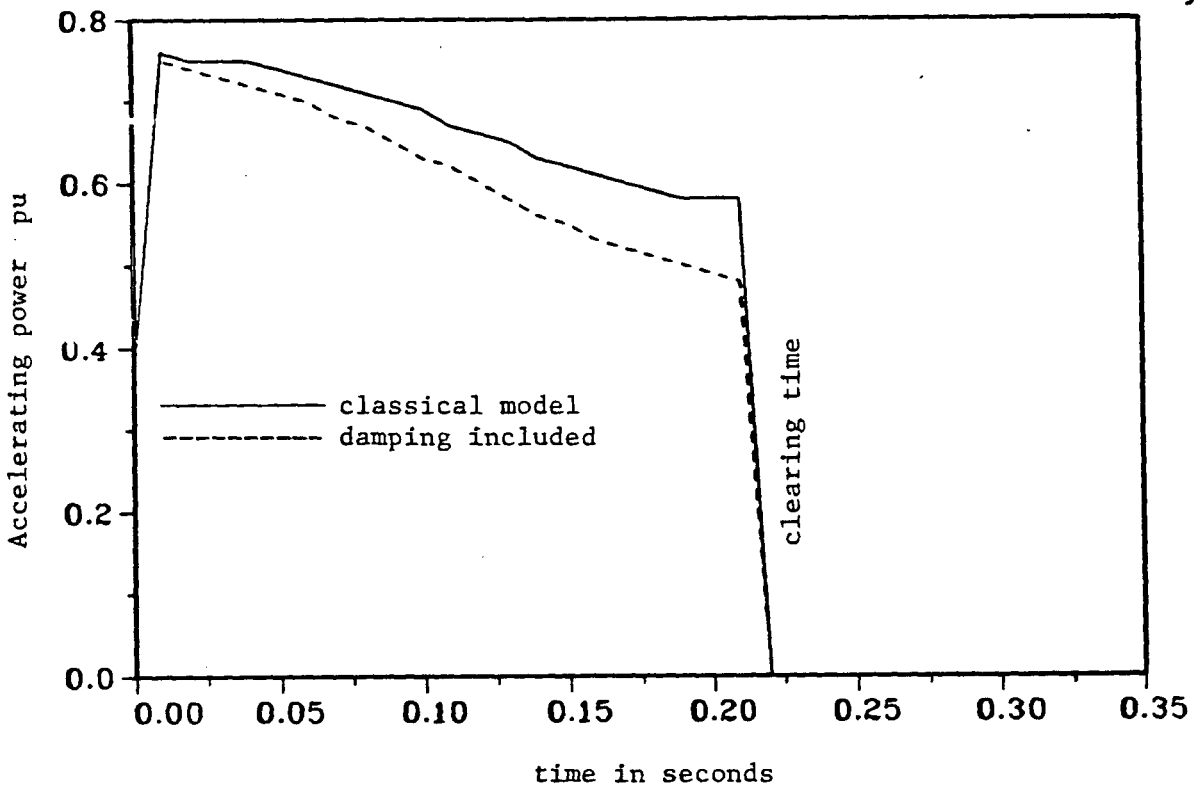

Fig. 5.1

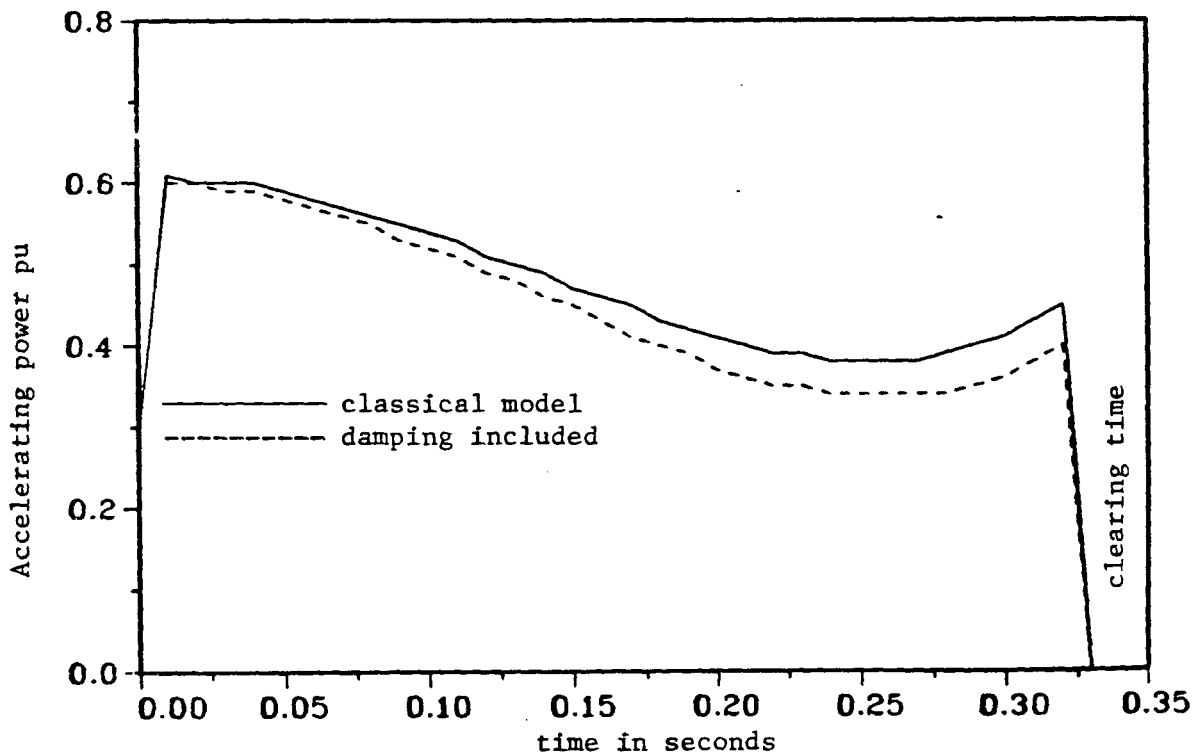

Fig. 5.2 Effect of damping inclusion on the accelerating power during the fault-on period for two test cases.

The vector diagram for the transient state of a cylindrical rotor generator is given in Fig. 5.3. We assume that the internal voltage E_i lags behind the q-axis by a constant angle ϕ_i all the time.

The equations of motion of generator i in an n-machine power system with field flux decay and excitation response are expressed as follows

$$M_i \ddot{\delta}_i = P_{mi} - \sum_{j=1}^{n} (D_{ij} \cos \delta_{ij} + C_{ij} \sin \delta_{ij})$$

and

$$T'_{doi} \frac{dE'_{qi}}{dt} = E_{fdi} - E'_{qi} - (X_{di} - X'_{di})\, i_{di} \tag{5.12}$$

where

T'_{doi} : d-axis transient open circuit time constant

E'_{qi} : voltage along the q-axis related to E_i by angle ϕ_i.

E_{fdi} : excitation voltage applied to field winding.

X_{di}, X'_{di}: d-axis synchronous and transient reactance.

i_{di} : d-axis current.

The terms of the swing equation were previously defined. From the vector diagram of Fig. 5.3, and since ϕ_i is constant

$$E'_{qi} = E_i \cos \phi_i$$

Equation (5.12) becomes

$$T'_{doi} \frac{d\, E_i}{dt} = \frac{E_{fdi}}{\cos \phi_i} - E_i - (X_{di} - X'_{di}) i\, d_i \tag{5.13}$$

Equation (5.13) can be modified in terms of the power equation and assuming that ϕ_i is small we obtain [56]:

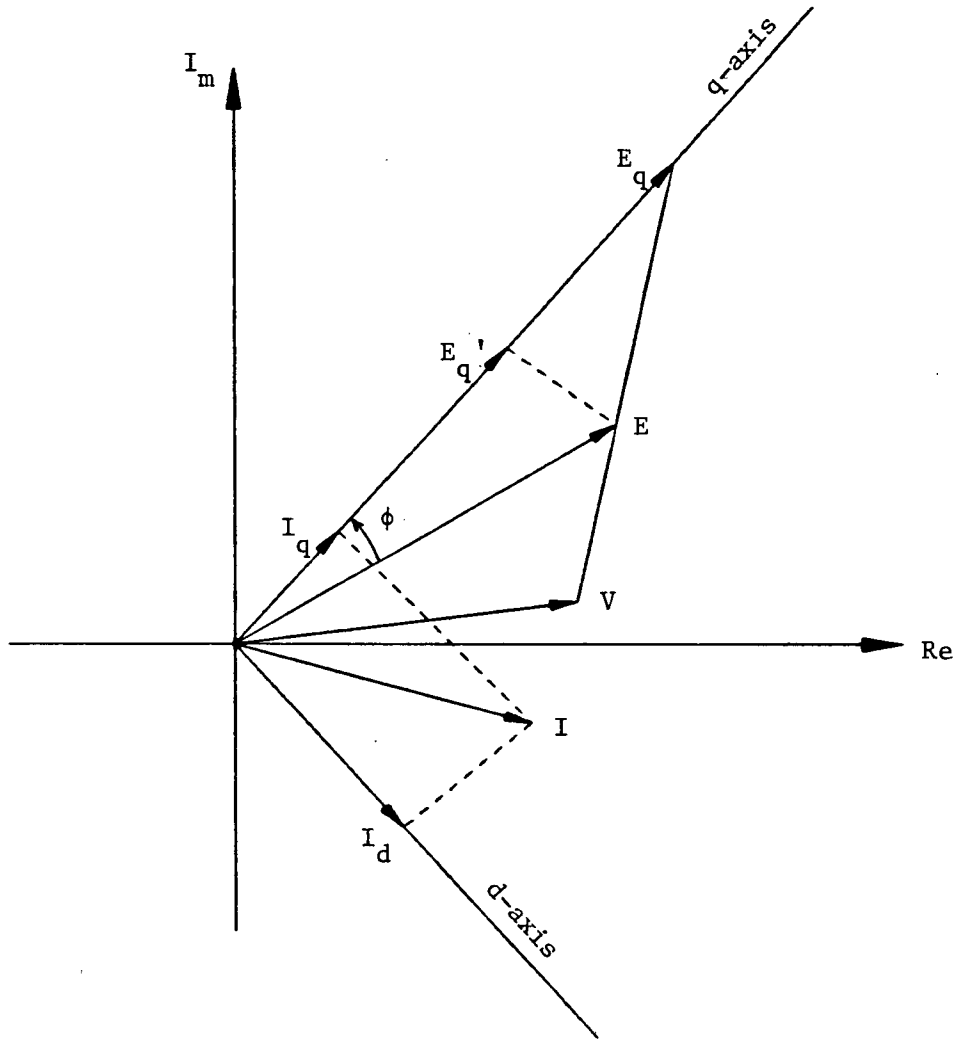

Fig. 5.3 The vector diagram of the generator internal quantities for the transient state.

$$T'_{doi} \frac{d E_i}{dt} = \frac{E_{fdi}}{\cos\phi_i} - E_i - (X_{di} - X'_{di}) \sum_{j=1}^{n} (g_{ij}E_j\cos\delta_{ij} + b_{ij}E_j\sin\delta_{ij}) \qquad (5.14)$$

The first term of the R.H.S. of equation (5.14) represents the exciter response while the second and third terms represent the drop in the internal voltage due to the flux decay. It is clear that if E_{fdi} is fast and high then the drop of internal voltage (E_i) due to the flux decay can be eliminated.

A typical excitation voltage-time response curve is shown in Fig. 5.4. OA is the generator rated load field voltage before disturbance occurs. The straight line AC is drawn such that the area ACD is equal to the area ABD enclosed by the actual response. The exciter response is given by the rate of increase or decrease of the exciter voltage, i.e., the slope determined by $\frac{CE - AO}{OE}$ in Fig. 5.4. The time, in seconds, for the exciter voltage to reach 95 percent of ceiling voltage is known as exciter voltage response time [57]. An exciter with a voltage response time of 0.1 second or less is taken to be a fast high initial response exciter.

The exciter voltage response is given by

$$E_{fdi} = E_o + (E_c - E_o)(1 - e^{-t/\tau_e}) \qquad (5.15)$$

where E_o is the initial exciter voltage

E_c maximum ceiling voltage

τ_e excitation system time constant

Substituting by E_{fdi} in equation (5.14) we get

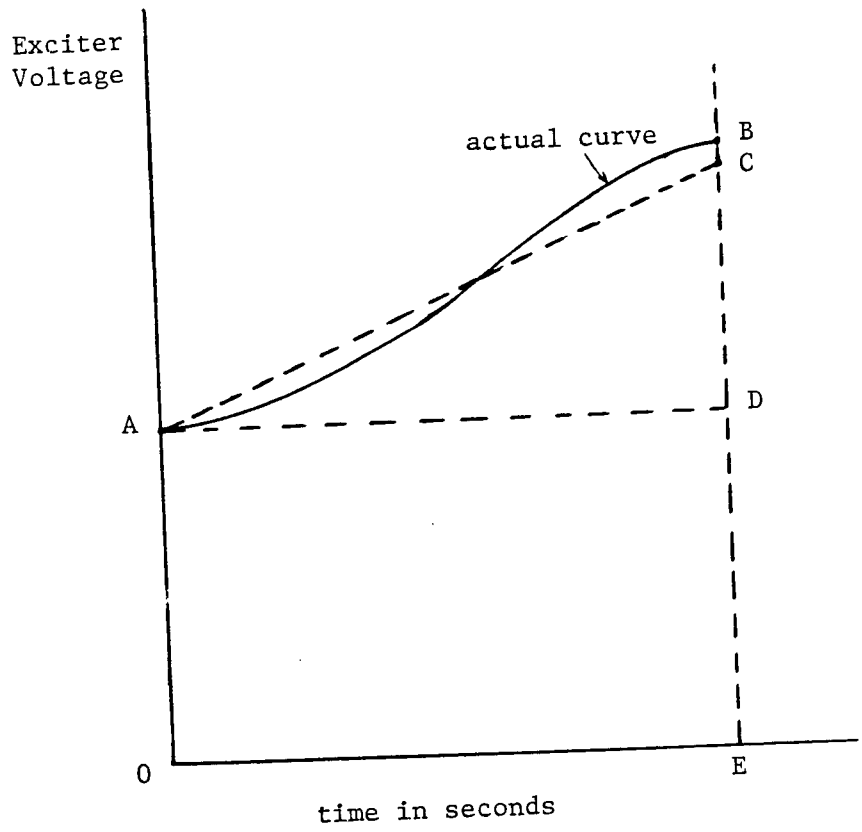

Fig. 5.4 The typical excitation voltage-time response

$$T'_{doi} \frac{d\,E_i}{dt} = F(t) = \frac{E_c - (E_c - E_o)e^{t/\tau_e}}{\cos\,\phi_i}$$

$$-E_i - (X_{di} - X'_{di}) \sum_{j=1}^{n} (g_{ij}E_j \cos\,\delta_{ij} + b_{ij}E_j \sin\,\delta_{ij}) \quad (5.16)$$

The function F(t) will now be expanded in a Taylor series to evaluate equation (5.16) for the transient period (t < .5s). F(t) is expanded around t=0 as follows

$$F(t)\Big|_{t=0} \simeq F^{(0)} + F^{(1)} + \frac{F^{(2)}}{2!} t^2 + \ldots \quad (5.17)$$

where

$$F^{(n)} = \frac{d^n F(t)}{dt^n}\Big|_{t=0}$$

Therefore

$$F^{(0)} = \frac{E_o}{\cos\phi_i} - E_i(0) - (X_{qi} - X'_{di}) \sum_{j=1}^{n} (g_{ij}E_j \cos\delta_{ij}^{0} + b_{ij}E_j \sin\delta_{ij}^{0})$$

(5.18)

$$F^{(1)} = \frac{d\,F(t)}{dt}\Big|_{t=0}$$

$$= \frac{1}{\tau_e} \frac{(E_c - E_o)e^{-t/\tau_c}}{\cos\phi_i} - \frac{d\,E_i}{dt} - (X_{qi} - X'_{di}) \sum_{j=1}^{n} (-g_{ij}E_j \sin\delta_{ij}$$

$$+ b_{ij}E_j \cos\delta_{ij})\dot{\delta}_{ij}$$

at t = 0

$$\dot{\delta}_{ij} = 0, \quad \frac{d\,E_i}{dt} = \frac{1}{\tau'_{doi}} F^{(0)}$$

Thus

$$F^{(1)} = \frac{1}{\tau_e} \frac{(E_c - E_o)}{\cos\phi_i} - \frac{F^{(0)}}{T'_{doi}} \tag{5.19}$$

$F^{(2)}$, $F^{(3)} \ldots F^{(n)}$ can be evaluated in the same way. Equation (5.16) is evaluated using (5.17), and we get

$$E_i = E(o) + F^{(0)}t + \frac{F^{(1)}\,t^2}{2} + \frac{F^{(2)}t^3}{6} \tag{5.20}$$

where E(o) is the initial generator internal voltage at t=to-.

Equation (5.20) represents the generator internal voltage during the transient period including exciter response and flux decay. Truncation of E_i depends on the length of the transient period. As we explained in the previous chapter the Taylor series method can give good results up to a period of .5 seconds. In practice, faults are usually cleared faster than the .5 s period (a typical clearing time in large power systems is .1 second).

Equation (5.20) can be used with the method presented in Section 4.3 to include excitation response and flux decay in the assessment of transient stability. The swing equation of the critical machine i in an n-machine system is given by

$$M_i \ddot{\delta}_i = P_{mi} - \sum_{j=1}^{n} E_i E_j \, (g_{ij} \cos \delta_{ij} + b_{ij} \sin \delta_{ij}) \tag{5.21}$$

$$= P_{ai}$$

From equation (5.20) let the internal voltage of the critical machine be

$$E_i = E(o) + F^{(0)} t + \frac{F^{(1)} t^2}{2} + \frac{F^{(2)} t^3}{6} \tag{5.22}$$

Substitute (5.22) in (5.21) and expand P_{ai} in a Taylor series as in Section 4.3 to obtain

$$P_{ai} = P_a^{(0)} + P_a^{(1)} t + \frac{P_a^{(2)} t^2}{2!} + \ldots$$

where $P_a^{(n)} = \left. \dfrac{d^n P_{ai}}{dt^n} \right|_{t=0}$

The accelerating power coefficients are evaluated and given as follows

$$P_a^{(0)} = P_{mi} - \sum_{j=1}^{n} E_i(0) E_j \, (g_{ij} \cos \delta_{ij}^0 + b_{ij} \sin \delta_{ij}^0) \tag{5.23}$$

$$P_a^{(1)} = - \sum_{j=1}^{n} F^{(0)} E_j \, (g_{ij} \cos \delta_{ij}^0 + b_{ij} \sin \delta_{ij}^o) \tag{5.24}$$

$$P_a^{(2)} = - \sum_{j=1}^{n} F^{(1)} E_j \, (g_{ij} \cos \delta_{ij}^0 + b_{ij} \sin \delta_{ij}^0)$$

$$+ \sum_{j=1}^{n} E_i(0) E_j \, (g_{ij} \sin \delta_{ij}^0 - b_{ij} \cos \delta_{ij}^0) \ddot{\delta}_{ij}^0 \qquad (5.25)$$

The derivation of these coefficients and $P_a^{(3)}$, $P_a^{(4)}$ are given in Appendix E.

The energy equilibrium surface (catastrophe manifold) can now be written down in terms of the accelerating power coefficients as in equation (5.9)

$$V_i = \int_0^{t_c} (P_{ai}^f - P_{ai}^p) dt + \int_0^{t_s} P_{ai}^p dt + V_{cr} = 0 \qquad (5.26)$$

Equation (5.26) is evaluated and truncated after the 4th order term to get the swallowtail catastrophe manifold. This truncation is valid for $t < .5$ second. Thus equation (5.26) becomes

$$V_i = A_4 t^4 + a_2 t^2 + A_1 t + A_0 + K_s + V_{cr} = 0 \qquad (5.27)$$

where

$$A_n = \frac{1}{n!} (P_{ai}^{f(n)} - P_{ai}^{p(n)})$$

$$K_s = \int_0^{t_c} P_{ao}^p \, dt = \text{constant}$$

$$V_{cr} = \text{critical energy}$$

Again we eliminate the third order term of equation (5.27) to get the standard swallowtail catastrophe (Appendix A) in the form

$$X^4 + uX^2 + vX + w = 0 \tag{5.28}$$

The effect of flux decay and exciter response on the accelerating power during the transient period is shown in Fig. 5.4 and Fig. 5.5 using examples shown in Fig. 3.5 and Fig. 4.1. It is apparent that the area under the accelerating power is reduced. This area represents the kinetic energy generated by the fault. Therefore, the degree of stability is increased and the critical clearing time is also increased. This means that when fast exciters are used the system can generate more power for the same clearing time.

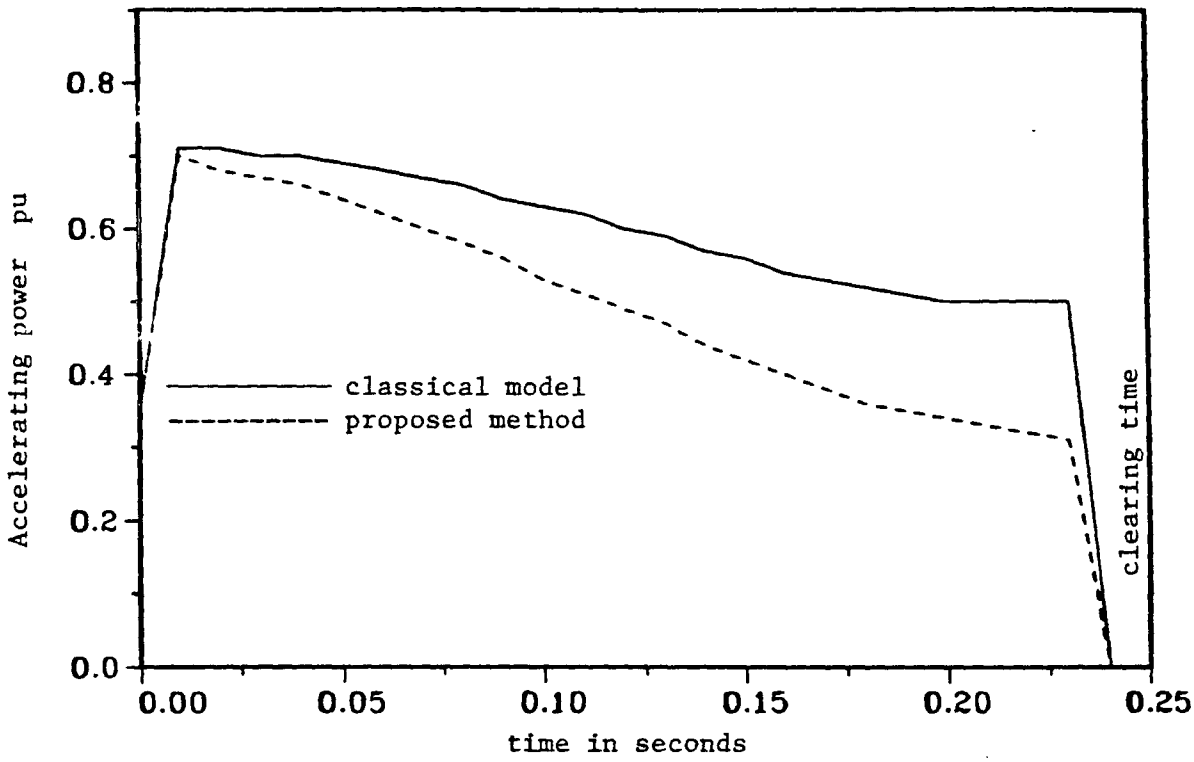

Fig. 5.5

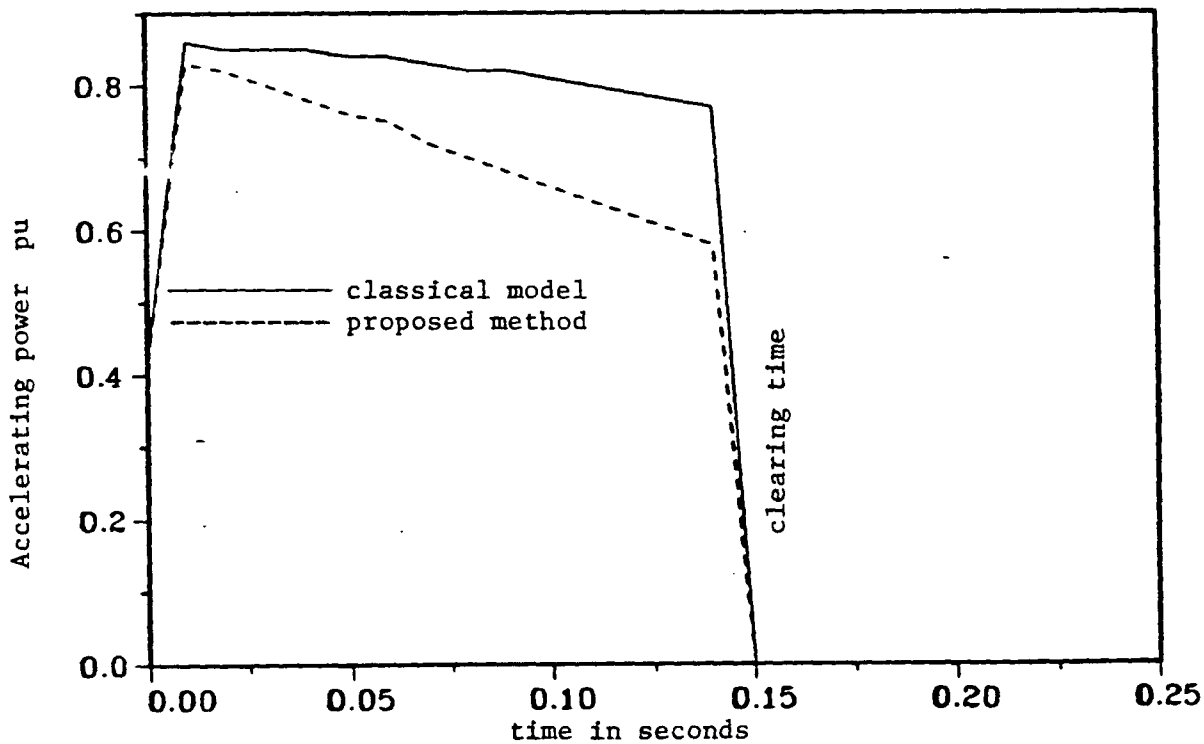

Fig. 5.6

The effect of flux decay and excitation response on the accelerating power during the transient period for two test cases.

CHAPTER 6

CONCLUSIONS

In this thesis, the transient energy function was efficiently used with catastrophe theory to define comprehensive transient stability regions for power systems. Explicit boundaries of the transient stability regions were identified by the bifurcation set of the catastrophe manifolds. The method is made practical by using the concept of critical machines since for a specified fault, only a few machines show significant oscillations during the transient period.

The thesis suggests two methods to solve the transient stability problem of multi-machine power systems. In the first method, the critical machine(s) is identified and a two-machine dynamic equivalent for the power system is formed. The critical machine is singled out and a center of angle group is formed for the rest of the system. The energy balance equation is derived from the equation of motion of the critical machine against the center of angle. At critical clearing, the energy balance equation forms the equilibirum surface of the catastrophe manifold from which the transient stability region is derived by the bifurcation technique. This stability region is valid for different loading conditions and fault locations. This method has the advantage that the critical energy is calculated directly by using the closest unstable equilibrium point. However, this method can only be used with the classical model.

In the second method, the critical machine is identified and a Taylor series expansion for its accelerating power for a specified fault is

constructed. The energy balance equation is then derived by integrating the accelerating power. The critical energy is calculated off-line by numerical integration for the fault considered. Again the energy balance equation at critical clearing represents the catastrophe manifold from which the transient stability region is determined. This region is bounded by the stability limits and is valid for different loading conditions and fault locations. This method is limited to a period of .5 second for best accuracy. However, this is adequate for most large power systems since typical clearing times are in the range of a few cycles or .1 second. Model improvements were made possible using this method. Excitation response, flux decay, and damping, were included in the stability analysis by the Taylor series expansion method.

The results obtained by the proposed methods are in good agreement with those obtained by the time solution method. A large number of simulations are presently needed in system planning in order to determine the critical clearing time or stability limits. The proposed methods give directly the critical clearing time and stability limits with good accuracy and less computation. Therefore, they can be used to greatly reduce the large number of time simulations in the system planning stage. In system operations, the proposed methods provide fast solutions to the transient stability problem with definite stability boundaries so that corrective action can be taken to prevent instability.

The major contributions of this research are the following:

1. For the first time, the catastrophe theory is applied to the transient stability problem. Comprehensive transient stability regions are

calculated in terms of the power system parameters. These regions are valid for any loading condition and fault location. All existing direct methods, on the other hand, require new computation for any change in operating conditions. This is an important consideration in implementing direct methods for real-time assessment of transient stability and system security.

2. Another unique advantage of the methods presented is the inclusion of the excitation response during the transient period in the stability analysis. All existing direct methods are limited to the classical model [47] which neglects the exciter response. With the inclusion of damping, flux decay and excitation response in the presented methods, all factors that directly effect transient stability are taken into account. This result makes the direct methods more realistic.

3. The methods presented predict any violation of stability limits and, therefore transient instability. This result is very important; it helps to ensure the security of power systems for any disturbance considered. It also enables power system planners to design proper stability controls to prevent system instability.

4. Existing direct methods either neglect or approximate the effect of the transfer conductances. However, in some cases transfer conductances can have an appreciable effect on system performance [50]. In this research, the transfer conductances are fully represented.

5. The application of catastrophe theory is extended to the steady state stability problem of cylindrical-rotor generators. The method

presented (Chapter 3) is also adaptable to include the effect of governors on steady state stability.

6. The achievements of this research have made the on-line security assessment more feasible than ever before. The important requirements for real-time applications are speed, accuracy and information. The methods presented need minimal calculations to locate the system parameters with respect to the stability region. Good agreement with the time solution method were obtained (Chapter 4). The location of the system parameters, for each case, on the transient stability region gives enough information on the degree of stability of the power system.

The outcome of this thesis gives new motivation to the application of fast direct methods to the transient stability problem of power systems. New areas of research need to be explored in order to reach the ultimate goal of the direct methods which is on-line assessment of transient stability. The future research should include the following:

1. The calculation of the critical energy of the post-fault network is still time consuming and needs to be done off-line. With some approximations, the dynamic equivalent method can give fast answers by calculating the closest unstable equilibrium points. However, a fast and exact method is still needed in order to complete the overall on-line approach.
2. Stability controls such as fast valving, braking resistors, single pole switchings, series capacitors and generator trippings are usually applied in practice to restore transient stability of power systems.

The inclusion of these controls in the proposed direct methods is of great interest to power utilities.

3. This research considered only single disturbances. Multiple disturbances should also be considered in future research.

4. More can also be done in the area of steady state stability. The presented method (Chapter 3) is adaptable to include speed governor control systems. This is an interesting area to investigate and an on-line steady state stability assessment approach can be developed using the catastrophe theory.

REFERENCES

[1] E.W. Kimbark, "Power System Stability", Vol. I, John Wiley & Sons Inc., New York, 1948.

[2] P.M. Anderson and A.A. Fouad, "Power System Control and Stability", Vol. I, Iowa State University Press, Ames, Iowa, 1977.

[3] G.W. Stagg and A.H. El-Abiad, "Computer Methods in Power System Analysis", McGraw-Hill, 1968.

[4] C. Concordia, "Representation of Loads", IEEE PES Winter Meeting, paper 75 CH0970-4-PWR, 1975.

[5] IEEE Committee Report, "Dynamic Load Dynamics Simulation Effects and Determination of Load Constants", Paper T73-089-0, IEEE Trans. PAS, Vol. 92, March/April 1973, pp. 600-609.

[6] F. John Meyer and K.Y. Lee, "Improved Dynamic Load Model for Power System Stability Studies", IEEE PES, Winter Meeting 1982, 82 WM 126-1.

[7] A.M. Sasson, "The Power System Stability Problems and its Solution Methods", IEEE PES Summer Meeting, Los Angeles, Calif., July 1970.

[8] W.D. Humpage and B. Stott, "Predictor-Corrector Methods of Numerical Integration in Digital Computer Analysis of Power System Transient Stability", Proc. IEE, Vol. 112, pp. 1557-1565, 1965.

[9] N.D. Rao and H.N. Rao, "Solution of Transient Stability Problems through the Number Series Approach", Proc. IEE, Vol. 111, pp. 775-788, 1964.

[10] D.L. Johnson, J.B. Ward, "The Solution of Power System Stability Problems by Means of Digital Computers", Trans. AIEE-PAS, Vol. 75, pp. 1321-1329, 1957.

[11] S.N. Talukdar, "Iterative Multi-Step Methods for Transient Stability Studies", IEEE Paper No. 70TP 48-PWR, Winter Power Meeting, New York, 1970.

[12] N.D. Rao and H.N. Rao, "Phase-Plane Techniques for the Solution of Transient Stability Problems", Proc. IEE, Vol. 110, 1963, pp. 1451-1461.

[13] K.N. Stanton and S.N. Tulukdar, "New Integration Algorithms for Transient Stability Studies", IEEE Trans., Vol. PAS-89, May/June 1970, pp. 785-991.

[14] H.W. Dommel and N. Sato, "Fast Transient Stability Solutions", IEEE Trans., Vol. PAS-91, July/August 1972, pp. 1643-1650.

[15] K. Prabhashanker and W. Janischewsyj, "Digital Simulationof Multi-Machine Power Systems for Stability Studies", IEEE Trans., Vol. PAS-87, Jan. 1968, pp. 73-80.

[16] L.H. Michaels, "The AC/Hybrid Power System Simulator and its Role in System Security", Proc. of the Power Industry Computer Applications Conference, Boston, Mass., May 1971, pp. 128-136.

[17] A.H. El-Abiad and K. Naguppun, "Transient Stability Regions of Multi-Machine Power Systems", IEEE Trans., Vol. PAS-85, pp. 169-179.

[18] J.L. Willems and J.C. Willems, "The Application of Lyapunov Methods to the Computations of Transient Stability Regions for Multi-Machine Power Systems", IEEE Trans. PAS., vol. 89, No. 5/6, pp. 795-801, May/June 1970.

[19] F.S. Prabhakara and A.H. El-Abiad, "A Simplified Determination of Transient Stability Regions for Lyapunov Methods", IEEE Trans. PAS, Vol.-94, No. 2, March/April 1975, pp. 672-689.

[20] M.A. Pai, "Power System Stability", Vol. 3, North Holland Publishing Co.

[21] M. Ribbens-Pavella and F.J. Evans, "Direct Methods for Studying Dynamics of Large-Scale Electric Power Systems - A Survey", Automatica, Vol. 21, No. 1, pp. 1-21, 1985.

[22] T. Athay, R. Podmore and S. Vivmani, "A Practical Method for Direct Analysis of Transient Stability", IEEE Trans., PAS-98, March/April 1979, pp. 573-584.

[23] A.A. Fouad and S.E. Stanton, "Transient Stability of Multi-Machine Power System Part I and II", IEEE Trans. PAS-100, pp. 3808-3424, Aug. 1981.

[24] M. Ribbens-Pavella, Th. Nan Cutsem, R. Ohifoui and B. Toumi, "Energy Type Lyapunov-Like Direct Criteria for Rapid Transient Stability Analysis", Proceedings of International Symposium on Power Systems Stability, Ames, Iowa, May 1985.

[25] A.A. Fouad, "Application of Transient Energy Functions to Practical Power System Problems", IEEE Speical Publication on Rapid Analysis of Transient Stability, Power Winter Meeting, 1987.

[26] A. Valveer, et al., "Relative Transient Stability Power System Margin Index", IEEE PES Summer Meeting and EHV/UHV Conference, Paper C73 474-4, Vancouver, Canada, July 1973.

[27] C.K. Pang, F.S. Prabhakara, A.H. El-Abiad and A.J. Koivo, "Security Evaluation in Power Systems Using Pattern Recognition", IEEE PES Winter Meeting, New York, Feb. 1973.

[28] K.S. Fu, "Sequential Method in Pattern Recognition and Machine Learning", Academic Press, 1968.

[29] W. Meisel, "Computer Oriented Approaches to Pattern Recognition", Academic Press, 1972.

[30] K.S. Fu and J.M. Mendel, "Adaptive Learning and Pattern Recognition", Academic Press, 1970.

[31] G. Hadley, "Linear Programming", Addison Wesley, 1962.

[32] P.H. Mengert, "Solution of Linear Inequalities", IEEE Trans. on Computers, Vol. C-19, pp. 124-131, 1970.

[33] C.L. Gupta, "Transient Security Assessment of Power Systems by Pattern Recognition and Lyapunov's Direct Method", Ph.D. thesis, Purdue University, West Lafayette, Indiana, 1976.

[34] H. Hakkimmashhadi, "Fast Transient Stability Assessment", Ph.D. thesis, Purdue University, West Lafayette, Indiana, Aug. 1982.

[35] S. Yamashira, T. Koike, A.H. El-Abiod, "Fast Transient Security Assessment and Enhancement Using Pattern Recognition", Proc. of 8th PSCC, Aug. 1984.

[36] T. Poston and I. Stewart, "Catastrophe Theory and Its Applications", Pitman Publishing Co., London, 1979.

[37] A.A. Sallam and J.L. Dineley, "Catastrophe theory as a Tool for Determining Synchronous Power System Dynamic Stability", IEEE Trans. PAS, Vol. 102, pp. 622-630, March 1983.

[38] R. Thom, "Structural Stability and Morphogenesis", Benjamin-Addison Wesley, New York, 1975.

[39] I. Stewart, "Elementary Catastrophe Theory", IEEE Trans. on Circuits and Systems, Vol. CAS-30, pp. 578-586, August 1983.

[40] P.T. Saunders, "An Introduction to Catastrophe Theory", Cambridge University Press, 1980.

[41] R.F. Chu, Discussion to Reference [37], IEEE Trans. PAS, Vol.-102, pp. 629-630, March 1983.

[42] M.D. Wvong and A.M. Mihirig, "Catastrophe Theory Applied to Transient Stability Assessment of Power Systems", Proc. IEE, Vol. 133, Pt. C, No. 6, Sept. 1986.

[43] M. Ribbens-Pavella, Thn Van Cutsem, R. Odifaoui and B. Toumi, "Energy Type Liapuniv-Like Direct Criteria for Rapid Transient Stability Analysis", Proc. of the International Symposium on Power System Stability, Ames, Iowa, May 1985.

[44] A.M. Mihirig and M.D. Wvong, "Application of Catastrophe Theory to Transient Stability Analysis of Power Systems", Proceedings of IASTED International Conference on High Technology in the Power Industry, Bosman, Montana, August 1986.

[45] Y. Xue, Th. Van. Cutsem and Ribbens-Pauella, "A Simple Direct Method for Fast Transient Stability Assessment of Large Power Systems", IEEE PES Winter Meeting, New Orleans, Louisiana, February 1-6, 1987.

[46] R. Rahimi and G. Schaffer, "Power System Transient Stabiliuty Indexes for On-Line Analysis of 'Worst Case' dynamic Contingencies", IEEE PES Summer Meeting, Paper 86 SM332-1, Mexico City, Mexico, July 20-25, 1986.

[47] A.N. Michel, A.A. Fouad and V. Vittal, "Power System Transient Stability Using Individual Machine Energy Functions", IEEE Trans., CAS-30, May 1983, pp. 266-276.

[48] N. Kakimoto, Y. Ohnogi, H. Matsuda and H. Shibuya, "Transient Stability Analysis of Large-Scale Power System by Lyapunov's Direct Method", IEEE/PES, 83SM 403-3, July, 1983.

[49] A.A. Fouad, "Application of Transient Energy functions to Practical Power System Problems", IEEE Special Publication on Rapid Analysis of Transient Stability, No. 87 TH0169-3-PWR.

[50] V.R. Sastry, "Validity of Nelgecting Transfer Conductances in Transient Stability Studies", Proc. IEE, Vol. 120, No. 12, December 1973.

[51] A.A. Fouad and S.E. Stanton, "Transient Stability of A Multi-Machine Power System", Part I and II, IEEE Trans., Vol. PAS-100, pp. 3408-3424, July 1981.

[52] S. Furuya and S. Iwamoto, "Fast Transient Stability Solution Using Taylor Expansion and Energy Function", EE in Japan, Vol. 105, No. 3, 1985.

[53] C. Concordia and P.G. Brown, "Effects of Trends in Large Steam Turbine Generator Parameters on Power System Stability", IEEE Trans. PAS-90, pp. 993-1000, 1971.

[54] S.B. Crary, "Power System Stability", Vol. 2, John Wiley & Sons, Inc., New York, 1947.

[55] IEEE Work Group on Special Stability Controls PSEC, "A Bibliography on the Application of Discrete Supplementary Controls to Improve Power System Stability", IEEE Trans., Vol. PWRS-2, No. 2, May 1987.

[56] N. Kakimoto, Y. Ohsawa and M. Hayashi, "Transient Stability Analysis of Multi-machine Power Systems with Field Flux Decays Via Lyapunov's Direct Method", IEEE Trans., Vol. PAS-99, No. 5, Sept/Oct. 1980.

[57] M.S. Sarma, "Synchronous Machines (Their theory, Stability and Excitation Systems)", Gordon and Breach Science Publishers, New York.

APPENDIX A

The swallowtail catastrophe:

The potential function is

$$V(X) = X^5 + uX^3 + \upsilon X^2 + wX$$

The equilibrium surface M is the hyper surface

$$5X^4 + 3uX^2 + 2\upsilon X + w = 0 \tag{A.1}$$

and the singularity set i the subset of M for which the equation

$$20X^3 + 6u\chi + 2\upsilon = 0 \tag{A.2}$$

The bifurcation set, B, is a three-dimensional surface in the control space u, υ and w.

Since we are concerned only with the qualitative behaviour of the system, and therefore want primarily to be able to plot the bifurcation set B. Let C_u be a plane u = constant in C (the control space), B_u will be a surve in C, and if we can sketch this curve for all values of u we can build up the complete surface B.

Equation (A.2) implies that υ is an odd function of X, and that is together with (A.1), implies that w is an even function X. Hence w is an even function of υ, and so for any u the curve B_u is symmetric about the w-axis.

Nest we differentiate (A.1) and (A.2) obtaining

$$\frac{dw}{dX} = -\ 2X\ \frac{d\upsilon}{dX} \tag{A.3}$$

and $$\frac{dw}{dX} = -\ (30X^2 + 3u) \tag{A.4}$$

the rest of the term in (A.3) having vanished in account of (A.2). We now have to consider the cases $u > 0$ and $u < 0$ separately.

If U is positive, then $\frac{du}{dX}$ cannot vanish. Hence υ is a strictly monotone function of X and the equation

$$\frac{dw}{d\upsilon} = -\ 2 \tag{A.5}$$

is valid everywhere. Moreover, equation (A.2) implies that $X\upsilon < 0$ with equality only when $X = \upsilon = 0$, at which point w also vanishes.

It follows that B_u is smooth, that w is large when $|X|$ is large, and that the signal of $\frac{dw}{d\upsilon}$ is the same as that of υ, vanishing only at the origin. This enables us to draw Fig. (A.1).

If u is negative, then $\frac{du}{dX}$ vanishes for two real values of X, $\pm\sqrt{\frac{-u}{10}}$. Consequently, $\frac{dw}{dX}$ vanishes for three values of X, these two together with $X = 0$ as before, and it follows that B_u has a critical point at $X = 0$ and cusps at the other two points.

To determine the type of the critical point, we notice that Equation (A.2) implies that for $|X| < \sqrt{\frac{-3u}{10}}$ the product $X\upsilon$ cannot be negative. Since X and υ also vanish together, it follows that if υ is small and positive so is X, and $\frac{dw}{d\upsilon}$ is then negative. This together with the fact that B_u is

symmetric about the w-axis, establishes that the critical point is a relative maximum.

Finally, we note that if $\upsilon = 0$ then either $X = 0$ or $X = \pm\sqrt{\frac{-3u}{10}}$. We have just seen that $X = 0$ corresponds to a maximum at the origin, and substituting into equation (A.1) we find that both the other roots give $w = \frac{9u^2}{20}$. Hence B_u has a point of self-intersection on the positive w-axis. We then check that $|X|$ large implies that both $|\upsilon|$ and w are also large and then, using the values of the parameter X to tell us that the order of the points we have found is: self-interseciton, cusp, maximum, cusp self-intersection, we can draw Fig. (A.2). And since the equation of the line of points of self-intersection is the parabola

$$w = \frac{9u^2}{20}, \quad \upsilon = 0$$

We can put the curves B_u together to form the surface B shown in Fig. (A.3). The origin of the name "swallowtail" is now apparent.

To find the form of the potential in each of the three regions into which B divides C, it is sufficient to consider points for which $\upsilon = 0$ and $u < 0$ then the solution of Equation (A.1) is

$$X^2 = \frac{1}{10}\left(-3u \pm \sqrt{(9u^2 - 20w)}\right)$$

There are three cases:

(a) $w > \frac{9u^2}{20}$ Equation (A.1) has no real roots and V has no critical

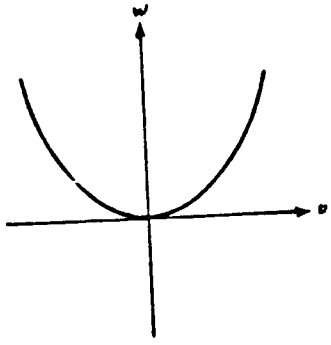

Fig.(A.1)

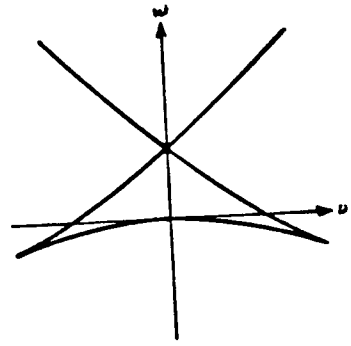

Fig.(A.2)

Cross section of the bifurcation set for

$u > 0$ and $u < 0$

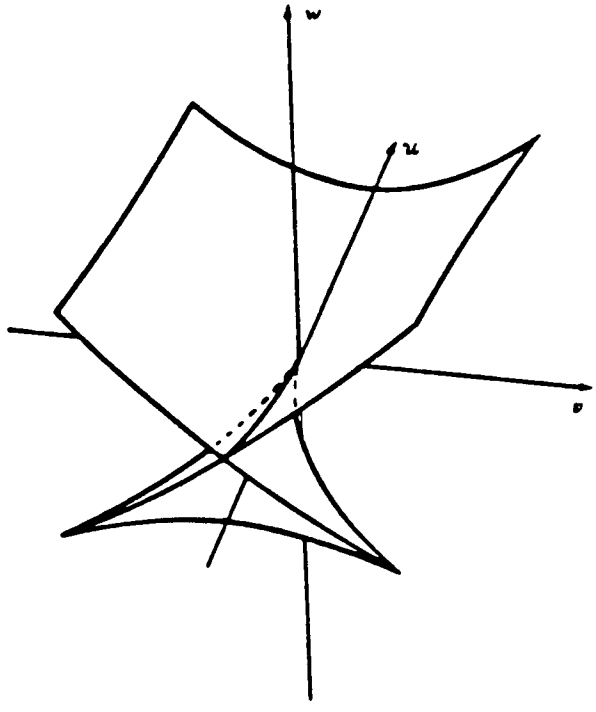

Fig.(A.3)

The bifurcation set of the swallowtail

points.

(b) $0 < w < \frac{9u^2}{20}$ Because $\sqrt{(9u^2 - 20w)}$ is real and less than the real and positive $-3u$, both solutions for X^2 are real and positive and V has four critical points, two maxima and two minima.

(c) $w < 0$ Both solutions for X^2 are real but one is negative. Consequently V has only two critical points, one minimum and one maximum.

APPENDIX B

The cusp catastrophe:

The potential function is

$$V(X) = X^4 + uX^2 + \upsilon X \tag{B.1}$$

so the equilibrium surface is a three-dimensional space in x, u and υ given by

$$4X^3 + 2uX + \upsilon = 0 \tag{B.2}$$

and the singularity set is the subset of the equilibrium surface such that the derivative of (B.2) is also equal to zero. It is given by

$$12X^2 + 2u = 0 \tag{B.3}$$

We find the bifurcation set by eliminating the state variable X from (B.2) and (B.3), we obtain

$$8u^3 + 27\upsilon^2 = 0 \tag{B.4}$$

Equation (B.4) is the projection of the three-dimensional manifold of equation (B.2) onto the control space (u-υ). The cusp manifold and the bifurcation set is shown in Fig. (B.1).

Equation (B.2) has three real roots within the bifurcation set region, or when

$$8u^3 + 27\upsilon^2 < 0$$

But when

$$8u^3 + 27\upsilon^2 > 0$$

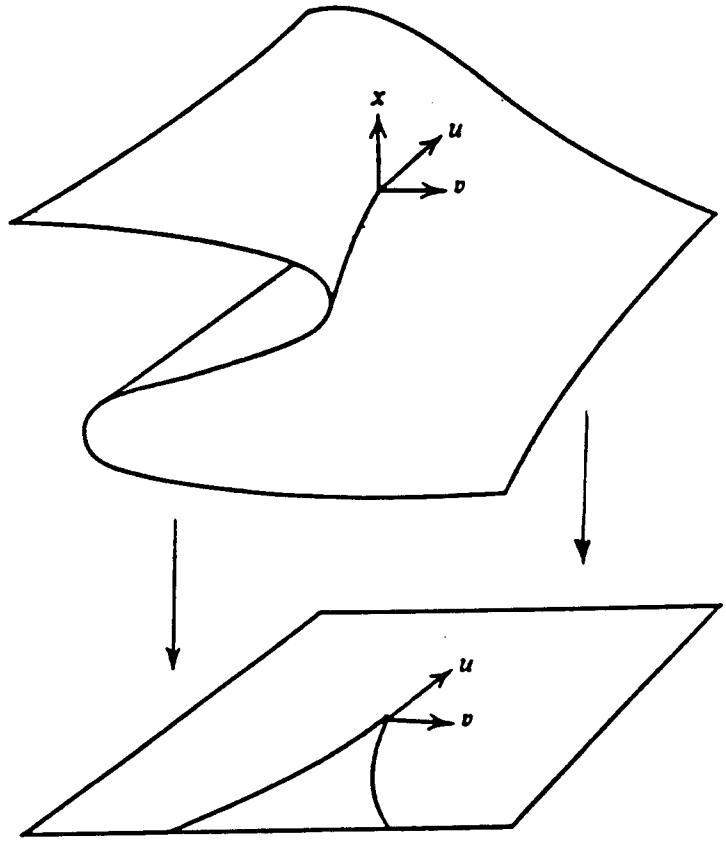

Fig. B.1 The cusp manifold and its bifurcation set.

there is only one real root.

Figure (B.2) shows the bifurcation set of u-υ plane in which the fuctions V(X) is sketched for different values of the parameters u and υ.

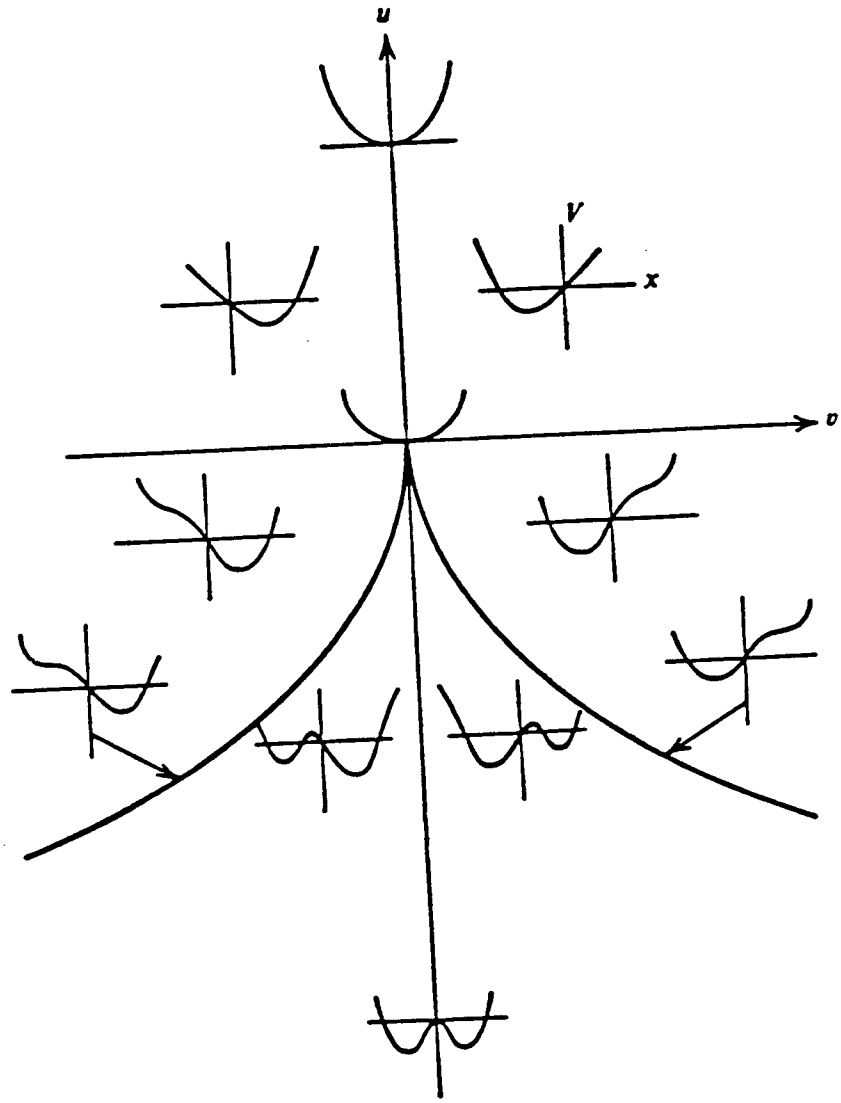

Fig. B.2 The cusp potential function V(X) at different values of the control variables.

APPENDIX C

Taylor series expansion of the accelerating power:

The accelerating power of machine i in an n-machine power system is given by (Equation 4.22)

$$P_{ai} = P_{mi} - \sum_{i=1}^{n} (D_{ij} \cos \delta_{ij} + c_{ij} \sin \delta_{ij}) \tag{C.1}$$

We expand P_{ai} in the neighborhood of t=0 to obtain,

$$P_{ai}(t) = P_a^{(0)} + \frac{1}{1!} P_a^{(1)} t + \frac{1}{2!} P_a^{(3)} t^2 + \ldots + \frac{1}{m!} P_a^{(n)} t^m \tag{C.2}$$

where

$$P_a^{(m)} = \left. \frac{d^m P_a}{dt^m} \right|_{t=0}$$

We note that at t=0, ω_i (speed deviation) = 0

and $\delta_i = \delta_i^{\,0}$ (initial angle)

therefore $$P_a^{(0)} = p_{mi} - \sum_{j=1}^{n} (D_{ij} \cos \delta_{ij}^{\,0} + c_{ij} \sin \delta_{ij}^{\,0}) \tag{C.3}$$

$$P_a^{(1)} = \left. \frac{d}{dt} (P_{ai}) \right|_{t=0} = \sum_{j=1}^{n} (D_{ij} \sin \delta_{ij}^{\,0} - c_{ij} \cos \delta_{ij}^{\,0})$$

Since $$\left. \dot{\delta}_{ij} \right|_{t=0} = \omega_{ij} = 0$$

therefore $$P_a^{(1)} = 0 \tag{C.4}$$

To simplify the derivative equations we let

$$A = \sum_{j=1}^{n} (D_{ij} \cos \delta_{ij}^{0} + c_{ij} \sin \delta_{ij}^{0}) \tag{C.5}$$

and

$$B = \sum_{j=1}^{n} (D_{ij} \sin \delta_{ij}^{0} - c_{ij} \cos \delta_{ij}^{0}) \tag{C.6}$$

the derivatives of A and B with respect to time are

$$\frac{d(A)}{dt} = - B \dot{\delta}_{ij} \quad , \quad \frac{d(B)}{dt} = A \dot{\delta}_{ij}$$

for convenience let $\delta_{ij}^{(1)} = \dot{\delta}_{ij}$, $\delta_{ij}^{(2)} = \ddot{\delta}_{ij}$ ... and so on

therefore

$$P_a^{(0)} = P_{mi} - A$$

$$P_a^{(1)} = \frac{d}{dt} P_a^{(0)} = B \, \delta_{ij}^{(1)} = 0$$

$$P_a^{(3)} = \frac{d}{dt} P_a^{(1)} = \frac{d}{dt} (B \, \delta_{ij}^{(1)})$$

$$= A \, \delta_{ij}^{(1)} + B \, \delta_{ij}^{(2)} = B \, \delta_{ij}^{(2)} \tag{C.7}$$

$$P_a^{(3)} = \frac{d}{dt} P_a^{(2)} = 2A \, \delta_{ij}^{(1)} \, \delta_{ij}^{(2)} - B \, \delta_{ij}^{(1)^3} + A \, \delta_{ij}^{(1)} \, \delta_{ij}^{(2)} + B \, \delta_{ij}^{(3)}$$

$$= 0 \tag{C.8}$$

where $\delta_{ij}^{(3)} = \frac{P_{ai}^{(1)}}{M_i} - \frac{P_{ai}^{(1)}}{M_j} = 0$

$$P_a^{(4)} = \frac{d}{dt} P_a^{(3)} = B\ \delta_{ij}^{(4)} + A\ \delta_{ij}^{(1)}\ \delta_{ij}^{(3)}$$

$$+ 2A\ \delta_{ij}^{(2)^2} - B\ \delta_{ij}^{(1)^2}\ \delta_{ij}^{(2)} + 2\ A\ \delta_{ij}^{(1)}\delta_{ij}^{(3)} - 2B\ \delta_{ij}^{(1)^2}\ \delta_{ij}^{(2)}$$

$$- 3\ B\ \delta_{ij}^{(1)^2}\ \delta_{ij}^{(2)} - A\ \delta_{ij}^{(1)^4}$$

$$P_a^{(4)} = B\ \delta_{ij}^{(4)} + 3\ A\ \delta_{ij}^{(2)^2} \tag{C.9}$$

$$P_a^{(5)} = \frac{d}{dt} P_a^{(4)} = B\ \delta_{ij}^{(5)} + 5A\ \delta_{ij}^{(1)}\delta_{ij}^{(4)} + 10\ A\ \delta_{ij}^{(2)}\ \delta_{ij}^{(3)} - 10\ B\ \delta_{ij}^{(1)^2}\delta_{ij}^{(3)}$$

$$- 15\ B\ \delta_{ij}^{(2)^2}\delta_{ij}^{(1)} - 10\ A\ \delta_{ij}^{(1)^3}\delta_{ij}^{(2)} + B\ \delta_{ij}^{(1)^5} = 0 \tag{C.10}$$

$$P_a^{(6)} = \frac{d}{dt} P_a^{(5)} = B\ \delta_{ij}^{(6)} + 6\ A\ \delta_{ij}^{(1)}\delta_{ij}^{(5)} + 15\ A\ \delta_{ij}^{(2)}\delta_{ij}^{(4)} - 15\ B\ \delta_{ij}^{(1)^2}\delta_{ij}^{(4)}$$

$$+ 10\ A\ \delta_{ij}^{(3)^2} - 60\ B\ \delta_{ij}^{(1)}\delta_{ij}^{(2)}\delta_{ij}^{(3)} - 20\ A\ \delta_{ij}^{(1)^3}\delta_{ij}^{(3)} - 15\ B\ \delta_{ij}^{(2)^3}$$

$$- 45\ A\ \delta_{ij}^{(1)}\delta_{ij}^{(2)^2} + 15\ B\ \delta_{ij}^{(1)^4}\delta_{ij}^{(2)} + A\ \delta_{ij}^{(1)^6}$$

$$= B\ \delta_{ij}^{(6)} + 15\ A\ \delta_{ij}^{(2)}\delta_{ij}^{(4)} - 15\ B\ \delta_{ij}^{(2)^3} \tag{C.11}$$

Note that $\delta_{ij}^{(1)} = \delta_{ij}^{(3)} = \delta_{ij}^{(5)} = \delta_{ij}^{(7)} \ldots = 0$

APPENDIX D

Derivation of $P_{ai}^{(3)}$ and $P_{ai}^{(4)}$ including damping:

$$P_{ai}^{(3)} = \frac{d}{dt} P_{ai}^{(2)}$$

From equation (C.8) of Appendix C

$$P_{ai}^{(3)} \text{ (without damping)} = 0$$

Therefore

$$P_{ai}^{(3)} = - D\ \delta_{ij}^{(4)} \tag{D.1}$$

Also

$$P_{ai}^{(4)} = \frac{d}{dt} P_{ai}^{(3)}$$

From equation (C.4) we obtain

$$P_{ai}^{(4)} = B\ \delta_{ij}^{(4)} + 3\ A\ \delta_{ij}^{(2)^2} - D\ \delta_{ij}^{(5)}$$

Since $\delta_{ij}^{(5)} = 0$

then

$$P_{ai}^{(4)} = B\ \delta_{ij}^{(4)} + 3\ A\ \delta_{ij}^{(2)^2}$$

$$= \sum_{j=1}^{n} (D_{ij} \sin\ \delta_{ij}^{0} - c_{ij} \cos\ \delta_{ij}^{0}) \delta_{ij}^{(4)} + 3 \sum_{j=1}^{n} (D_{ij} \cos \delta_{ij}^{0}$$

$$+ c_{ij} \sin\ \delta_{ij}^{0})\ \delta_{ij}^{(2)^2} \tag{D.2}$$

APPENDIX E

Taylor series coefficients of the accelerating power including excitation response.

The accelerating power of machine i is

$$P_{ai} = P_{mi} - \sum_{j=1}^{n} E_i E_j \, (g_{ij} \cos \delta_{ij} + b_{ij} \sin \delta_{ij}) \tag{E.1}$$

and

$$E_i = E(0) + F^{(0)} t + \frac{F^{(1)}}{2} t^2 + \ldots \tag{E.2}$$

Recalling equation (5.16)

$$T_{d0_i}' \frac{d\,E_i}{dt} = F(t) = \frac{E_c - (E_c - E_0)}{\cos \phi_i} e^{-t/\tau_e} - E_i - (X_{qi} - X_{di}')$$

$$\sum_{j=1}^{n} E_j \, (g_{ij} \cos \delta_{ij} + b_{ij} \sin \delta_{ij}) \tag{E.3}$$

the coefficients $F^{(0)}$, $F^{(1)}$ are given in Section (5.3), $F^{(2)}$, $F^{(3)}$ are derived from (E.3) and given as follows.

$$F^{(2)} = \frac{-1}{\tau_e^{\,2}} \frac{(E_c - E_0)}{\cos \phi_i} \frac{F^{(1)}}{\tau_{doi}'} + (X_{qi} - X_{di}') \sum_{j=1}^{n} E_j (g_{ij} \sin \delta_{ij}^{0}$$

$$- b_{ij} \cos \delta_{ij}^{0}) \tag{E.4}$$

$$F^{(3)} = \frac{1}{\tau_e^{\,3}} \frac{(E_c - E_0)}{\cos \phi_i} - \frac{F^{(2)}}{\tau_{doi}'} \tag{E.5}$$

The derivation of the accelerating power coefficients are as follows

Let $A_{ij} = E_j \, (g_{ij} \cos \delta_{ij} + b_{ij} \sin \delta_{ij}^{0})$

$$B_{ij} = E_j \, (g_{ij} \sin \delta_{ij}^{0} - b_{ij} \cos \delta_{ij}^{0}) \tag{B.6}$$

then $\dfrac{d\, A_{ij}}{dt} = - B_{ij} \, \dot{\delta}_{ij}^{0}$

$$\frac{d\, B_{ij}}{dt} = A_{ij} \, \dot{\delta}_{ij}^{0}$$

Let $\dot{\delta}_{ij}^{0} = \delta_{ij}^{(1)}$, $\ddot{\delta}_{ij}^{(1)} = \delta_{ij}^{(2)}$, ... etc.

Substituting equations (E.6), and (E.2) to (E.1) to obtain the Taylor series coefficients of P_{ai} we get

$$P_a^{(0)} = P_{mi} - \sum_{j=1}^{n} E_i^{(0)} \, A_{ij} \tag{E.7}$$

$$P_a^{(1)} = \left. \frac{d\, P_{ai}}{dt} \right|_{t=0} = - \sum_{j=1}^{n} (F^{(0)} A_{ij} - E(0) \, B_{ij} \, \delta_{ij}^{(1)})$$

$$= - \sum_{j=1}^{n} F^{(0)} \, A_{ij} \tag{E.8}$$

$$P_a^{(2)} = \left.\frac{d^2 P_{ai}}{dt^2}\right|_{t=0} = \sum_{j=1}^{n} (E(0)\, B_{ij}\, \delta_{ij}^{(2)} - F^{(1)}\, A_{ij}) \tag{B.9}$$

$$P_a^{(3)} = \left.\frac{d^3 P_{ai}}{dt^3}\right|_{t=0} = \sum_{j=1}^{n} (-F^{(2)}\, A_{ij} + 3\, F^{(0)}\, B_{ij}\, \delta_{ij}^{(2)}) \tag{E.10}$$

$$P_a^{(4)} = \left.\frac{d^4 P_{ai}}{dt^4}\right|_{t=0} = \sum_{j=1}^{n} [6\, F^{(1)}\, B_{ij}\, \delta_{ij}^{(2)} + 3\, E(0)\, A_{ij}\, \delta_{ij}^{(2)^2}$$

$$+ E(0)\, B_{ij}\, \delta_{ij}^{(4)} - F^{(3)}\, A_{ij}] \tag{E.11}$$